

**Integrated Ocean Drilling Program
Expedition 325 Preliminary Report**

Great Barrier Reef environmental changes

**The last deglacial sea level rise in the South Pacific:
offshore drilling northeast Australia**

Platform operations
11 February–7 April 2010

Onshore Science Party
2–16 July 2010

Expedition 325 Scientists



Published by
Integrated Ocean Drilling Program Management International, Inc.,
for the Integrated Ocean Drilling Program

Publisher's notes

Material in this publication may be copied without restraint for library, abstract service, educational, or personal research purposes; however, this source should be appropriately acknowledged. Core samples and the wider set of data from the science program covered in this report are under moratorium and accessible only to Science Party members until 16 July 2011.

Citation:

Expedition 325 Scientists, 2010. Great Barrier Reef environmental changes: the last deglacial sea level rise in the South Pacific: offshore drilling northeast Australia. *IODP Prel. Rept.*, 325. doi:10.2204/iodp.pr.325.2010

Distribution:

Electronic copies of this series may be obtained from the Integrated Ocean Drilling Program (IODP) Scientific Publications homepage on the World Wide Web at www.iodp.org/scientific-publications/.

Published by Integrated Ocean Drilling Program Management International (IODP-MI), Inc., for the Integrated Ocean Drilling Program and prepared by the European Consortium of Ocean Research Drilling (ECORD) Science Operator. Funding for the program is provided by the following agencies:

National Science Foundation (NSF), United States

Ministry of Education, Culture, Sports, Science and Technology (MEXT), Japan

European Consortium for Ocean Research Drilling (ECORD)

Ministry of Science and Technology (MOST), People's Republic of China

Korea Institute of Geoscience and Mineral Resources (KIGAM)

Australian Research Council (ARC) and New Zealand Institute for Geological and Nuclear Sciences (GNS), Australian/New Zealand Consortium

Ministry of Earth Sciences (MoES), India

Disclaimer

Any opinions, findings, and conclusions or recommendations expressed in this publication are those of the author(s) and do not necessarily reflect the views of the participating agencies, IODP Management International, Inc., British Geological Survey, European Petrophysics Consortium, University of Bremen, or the authors' institutions.

Expedition 325 participants

Expedition 325 scientists

Jody M. Webster*
Co-Chief Scientist
School of Geosciences
The University of Sydney
Sydney NSW 2006
Australia
jody.webster@sydney.edu.au

Yusuke Yokoyama*
Co-Chief Scientist
Atmosphere and Ocean Research Institute
University of Tokyo
5-1-5 Kashiwanoha, Kashiwa
Chiba 277-8564
Japan
yokoyama@ori.u-tokyo.ac.jp

Carol Cotterill*
Staff Scientist
British Geological Survey
Murchison House
Edinburgh
Scotland
EH9 3LA
United Kingdom
cjcott@bgs.ac.uk

Louise Anderson*
Petrophysics Staff Scientist
University of Leicester
Department of Geology
University Road
Leicester
LE1 7RH
United Kingdom
lma9@le.ac.uk

Sophie Green*
Staff Scientist in Training
British Geological Survey
Murchison House
Edinburgh
Scotland
EH9 3LA
United Kingdom
soph@bgs.ac.uk

Raphael Bourillot
Carbonate Sedimentologist
Laboratory Biogeosciences
Universite de Bourgogne
6 Bd Gabriel
F-21000 Dijon
France
raphael.bourillot@u-bourgogne.fr

Juan Carlos Braga*
Coral Specialist
Departamento de Estratigrafia y Paleontologia
Facultad de Ciencias
Universidad de Granada
Campus Fuentenueva
18002 Granada
Spain
jbraga@ugr.es

Andre Droxler
Carbonate Sedimentologist
Department of Earth Science
Rice University
MS-126
PO Box 1892
Houston TX 77251-1892
USA
andre@rice.edu

Tezer Esat
Dating Specialist
Institute for Environmental Research
Australian Nuclear Science and Technology
Organisation and Australian National
University RSES
Private Mail Bag 1
B53
Menai NSW 2234
Australia
Tezer.esat@anu.edu.au

*Expedition scientists who are participating offshore.

Thomas Felis
Paleoclimatologist
MARUM—Center for Marine Environmental
Sciences
University of Bremen
GEO Building
Klagenfurter Strasse
28359 Bremen
Germany
tfelis@uni-bremen.de

Kazuhiko Fujita
Micropaleontologist (benthic foraminifers)
Department of Physics and Earth Sciences
University of the Ryukyus
1 Senbaru, Nishihara
Okinawa 903-0213
Japan
fujitaka@sci.u-ryukyu.ac.jp

Michael Gagan
Paleoclimatologist
Research School of Earth Sciences
The Australian National University
1 Jaeger Building 61
Mills Road
Canberra ACT 0200
Australia
michael.gagan@anu.edu.au

Eberhard Gischler
Carbonate Sedimentologist
Institut fuer Geowissenschaften
J. W. Goethe-Universitaet
Altenhoferallee 1
60438 Frankfurt am Main
Germany
gischler@em.uni-frankfurt.de

Emilio Herrero-Bervera
Paleomagnetist
School of Ocean Earth Science and
Technology
Hawaii Institute of Geophysics
1680 East West Road
Honolulu HI 96822
USA
herrero@soest.hawaii.edu

Jiang Hongchen*
Microbiologist
School of Earth Sciences and Resources
China University of Geosciences
29 Xueyuan Road
Haidan District
Beijing
P.R. China
hongchen.jiang@gmail.com

Marc Humblet
Coral Specialist
Atmosphere and Ocean Research Institute
Ocean Floor Geoscience
University of Tokyo
5-1-5 Kashiwanoha, Kashiwa
Chiba 277-8564
Japan
m-hum@aori.u-tokyo.ac.jp

Mayuri Inoue
Paleoclimatologist
Ocean Floor Geoscience
Atmosphere and Ocean Research Institute
University of Tokyo
5-1-5 Kashiwanoha, Kashiwa
Chiba 277-8564
Japan
mayuri-inoue@aori.u-tokyo.ac.jp

Tania Lado Insua
Physical Properties Specialist
University of Rhode Island
Department of Ocean Engineering
Sheets Building
Bay Campus
Narragansett RI 02882
USA
ladoinsuat@egr.uri.edu
Tania_insua@yahoo.es

Yasufumi Iryu
Coral Specialist
Department of Earth and Planetary Sciences
Graduate School of Environmental Studies
Nagoya University
Furo-cho, Chikusa-ku
Nagoya 464-8601
Japan
iryu.yasufumi@a.mbox.nagoya-u.ac.jp

Luigi Jovane*
Paleomagnetist
Geology Department
Western Washington University
516 High Street
MS 908
Bellingham WA 98225
USA
luigijovane@gmail.com

Hironobu Kan
Carbonate Sedimentologist
Graduate School of Education
Okayama University
3-1-1 Tsushima Naka
Okayama 700-8530
Japan
kan@cc.okayama-u.ac.jp

Braddock Linsley
Paleoclimatologist
Atmospheric and Environmental Science
State University of New York
ES 351
1400 Washington Avenue
Albany NY 12222
USA
blinsley@albany.edu

Didier Loggia
Physical Properties
Universite Montpellier 2
Laboratoire Geosciences
Place Eugene Bataillon
34095 Montpellier Cedex 5
France
loggia@univ-montp2.fr

Heath Mills
Microbiologist
Department of Oceanography
Texas A&M University
716A Eller O&M Building
College Station TX 77843
USA
hmills@ocean.tamu.edu

Donald Potts*
Coral Specialist
Ecology and Evolutionary Biology and
Institute of Marine Sciences
University of California
A316 Earth and Sciences Building
Santa Cruz CA 95064
USA
potts@biology.ucsc.edu

Claire Searđ
Carbonate Sedimentologist
CEREGE
Europole Mediterranee de l'Arbois
BP 80
13545 Aix-en-Provence Cedex 4
France
seard@cerege.fr

Atsushi Suzuki*
Paleoclimatologist
Institute of Geology and Geoinformation
Geological Survey of Japan
Tsukuba Central 7
1-1-1 Higashi, Tsukuba
Ibaraki, 305-8567
Japan
a.suzuki@aist.go.jp

Alex Thomas
Dating Specialist
Department of Earth Sciences
University of Oxford
Parks Road
Oxford, OX1 3PR
United Kingdom
alexth@earth.ox.ac.uk

William Thompson
Dating Specialist
Department of Geology and Geophysics
Woods Hole Oceanographic Institution
113A Clark Laboratory
MS #23
Woods Hole MA 02543
USA
wthompson@whoi.edu

Manish Tiwari
Paleoclimatologist
National Centre for Antarctic and Ocean
Research
Headland Sada
Vasco-da-Gama-403804
Goa
India
manish@ncaor.org

Alexander Tudhope
Paleoclimatologist
Grant Institute
University of Edinburgh
West Mains Road
Edinburgh, EH9 3JW
United Kingdom
sandy.tudhope@ed.ac.uk

Operational and technical staff

ECORD Science Operator and technical representatives

Dave Smith[†]
Operations Manager

Ursula Röhl
Laboratory and Curation Manager

Lee Baines[†]
Drilling Coordinator

Leigh-Anne Baker
Yeoperson in Training

Simon Barry[†]
Logging Engineer

Annick Fehr
EPC Petrophysicist

Alan Douglas
IT Support

Thomas Frederichs
ESO Paleomagnetist

Lydia Gerullis
Photography/Database

Eileen Gillespie
Yeoperson

Colin Graham[†]
Database Manager

Walter Hale
Core Curator

Rhonda Kappler
Publications Specialist (USIO)

Eleanor John
EPC Petrophysics Technician

Rob Knight
EPC Petrophysics Technician

Johanna Lofi
EPC Petrophysicist

Brit Kockisch
LECO Operator

Martin Kölling[†]
ESO Geochemist

Jan Hoffman[†]
ESO Geochemist

Holger Kuhlmann
Core Curator/Assistant Laboratory
Manager

Vera Lukies
ESO Petrophysics Technician

Dave McInroy
ESO Science Manager

Sally Morgan[†]
EPC Petrophysicist

Mary Mowat[†]
Database Manager

Richard le Provost[†]
Logging Engineer

Scott Renshaw
Core Technician

Johanna Schietke
Photography/Database

Luzie Schnieders
ESO Geochemist

[†]Participated in shipboard operations.

Ali Skinner
Drilling Consultant

Graham Tulloch[†]
Drilling Coordinator

Christoph Vogt
XRD Specialist

Dave Wallis[†]
Electronics Engineer

Hans-Joachim Wallrabe-Adams
Database Operator

Thomas Westerhold
ESO Petrophysicist

Alex Wülbers[†]
Core Curator/Logistics

University of Bremen (temporary student assistants)

Katharina Alter
Catering

Mechthild Böthig
Catering

Patrizia Geprägs
Sampling

Katharina Hochmuth
Core Splitter

Jennifer Kuhr
Sampling

Silvana Pape
Geochem Lab

Alexander Petrovic
Core Splitter

Nadine Rippert
Catering

Melanie Siegburg
Core Splitter

Christian Sommerfield[†]
Core Curator/Sampling

Bluestone personnel

Sukhwinder Singh Gill
Party Chief

Govindasamy Paneer Selvam
Exploration Manager

Sufyan Bin Abdullah Bin Diab
QHSE Manager

Ajith Dsouza
CPT Operator/Roughneck

Simon Steevan Dsouza
CPT Operator/Roughneck

Jason Harvie
Surveyor

Mulyadi Haryadi
HSE Advisor

Packrisamy Kanesan
Driller

Gatot Letariono
Party Chief 1

Vikram s/o Raju
Roughneck /Assistant Driller

Vimal s/o Raju
Roughneck 3

Ismail Ressay
Roughneck/Assistant Driller

Edy Safrudin
ISOS Medic

Bernard Silitonga
Roughneck/Assistant Driller

Grant Smith
Surveyor

Andi Sujito
ISOS Medic

Amerda Lingam s/o Verayan
Roughneck 1

Mikheev Vladimir
Driller

GBRMPA personnel

Jessica Hoey
Environmental Site Supervisor

Mike Stanton
Hydrographers' Pilot

GC Rieber personnel

Hallgeir Johansen
Master

Lester Bryan Anino
Steward 2

Honorato Jr. Arriola
AB 1

Lyonidd Capacite Cimafranca
2nd Officer / DPO 1

Wojciech Frackowiak
Amos Puncher

Jeferson Villanueva Garcia
Chief Cook

Ryan Ronnel Manimtim Gomez
Steward 1

Nicolas Rivas Giray
3rd Engineer

Frank Hammero
Chief Officer/DPO

Kasten Koop
Electrician

Nils Erik Leikvoll
2nd Officer/DPO

Edgardo Manio
Cook 2

Leo Caga Anan Mutia
2nd Officer/DPO

Michael Nacion
Steward 3

Jan Mathiesen
Chief Engineer

Jose Odquin
Fitter

Joven Palicato
2nd Engineer

Glenn Galon Dela Pena
Oiler

Edwin Reyes
Bosun

Dennis Delos Santos
AB 2

Andre Skadal
2nd Engineer

Geir H. Strand
Chief Engineer

Elin Tasas
Chief Steward

Kare Thorholm
Master (DPO)

Abstract

Integrated Ocean Drilling Program (IODP) Expedition 325, designed to investigate the fossil reefs on the shelf edge of the Great Barrier Reef, was the fourth expedition to utilize a mission-specific platform and was conducted by the European Consortium for Ocean Research Drilling (ECORD) Science Operator (ESO). The objectives of Expedition 325 are to establish the course of sea level change, to define sea-surface temperature variations, and to analyze the impact of these environmental changes on reef growth and geometry for the region over the period of 20–10 ka. To meet these objectives, a succession of fossil reef structures preserved on the shelf edge seaward of the modern barrier reef were cored from a dynamically positioned vessel in February–April 2010. A total of 34 boreholes across 17 sites were cored in depths ranging from 42.27 to 167.14 meters below sea level (lowest astronomical tide [LAT] taken from corrected EM300 multibeam bathymetry data). Borehole logging operations in four boreholes provided continuous geophysical information about the drilled strata. The cores were described during the Onshore Science Party (OSP) at the IODP Bremen Core Repository (Germany) in July 2010, where minimum and some standard measurements were made. Preliminary shipboard dating of core catcher samples and initial observations of the cores made during the OSP confirm that coral reef material ranging in age from >30 to 9 ka was recovered during Expedition 325. Further post-cruise research on samples taken during the OSP is expected to fulfill the objectives of the expedition.

Introduction

The timing and courses of deglaciations are considered an essential component for understanding the dynamics of large ice sheets (Lindstrom and MacAyeal, 1993; Denton et al., 2010) and their effects on Earth's isostasy (Nakada and Lambeck, 1987; Lambeck, 1993; Peltier, 1994). Moreover, the disappearance of glacial ice sheets was responsible for dramatic changes in the freshwater fluxes to the oceans, which disturbed the thermohaline circulation and hence global climate (e.g., Stocker and Wright, 1991). Coral reefs are excellent sea level indicators, and their accurate dating by mass spectrometry is of prime importance for determining the timing of deglaciation events and thus for understanding the mechanisms driving the glacial–interglacial as well as millennial scale cycles. Furthermore, scleractinian coral colonies can monitor sea-surface temperatures (SSTs) and other oceanographic parameters (e.g., salinity and sediment run-off), and fossil corals can be used as recorders of past varia-

tions in these parameters. Finally, assessing the impact of sea level and paleoclimate changes on fossil coral reefs may represent an important advance in understanding how coral reef systems—in particular the Great Barrier Reef—respond to environmental stress.

Background

Sea level change as a global climate indicator

Prior to Integrated Ocean Drilling Program (IODP) Expedition 310 (Tahiti Sea Level), only a few sea level curves based on coral reef records had been accurately dated for the last deglaciation: in Barbados between 19,000 and 8,000 calendar years before present (cal. y BP; A.D. 1950) (Fairbanks, 1989; Bard et al., 1990a, 1990b; Peltier and Fairbanks, 2006), in New Guinea between 13,000 and 6,000 cal. y BP (Chappell and Polach, 1991; Edwards et al., 1993), in Vanuatu between 23,000 and 6 cal. y BP (Cabioch et al., 2003), and in Tahiti between 13,750 cal. y BP and 2,380 radiocarbon years before present (^{14}C y BP) (Bard et al., 1996) (Fig. F1A). Until recently, the Barbados and Vanuatu curves were the only ones to encompass the entire deglaciation. However, these sites, like New Guinea, are located above active subduction zones where tectonic movements can be large and discontinuous. Therefore, the reconstructed sea levels may be biased by variations in the rate of tectonic uplift and/or abrupt coseismic vertical motions. Also, Barbados is under the influence of glacial isostatic adjustment because of the waxing and waning of the North American ice sheet (Lambeck et al., 2002; Milne et al., 2009). Hence, there is a clear need to study past sea level changes in tectonically stable regions (or in areas where vertical crustal deformation is slow and/or regular) located far away from former ice-covered regions (far-field). The expeditions linked to IODP Proposal 519 (Expedition 310, Tahiti Sea Level, and Expedition 325, Great Barrier Reef Environmental Changes [GBREC]) aim to provide the most comprehensive deglaciation curves from tectonically stable regions by conducting offshore drilling of fossil coral reefs now preserved at 40–120 m below present sea level. Expedition 310 was successfully completed in 2005 (offshore phase) and 2006 (Onshore Science Party) (Camoin, Iryu, McInroy, et al., 2007).

The Barbados record suggested that the last deglaciation was characterized by three brief periods of accelerated melting superimposed on a smooth and continuous rise of sea level with no reversals (Fig. F1A). These so-called meltwater pulse (MWP) events—19ka-MWP (Yokoyama et al., 2000; Clark et al., 2004; DeDeckker and

Yokoyama 2009; Hanebuth et al., 2009), MWP-1A, and MWP-1B (~13,800 and 11,300 cal. y BP; Fairbanks, 1989; Bard et al., 1990)—were interpreted to be a consequence of massive inputs of continental ice (~40–50 mm/y in sea level rise that is roughly equivalent to annual discharge rates of 16,000 km³ for MWP-1A). Originally, MWP-1A was thought to correspond to a short and intense cooling between 14,100 and 13,900 cal. y BP in the Greenland ice core records (Johnsen et al., 1992; Grootes et al., 1993) and therefore to postdate the initiation of the Bölling-Alleröd warm period at ~14,800 cal. y BP (Broecker, 1992). However, cumulative evidence from far-field sites suggests that the timing of MWP-1A was slightly older than originally proposed (e.g., ~14,600–14,700 cal. y BP; Hanebuth et al., 2000; Webster et al., 2004); this has been confirmed by the Expedition 310 Tahiti sea level record (Deschamps et al., unpubl. data).

The apparent sea level jump evident in the New Guinea Huon Peninsula coral record at ~11,000 cal. y BP (Edwards et al., 1993) lags MWP-1B by a few centuries compared to the coral record observed at Barbados (Fig. [F1A](#)). Two of the inferred meltwater pulses (MWP-1A and MWP-1B) may have induced reef-drowning events (Blanchon and Shaw, 1995). Two “give-up” reef levels have been reported at 90–100 and 55–65 meters below sea level (mbsl) on the Mayotte foreslopes (Comoro Islands) and have been related to MWP-1A and MWP-1B, respectively (Dullo et al., 1998), with similar features recorded in the Caribbean (MacIntyre et al., 1991; Grammer and Ginsburg, 1992). In contrast, the continuous coral record obtained from onshore Tahiti suggests that there are no major changes in the rate of sea level rise during the time of the inferred post-Younger Dryas (YD) meltwater pulse (MWP-1B) (Bard et al., 2010). A third *Acropora* reef-drowning event at ~7600 cal. y BP was reported by Blanchon and Shaw (1995).

Thus, there are still uncertainties about the general pattern of sea level rise during the last deglaciation, including the duration and amplitude of the maximum lowstand during the Last Glacial Maximum (LGM) and potential links between increased glacial meltwater and accelerated sea level rise (Broecker, 1990). Furthermore, sawtooth sea level fluctuations between 19,000 and 15,280 cal. y BP (Locker et al., 1996; Yokoyama et al., 2000, 2001c, 2006b); the precise timing, rate, and amplitude of MWP-1A; and a sea level fall coeval with climatic change around 11,000 cal. y BP are still controversial topics (Lambeck et al., 2002).

Obtaining direct sea level information based on coral reef records older than the last glacial is difficult, and few studies have been reported. The Expedition 310 Tahiti coral record extends back past the last interglacial and provides important insights into the

climate system during the penultimate deglaciation (Thomas et al., 2009; Fujita et al., 2010). Offshore drilling at the shelf edge of the Great Barrier Reef (GBR) will provide paleoclimate and sea level records extending into marine isotope Stage 3 and beyond.

Sea level compilations indicate that local sea level histories varied considerably around the world in relation to both the postglacial redistribution of water masses and to a combination of local processes (Lambeck, 1993; Peltier, 1994; Yokoyama et al., 2001b, 2001c; Lambeck et al., 2003, 2006; Milne et al., 2009), although significant deviations between model predictions and field data have been noted for several regions (Camoin et al., 1997). Post-LGM sea level changes at far-field sites provide basic information regarding the melting history of continental ice sheets and the rheological structure of Earth. The effect of hydro-isostasy on local sea level will depend on the size of the adjacent landmass: near small islands, the addition of meltwater will produce a small differential response between the island and the seafloor, whereas the meltwater load will produce significant differential vertical movement between larger islands (or continental margins) and the seafloor (Nakada, 1986; Yokoyama et al., 1996). Thus there is a need to establish the relative magnitudes of hydro-isostatic effects at two ideal sites, one on an oceanic island and another on a continental margin, located at a considerable distance from the major former ice sheets. It is essential that both sites are tectonically stable throughout the time period proposed for the investigation so that the proposed Northern and Southern Hemisphere deglaciation curves from Barbados and New Guinea can be rigorously tested. Tahiti (Expedition 310, completed in 2006) and the GBR (Expedition 325, completed in 2010) are ideal locations in which to perform these tests.

Climatic and oceanographic changes during the last deglaciation

The Quaternary period of Earth's history is marked by major cyclical changes in global climate reflected in the growth and decay of high-latitude ice sheets. We are currently in a relatively warm interglacial following the LGM, which occurred around 21,000 cal. y BP (Yokoyama et al., 2000; Mix et al., 2001). These glacial–interglacial climate oscillations are related to cyclical changes in the distribution of incoming solar radiation due to variations in Earth's orbit around the sun (so-called “Milankovich cycles”). However, it is also clear that strong feedbacks within the earth system operate to amplify and modify the initial forced changes. Understanding the nature of these feedbacks and the mechanisms through which they influence the timing, rates, and magnitude of climate change remain outstanding issues in climate science.

In this context, the tropical oceans play a crucial role in modulating global climate on glacial–interglacial to interannual (i.e., El Niño Southern Oscillation [ENSO]) timescales. One of the key objectives of Expedition 325 is to elucidate the timing, magnitude, and mechanisms of tropical climate change across a major climate transition—namely, from the peak of the last glaciation (the LGM) to the relative warmth of the early Holocene. Paleodata indicate that the LGM mean global surface temperature was cooler than it is at present by several degrees (Mix et al., 2001). However, there were large latitudinal differences in the magnitude of this cooling, with the tropics in general showing less difference (with respect to preindustrial temperatures) than the high latitudes. Estimates of tropical SSTs based on proxies in deep-sea sediment cores now indicate a mean LGM cooling of $\sim 1.7^{\circ}\text{C}$ compared to the present, with significant regional variations (MARGO Project Members, 2009; Otto-Bliesner et al., 2009) that include a $\sim 3^{\circ}\text{C}$ cooling in the western sector of the Western Pacific Warm Pool (WPWP) (e.g., Linsley et al., in press) (Fig. **F1B**). At a few sites, late-glacial age corals (although not LGM) have been used to estimate cooling (Guilderson et al., 1994; McCulloch et al., 1996; Beck et al., 1997; Gagan et al., 2000). Some of these estimates are similar to those derived from deep-sea sediments, whereas others indicate larger differences (e.g., up to 4° – 6°C cooling). Resolving the inconsistencies between proxy-based reconstructions remains an important priority; subtle diagenesis of some coral samples (e.g., Allison et al., 2005), possible changes in oceanic Sr/Ca affecting coral SST reconstructions (e.g., Stoll and Schrag, 1998; Martin et al., 1999), possible seasonal biases in climate reconstruction from deep-sea sediments, and real differences in regional climate are all possible contributing factors.

The main transition from glacial to interglacial climate occurred in the interval 19,000–9,000 cal. y BP. However, the rise in temperature (and sea level) was not simple and smooth, at least regionally. Greenland ice cores, as well as North Atlantic deep-sea sediment records, suggest that there was a severe climate reversal during the course of the last deglaciation around 12,000–13,000 cal. y BP during the YD (Fig. **F1A**). Outside the North Atlantic region, diverse paleoclimate evidence suggests synchronous climate events were widespread in the Northern Hemisphere (e.g., Wang et al., 2001; Yuan et al., 2004; Yokoyama et al., 2006a). However, until recently, there was sparse evidence for the YD in the tropics. A coral Sr/Ca-based SST reconstruction from Vanuatu was used to suggest that SST during the YD was $\sim 4^{\circ}\text{C}$ cooler (Corrège et al., 2004). Fossil coral records from Expedition 310 in Tahiti also captured $\sim 3^{\circ}\text{C}$ cooling (Asami et al., 2009) and oceanic environmental change during the YD (Inoue et al., 2010). More recently, Griffiths et al. (2010) made paired measurements of calcite $\delta^{18}\text{O}$ and fluid inclusion $\delta^{18}\text{O}$ in stalagmites from southern Indonesia to estimate

air temperatures $\sim 6^{\circ}\text{C}$ cooler during the YD. The same stalagmite $\delta^{18}\text{O}$ records indicate that the Indonesian-Australian monsoon was stronger during the YD, in contrast to the weaker YD monsoon recorded by stalagmite $\delta^{18}\text{O}$ records from China (e.g., Yuan et al., 2004). It is important to acknowledge that some of these stalagmite- and coral-based reconstructions of tropical temperatures show YD cooling that is significantly greater than that estimated from deep-sea sediment cores. More coral data are required to help resolve this issue.

Recent studies in the tropical western Pacific have documented Holocene climatic variations, including $\sim 0.5^{\circ}\text{--}1^{\circ}\text{C}$ warmer SSTs in the GBR and WPWP during the early Holocene, based on analysis of Sr/Ca in corals and Mg/Ca in planktonic foraminifers (Gagan et al., 2004; Stott et al., 2004; Linsley et al., in press), and parallel analyses of $\delta^{18}\text{O}$ indicate that the surface ocean in the WPWP freshened through the Holocene. Coral, lake, and geoarchaeological evidence suggest that ENSO variability was substantially reduced in the early to middle Holocene (e.g., Sandweiss et al., 1996; Rodbell et al., 1999; Tudhope et al., 2001; Moy et al., 2002; McGregor and Gagan, 2004), a finding that challenges state-of-the-art ocean-atmosphere general circulation models, which, for the most part, reconstruct more modest changes in ENSO for this interval (e.g., Liu et al., 2000; Otto-Bliesner et al., 2003; Brown et al., 2008). New speleothem $\delta^{18}\text{O}$ records from southern Indonesia also suggest that monsoonal rainfall was weaker during the early Holocene (Griffiths et al., 2009), and a coral record from Expedition 310 in Tahiti suggests local SSTs may have been cooler than they are at present (DeLong et al., 2010).

Given the continued uncertainties in constraining the full range of tropical western Pacific climate and the importance of this region to global climate, additional paleo-data are required. Some of the most debated points are

1. The precise dating and quantification of SST and salinity change and variability during the last deglaciation,
2. The extent of the early Holocene thermal maximum in the tropical western Pacific, and
3. The relationship of WPWP size and mean temperature to global and tropical climate and to interannual ENSO variability since the LGM.

New approaches to these long-standing challenges will be provided by IODP Expedition 325 at the GBR.

The Great Barrier Reef: its suitability, previous results, and promise

The GBR is the largest epicontinental reef system on Earth, extending 2000 km in a northwest–southeast direction along the northeast coast of Queensland (Australia) (Davies et al., 1989) (Fig. F2). The origin of this morphologically and biologically important sedimentary system is poorly constrained, with ages of <500 k.y. before present assigned to the initiation of the northern GBR system (McKenzie, Davies, Palmer-Julson, et al., 1993; Davies and Peerdeman, 1998; International Consortium, 2001; Webster and Davies, 2003; Braithwaite et al., 2004) and, more recently, ages between 560 and 670 k.y. before present assigned to the southern GBR (Dubois et al., 2008).

The northern, central, and southern GBR define ideal sites for the evaluation of sea level changes during the period from 20,000 to 8,000 cal. y BP. The reefs on the shelf edge east of Cooktown (Australia) form the semicontinuous outer barrier of the northern GBR. In this area, as well as in the far northern GBR, the reef is narrow, with ribbon reefs on its eastern edge and extensive coastal fringing reefs and patch reefs. In the south, the GBR broadens, with patch reefs separated by open water or narrow channels. On the outer shelf east-northeast of Townsville (Australia), modern reefs form a line of pinnacles seaward of the main reef edge with lateral growth on the windward margin. South of 15°30'S, the reefs are generally ≥ 30 km offshore and reach 100 km offshore at 22°30'S. Farther south, the shelf widens considerably to >200 km. East of Mackay (Australia), the modern reefs form a complex series of flood-tide deltaic reefs (i.e., Pompey Complex) (Hopley, 2006). The coastal lagoon between the main GBR reef tract and the mainland has a maximum depth of 145 m but rarely exceeds 60 m (Wolanski, 1982).

Studies of the GBR (McKenzie et al., 1993; Davies and Peerdeman, 1998) focused on the areas southeast of Townsville and east of Cooktown and defined the morphologic shape of the outer reef and upper continental slope, as well as the geological origin of the GBR itself. Based on high-resolution seismic profiles in the fore reef section in front of the GBR, Feary et al. (1993; in McKenzie et al., 1993) recognized three seismic mega-sequences that define a clearly aggradational upper sequence (0–490 ms), a transitional middle sequence (490–555 ms), and a progradational lower sequence (below 555 ms). In 1991, indirect evidence that the GBR is very young, having initiated during marine isotope Stages 9–11 (McKenzie et al., 1993; Davies and Peerdeman, 1998) was recovered during Ocean Drilling Program (ODP) Leg 133.

In 1995, a new phase of drilling at Boulder Reef (15°23.944'S, 145°26.182'E; 86 m core depth below seafloor [CSF-A]) and Ribbon Reef 5 (15°22.40'S, 145°47.149'E; 210 m CSF-A), using a reef-mounted jack-up platform, further enhanced this story, proving that the northern GBR is ~100 m thick and rests on a subreef subtropical red coralline algal facies that, in turn, overlies a deepwater temperate grainstone facies (Davies and Peerdeman, 1998; International Consortium, 2001). Strontium isotope and magnetostratigraphic data from the base of the Pleistocene coral reef sequence have confirmed that the origin of the GBR is very young, perhaps <500,000 y (International Consortium, 2001; Webster and Davies, 2003; Braithwaite et al., 2004). Detailed stratigraphic and sedimentary facies analysis of the 210 m long Ribbon Reef 5 drill core shows that the upper part of the platform is composed of cycles of transgressional cool-water coralline-dominated carbonates topped by shallow-water highstand coral reefs (Webster and Davies, 2003; Braga and Aguirre, 2004). However, the Holocene reef does not show this cyclic sedimentary couplet, as it is coral dominated from its inception at 8000 cal. y BP.

Previous sedimentological and geophysical studies on the shelf edge have identified a succession of subsea morphologic structures interpreted as drowned reefs at 100, 90, 60–50, and 35–40 mbsl (Carter and Johnson, 1986; Harris and Davies, 1989; Lacombe et al., 1995; Hopley, 2006; Beaman et al., 2008), especially in the following four areas:

1. Cooktown shelf and slope (Ribbon Reef),
2. Cairns (Australia) shelf and slope (Grafton Passage, Flora Passage, and Noggin Pass),
3. Townsville shelf and slope (Bowl, Viper Reef), and
4. Mackay shelf and slope (Hydrographer's Passage).

For example, a series of drowned linear reefs and lagoons occupy specific depths over at least a 30 km stretch on the outer continental shelf in the vicinity of Hydrographer's Passage in the southern GBR region.

Based on the R/V *Southern Surveyor* cruise in September–October 2007, Webster et al. (2008a, 2008b) identified five primary drill site transects from three of these key regions on the Cooktown, Cairns, and Mackay shelf edges (Fig. F2).

Proposed drill sites

Available site survey data at the Great Barrier Reef

The proposed drill sites on the GBR are distributed in three distinct regions (Fig. F2): Offshore Cooktown (Ribbon Reef 5 and 3), Offshore Cairns (Noggin Pass), and McKay shelf (Hydrographer's Passage).

From previous site survey data (described in detail in the June 2007 preliminary report to the Environmental Protection and Safety Panel [EPSP] and recently synthesized by Beaman et al., 2008), it was clear that a succession of barrier reefs occupy the outer shelf between 40 and 100 mbsl with terrace features at ~80–110 mbsl along much of the GBR. These features have not previously been investigated in detail. For example, with the exception of the Ribbon Reef 5 region, only limited systematic high-resolution swath bathymetry mapping, imaging, or sampling had ever been attempted. However, it is clear that these submerged reef structures have the potential to provide unique and critical information about the nature of sea level and climatic change off-shore eastern Australia and important information about their role as habitats and substrates for present-day biological communities.

Prior to Expedition 325, proponents led a site survey cruise to gather the most comprehensive data set ever collected from the GBR shelf edge (Webster et al., 2008b). The cruise on the *Southern Surveyor* acquired the remaining site survey information needed for IODP drilling operations in the GBR. Four study sites (Ribbon Reef, Noggin Pass, Viper Reef, and Hydrographer's Passage) were mapped along the Queensland margin where the approximate location of submerged reefs is known. The data types acquired and submitted to the IODP Site Survey Database (SSDB) were:

- EM300 swath bathymetry and backscatter;
- Subbottom sparker and Topas PS18 seismic reflection profiles;
- High-resolution underwater stereoscopic images and high-resolution multibeam bathymetry, acquired onboard a state-of-the-art Autonomous Underwater Vehicle (AUV);
- Continuous measurements establishing the present-day oceanographic conditions on the shelf edge, using the AUV's onboard Seabird concentration/temperature/depth recorder (CTD); and
- Dredged rock samples from the tops of the shelf edge reefs, acquired using a standard rock dredge and a Smith-McIntyre sediment grab.

These data were used to define specific drill targets for Expedition 325 drilling operations (see “**Operational strategy**” for proposed transect locations and available site survey information).

Summary of 2007 Great Barrier Reef site survey data for the proposed sites

Mackay shelf, Hydrographer’s Passage (HYD-01C and HYD-02A)

EM300 swath mapping of the Hydrographer’s Pass survey area covers 810.68 km². Based on a detailed examination of all available site survey data, we proposed to drill two transects of holes across the best developed fossil reef features, one in the northwest (HYD-01C) and the other in the southeast (HYD-02A). See Figure F2 for the general location, Figures F3 and F4 for detailed maps of HYD-01C, and Figures F5 and F6 for detailed maps of HYD-02A.

Site survey data from the northwest of Hydrographer’s Pass illustrate the succession of morphological features that define the HYD-01C transect:

- A double-fronted barrier reef 200 and 100 m wide separated by a lagoon 2 km wide and up to 70 m deep; barrier reefs occur at 51–55 mbsl. In some regions, the lagoon is characterized by prominent subbottom reflectors, as well as 50 m wide patch reefs rising to 55 mbsl.
- A steep sloping 500 m wide terrace with a sharp break in slope marking the 80 mbsl reef feature.
- A complex 1 km wide lagoon and reef terrace system. The lagoon at 87–85 mbsl is as wide as 600 m with numerous prominent subbottom reflectors. Seaward, the lagoon grades into a 400 m wide relatively flat terrace and a sharp break in slope that marks the 90 mbsl reef feature.
- A 700 m wide lagoon and reef pinnacle system. The lagoon, characterized by prominent subbottom reflectors, is 300 m wide and at 95 mbsl. The lagoon grades seaward into a dense system of patch reefs or pinnacles ~30–40 m across that range between 95 and 97 mbsl.
- A major break in slope that defines the 100 mbsl reef feature also has a series of smaller seaward pinnacles and terraces interpreted as reefs at 110 and 120 mbsl.
- A gentle upper slope characterized by >160 ms of fore reef slope sediments.

Site survey data from the southeast of Hydrographer’s Pass illustrate the succession of morphological features that define the HYD-02A transect:

- A submerged reef shoal 600 m wide at 31 mbsl with well-developed landward and seaward terraces at 40 mbsl.
- A double-fronted barrier reef 250 m and 150 m wide separated by a lagoon 2.5 km wide and as deep as 55 m; barrier reefs occur at 54–56 mbsl. The lagoon is characterized by numerous prominent subbottom reflectors and partially buried patch reefs. Patch reefs become more dense seaward between 60 and 70 mbsl.
- A steep slope 400 m seaward of the reef at 50 mbsl defined by a series of smaller pinnacles and terraces interpreted as distinct reefs at 65, 70, and 80 mbsl.
- A complex 2.3 km wide lagoon, reef pinnacle, and terrace system between 90 and 100 mbsl. The lagoon is 2 km wide and up to 102 m deep with prominent subbottom reflectors that are only interrupted by significant breaks in slope that define the 90 and 100 mbsl reef features.
- A major break in slope that occurs at 103 mbsl and defines the 100 mbsl reef feature, with a series of smaller pinnacles and terraces interpreted as reef features at 110 mbsl.
- A prominent 70 m wide reef terrace observed at 126–128 mbsl, interpreted to be the LGM reef.
- A gentle upper slope characterized by >160 ms of fore reef slope sediments.

Offshore Cooktown, Ribbon Reef 5 and 3 (RIB-01C and RIB-02A)

EM300 swath mapping of the Ribbon Reef survey area covers 1609.87 km². The Ribbon Reef 5 area was also surveyed by Webster and colleagues in 2005 using a Reson 8101 (240 kHz) swath mapping system and Datasonics CAP-6600 Chirp 3.5 kHz subbottom profiler (Beaman et al., 2008). Based on a detailed examination of all available site survey data (multibeam, backscatter, seismic profiles, AUV imagery, and bottom samples), the initial plan was to drill two transects of holes during Expedition 325, across the best developed fossil reef features, one off Ribbon Reef 5 (RIB-01C) and another off Ribbon Reef 3 (RIB-02A). However, only one transect (RIB-02A) was drilled, and so only the details regarding that particular transect are included in this report. See Figure F2 for the general location and Figures F7 and F8 for detailed maps.

Site survey data seaward of modern Ribbon Reef 3 illustrate the succession of morphological features that define the RIB-02A transect:

- A modern reef front talus zone that extends down to 44 mbsl.
- A well-developed reef detected on the shelf lying parallel to the shelf break at 47 mbsl that defines the 50 mbsl reef feature.

- A gently sloping terrace ~330 m wide at 55–80 mbsl, with prominent subbottom reflectors visible.
- A submerged reef observed at 80 mbsl, characterized by a subtle raised rim 1–2 m high, that defines the 70 mbsl reef feature.
- The main shelf break at 105 mbsl, characterized by a 3–5 m raised rim that forms the 100 mbsl reef feature. Below 500 mbsl, the upper slope is deeply incised by canyons that extend down into the Queensland Trough.

Offshore Cairns, Noggin Pass (NOG-01B)

EM300 swath mapping of the Noggin Pass survey area covered 1243.27 km². See Figure F2 for the general location and Figures F9 and F10 for detailed maps.

Available site survey data seaward of modern Noggin Reef illustrate the succession of morphological features that define the NOG-01B transect:

- A double-fronted barrier reef 250 m and 90 m wide separated by a lagoon 80 m wide; barrier reefs occur at 44–42 mbsl.
- A lagoon up to 250 m wide at a depth of 57–54 mbsl with reef pinnacles some 50 m wide and rising to a depth of 56 mbsl. The lagoon is characterized by prominent subbottom reflectors and is fronted by a discontinuous barrier, which tops at 55 mbsl and represents the 50 mbsl reef feature.
- A gently sloping terrace ~450 m wide at 60–80 mbsl. A break in slope at the edge of this terrace marks the 80 mbsl reef feature.
- A gently sloping terrace ~140 m wide at 91–99 mbsl. A distinct break in slope at the edge of this terrace marks the reef feature at 100 mbsl.
- A narrow 50 m terrace at 108 mbsl and a main shelf break that forms the 110 mbsl reef feature.
- A gentle upper slope characterized by >100 m of fore reef slope sediments. Below ~250 mbsl, the upper slope is deeply incised by a well-developed canyon system that extends down to 1400 m in the Queensland Trough.

Scientific objectives of Expedition 325

1. To establish the course of postglacial sea level rise at the Great Barrier Reef.

The first objective of Expedition 325 is to establish the course of postglacial sea level rise in the GBR—in other words, to define the exact shape of the deglaciation curve for the period from 20 to 10 ka. The expected results will achieve the following:

- Assess the validity, timing, and amplitude of MWP events (e.g., 19ka-MWP, MWP-1A, and MWP-1B);
- Assess the maximum sea level drop during the LGM and establish the timing of its termination;
- Prove or disprove the sawtooth pattern of sea level rise during the last deglaciation (Locker et al., 1996); and
- Test Glacio-hydro-isostatic modeling–predicted sea level based on different ice and rheological models.

The reconstruction of sea level curves will rely on the absolute dating of in situ corals and other reef-building biota provided by radiometric methods (U-Th by thermal ionization mass spectrometry [TIMS] and multicollector inductively coupled plasma–mass spectrometry [MC-ICP-MS]; ^{14}C by accelerator mass spectrometry [AMS]) and paleobathymetric information deduced from biological communities (corals, algae, benthic foraminifers, and mollusks) that live in a sufficiently narrow or specific depth range to be useful as absolute sea level indicators.

2. To define sea-surface temperature variations for the region over the period 20 to 10 ka.

The second objective of Expedition 325 is to define SST variations for the region over the period from 20 to 10 ka to better understand the following:

- The regional variation of SSTs in the southwest Pacific,
- The climatic variability and the identification of specific phenomena such as ENSO, and
- The global variation and relative timing of postglacial climate change in the Southern and Northern Hemispheres.

Methods include stable isotope ($\delta^{18}\text{O}$) and trace element (Sr/Ca ratios by inductively coupled plasma spectroscopy [ICP] and TIMS) analyses on high-resolution (i.e., at the monthly scale) sampling of massive coral colonies. Coupled analyses of $\delta^{18}\text{O}$ and Sr/Ca on the same sample may yield estimates of both temperature and salinity (Mc-

Culloch et al., 1996). $\delta^{13}\text{C}$ measurements, systematically coupled with those of $\delta^{18}\text{O}$ in coral skeletons, will provide information on other parameters (e.g., solar variations or metabolism processes). Geochemical methods will be coupled with measurements and analyses of band widths and microstructural variations in the coral skeletons.

3. To analyze the impact of sea level changes on reef growth and geometry.

The third objective of Expedition 325 is to analyze the impact of sea level changes on reef growth and geometry, especially the following:

- Glacial meltwater phases (identification of reef deepening and/or drowning events),
- The morphological and sedimentological evolution of the fore reef slopes (highstand versus lowstand processes),
- The modeling of reef building, and
- Environmental changes during reef development.

Numerical models (e.g., CARB3D, DIONISIS) simulating reef building will be used to study the effect of abrupt sea level rise events on reef geometry and to assess qualitatively the effect of sea level fluctuations on reef shape and composition, as well as age–depth relationships.

Expedition 325 will provide the opportunity to better constrain the postglacial history (Lambeck et al., 2002; Peltier, 1994; Fleming et al., 1998; Okuno and Nakada, 1999) by documenting the LGM lowstand in well-studied cores in the far-field and by comparing MWP-1A in the Pacific and the Atlantic. Furthermore, the study of LGM and very early postglacial coral material should allow calculation of the first Sr/Ca SSTs in the Pacific, which could then supplement the Barbados sample data (Guilderson et al., 1994), the study of Papua New Guinea marine isotope Stage 6 corals (McCulloch et al., 1999), and the results of Expedition 310 (Camoin, Iryu, McInroy, et al., 2007; Asami et al., 2010; DeLong et al., 2010; Inoue et al., 2010).

Operational strategy

The Barbados offshore drilling (Fairbanks, 1989) demonstrated that the reef sequences corresponding to the last deglaciation developed on slopes forming discontinuous successive terraces of various lateral extent and stratigraphic thickness.

Therefore, to recover the entire postglacial reef sequence, successive reef terraces that occur seaward of the living barrier reef must be drilled.

Our detailed analyses of the combined GBR site survey data sets have demonstrated the occurrence of successive reef features at various depths between 130 and 25 mbsl, which correspond to potential drilling targets. Thus, at each geographic location, we cored a transect of several holes in order to recover the entire postglacial reef sequence. Initial results obtained from Expedition 310 confirm that this drilling strategy is sound (Camoin et al., 2007).

Based on the results of seismic, bathymetric, and sample data acquired during the *Southern Surveyor* cruise in September–October 2007, four transects located within three geographical areas (Fig. F2) were drilled during Expedition 325: Hydrographer’s Passage (2 transects), Noggin Pass (1 transect), and Ribbon Reef 3 (1 transect). Depths at these locations ranged from 47.27 to 167.14 mbsl (LAT taken from corrected EM300 data).

The exact location of drill holes was determined during the expedition by checking the nature and morphology of the seafloor with a through-pipe camera system. This enabled the protection of benthic biota from any disturbance by drilling. Following the completion of each hole, the cored lithologies were assessed by the Co-Chief Scientists and onboard sedimentologists to refine the position of the next hole. All holes were sited within a 125 m radius around the proposed drilling sites approved by the EPSP and within the transect boundaries given in the research permit issued by the Great Barrier Reef Marine Park Authority (GBRMPA). Figures F3 and F11, F5 and F12, F7 and F13, and F9 and F14 show the general locations and enlargements of groupings of sites for the holes at HYD-01C, HYD-02A, RIB-02A, and NOG-01B, respectively.

Principal site results

Cores were recovered from 34 holes across 17 sites (M0030–M0058) (Table T1), with a conventionally calculated recovery of 26.63%. Hole depths ranged from 47.27 to 167.14 mbsl (LAT taken from corrected EM300 data), and cores were recovered from 42.27 to 208.5 mbsl. Four transects located within three geographical areas (Fig. F2) were drilled during Expedition 325: Hydrographer’s Passage (2 transects; north and south), Noggin Pass (1 transect), and Ribbon Reef (1 transect). All holes were drilled within 125 m radius areas around the sites approved by the EPSP and were located

within the transect areas defined by the GBRMPA. Borehole geophysical wireline logging was conducted at four holes.

Because of space limitations on the *Greatship Maya*, only limited analysis of the cores was possible offshore. The bulk of the description and measurements on the whole and split cores was conducted during the Onshore Science Party (OSP) at the IODP Bremen Core Repository (Germany).

Table T2 shows which measurements were conducted offshore and which ones at the OSP.

Sedimentology and biological assemblages

The core material shows that fossil reefs on the shelf edge of the GBR are composed of nine major lithologic types, defined as follows:

1. Modern seafloor sediment. These sediments are characterized by a mixture of unconsolidated bioclastic sand to pebbles, with preserved invertebrate skeletons, mud with planktonic components, and lithified crusts mainly consisting of coralline algae, encrusting corals, bryozoans, serpulid worm tubes, and encrusting foraminifers. Crusts commonly show reddish to dark brown stains.
2. Coralgal boundstone. These deposits are mainly built (bound) by corals and coralline algae that form well-developed frameworks. Microbialites are a minor component. Variable amounts of loose to lithified internal bioclastic sediments are observed.
3. Coralgal/microbialite boundstone. These deposits are built by varying proportions of coral and coralline algae and abundant microbialite forming well-developed frameworks. Variable amounts of loose to lithified internal bioclastic sediments are observed.
4. Microbialite boundstone. Microbialites exhibiting a range of morphologies/fabrics (e.g., stromatolitic and digitate) form the major component of this boundstone deposit with minor coral and coralline algae. Variable amounts of loose to lithified internal bioclastic sediments are observed.
5. Packstone/grainstone. These deposits are bioclastic, sand-sized, and clast-supported, with a high degree of lithification in the presence (packstone) or absence (grainstone) of a fine-grained matrix. Large benthic foraminifers, corals, *Halimeda*, and mollusk grains are the most common component grains.

6. Rudstone. Clast-supported bioclastic deposit with a high degree of lithification and >10% of grains of granule to pebble size. Coral, *Halimeda*, and mollusks are the most common components of larger clasts.
7. Lime sand. These unconsolidated sediments are composed of sand-sized carbonate grains dominated by large benthic foraminifers, corals, *Halimeda*, and mollusks.
8. Lime pebbles. These are unconsolidated sediments with >10% pebble-sized clasts. The most common components are corals, *Halimeda*, and mollusks.
9. Mud. These unconsolidated sediments are composed fine-grained (silt to clay sized) carbonate and/or siliciclastic grains.

It is important to note that lithologic types of the same designation at different holes are not necessarily correlative in time. Comprehensive definition of distinct lithologic units and their correlation between sites will only be possible after a detailed analysis of the sedimentary facies and chronology data obtained during postcruise research.

HYD-01C transect: Holes M0030A–M0039A

The northern Hydrographer's Passage transect, HYD-01C, includes (landward to seaward) Holes M0034A, M0030A and M0030B, M0031A, M0032A, M0033A, M0035A, M0036A, M0038A, M0039A, and M0037A at depths between 51.0 and 122.3 mbsl. Numerous holes are closely spaced (i.e., <20 m apart) and could be considered as a composite hole through distinct reef targets: Holes M0030A and M0030B in the 80 mbsl reef target, Holes M0031A–M0033A in the 90 mbsl reef target, and Holes M0038A, and M0039A in the 110 mbsl reef target. Figure F15 summarizes the major lithologic types and their distribution and recovery for the HYD-01C transect.

Sedimentology and biological assemblages

Coralgal and coralgal-microbialite boundstones are the dominant lithologies recovered along the HYD-01C transect. Just below the modern seafloor, between one and three coralgal boundstone and coralgal-microbialite boundstone intervals occur in all the HYD-01C holes, except for Holes M0030A and M0030B, in which the recovery was low, and Hole M0037A, the most distal and deepest site on the transect (at 122 mbsl).

Coralgal intervals (one or two, depending on the hole) contain little or no microbialite. Their thicknesses range from <1 m in Hole M0032A to 8 m in Hole M0031A. Coralgal intervals systematically overlie coralgal-microbialite intervals in Holes M0031A, M0032A, M0033A, M0035A, M0036A, M0038A, and M0039A. In Hole M0034A, a 2 m thick coral boundstone underlies an 18 m thick coralgal-microbialite interval, whereas in Hole M0036A, the coralgal boundstone is interbedded with 6 m of unconsolidated sediments. The main corals in the coralgal intervals are massive *Isopora* with smaller amounts of massive *Porites*, submassive to massive *Montipora*, and branching *Acropora*.

Coralgal-microbialite intervals are dominated volumetrically by microbialites, and these boundstones are the thickest lithologies in every hole except Hole M0037A. They range in thickness from 10 m in Hole M0031A to ~30 m in Hole M0033A. Coral assemblages in the coralgal-microbialite intervals are diverse. Although dominated by massive *Isopora*, branching *Acropora*, and *Seriatopora*, other corals such as massive *Porites* and *Faviidae* are the principal corals in localized intervals.

In six of the eleven holes along the HYD-01C transect, an unconsolidated sediment interval ranging from <1 to 19 m thick underlies the upper coralgal-microbialite framework interval. In Hole M0034A, the unconsolidated interval is overlain by a coralgal level, whereas in Hole M0036A, the unconsolidated interval is included within the coralgal interval. This unconsolidated sediment interval was probably partly disturbed by coring operations and is composed of bioclastic lime sand to pebbles containing mollusks, larger benthic foraminifers, *Halimeda*, fragments of corals and red algae, bryozoans, echinoderms, and sea urchin spines.

A thin (<3 m) skeletal packstone to grainstone interval rich in large benthic foraminifers, calcareous algae, and/or a dark coralgal-worm tube boundstone is interbedded with, or underlies, the unconsolidated sediment interval in Holes M0031A, M0032A, M0033A, M0035A, M0036A, M0038A, and M0039A. A second unconsolidated interval, similar to the first, forms the base of the recovered sequences in Holes M0031A and M0036A.

As the most distal and deepest site (at 122 mbsl) along the HYD-01C transect, Hole M0037A also has a different sedimentary composition and lithologic succession, with a 12 m thick interval of unconsolidated lime sands to pebbles from the seafloor to the base of the hole. There is clear evidence of downhole contamination in the upper part of each section. This interval overlies very thin foraminifers, coralline algae, and coral

fragment-rich grainstone. The base of the hole consists of an 8 m thick lime sand rich in large benthic foraminifers and mollusks. These deposits appear to be undisturbed and therefore are probably in situ with minimal disturbance from downhole contamination.

Physical properties

Partial recovery was achieved in holes drilled on the HYD-01C transect. With regard to physical property measurements, cores were only partially saturated and often underfilled, impacting the different types of data coverage and quality. Borehole depths are as follows:

Hole M0031A = 90.05 mbsl, 43 m drilling depth below seafloor (DSF-A).

Hole M0032A = 91.58 mbsl, 36.70 m DSF-A.

Hole M0033A = 91.30 mbsl, 32.80 m DSF-A.

Hole M0034A = 51 mbsl, 23.10 m DSF-A.

Hole M0035A = 100 mbsl, 29.9 m DSF-A.

Hole M0036A = 103.21 mbsl, 34 m DSF-A.

Hole M0037A = 122.29 mbsl, 21 m DSF-A.

Hole M0039A = 107.04 mbsl, 28.4 m DSF-A.

In general, recovery was low, and the intervals recovered were often disturbed by drilling or partially unsaturated because of the unlithified to semilithified nature of the cored formations.

Density and porosity

Density and porosity vary similarly in all of the boreholes drilled across the HYD-01C transect. Discrete sample porosity ranges from 20% to 50%. This is due to significant variability in the pore systems (e.g., moldic, vuggy, growth framework, and intergranular) (Fig. F16). Bulk densities of discrete samples vary between 1.7 and 2.4 g/cm³. Densities measured on whole cores with the multisensor core logger (MSCL) are <2 g/cm³. This is likely due in part to the partial saturation of the cores but also due to the majority of the core comprising unconsolidated fragments. There is a classic linear correlation between the porosity (ϕ) and the bulk density (ρ) of the discrete samples (Fig. F17):

$$\rho = \rho_s(1 - \phi) + \rho_w\phi,$$

where

ρ_s = average grain density and

ρ_w = fluid density.

This correlation demonstrates that the average grain density along the HYD-01C transect is 2.77 g/cm³. Grain density varies between 2.7 and 2.85 g/cm³ and may correspond to a value between the density of calcite (2.71 g/cm³) and aragonite (2.93 g/cm³).

P-wave velocity

A crossplot of velocity versus porosity (both from discrete samples) for all sites shows an inverse relationship (Fig. F18) between acoustic velocity (V_p) and porosity. MSCL data, which were acquired cross core (over ~6.5 cm), range from 1500.34 to 1937.94 m/s, much lower values than discrete measurements acquired on core plugs. The scale dependency of petrophysical measurements, along with the (inevitable) difference in “selective” sampling of core as opposed to bulk MSCL measurements is evident: for a given porosity value, discrete measurements have higher V_p values than MSCL measurements. On the high end of the range in velocity for a given porosity, these differences can be interpreted as the added effect of pore characteristics, such as pore shape and connectivity, and textural properties of the coral and microbialite units. The differences on the low end of the range in velocity for a given porosity may originate from lack of burial compaction and/or pronounced diagenesis.

Magnetic susceptibility

MSCL magnetic susceptibility data collected at this transect are difficult to interpret as a result of gaps in the data due to limited core recovery. However, it is clear that the majority of data falls between -5×10^{-5} and 5×10^{-5} SI across all the holes with occasional clear magnetic susceptibility highs defined by smooth curves.

Electrical resistivity

The electrical conductivity of rock depends linearly on the electrical conductivity of the saturating fluid. In the presence of clays, an additional surface conductivity may be added to the previous volume conductivity. The volume conductivity of the rock is sensitive to the microgeometrical properties of the rock, such as porosity and tortuosity. Reliable resistivity measurements were difficult to obtain using the MSCL because of the presence of loose sediments or partially saturated rocks. When resistivity

was measured on unconsolidated or sandy sediments, low resistivity values were found (e.g., Hole M0037A, 1–2 m CSF, where resistivity is between 1 and 2 Ωm). Relatively higher resistivities were found when measuring more consolidated sediments (e.g., Hole M0034A, 12–14 m CSF, where resistivity is between 10 and 30 Ωm [coral framework and microbialite]). A more detailed study of electrical properties of the sediments would require measurements with fully saturated discrete samples.

Color reflectance

The values of color reflectance spectrophotometry were calculated for each of the boreholes as discrete measurements. The main parameters measured are total reflectance (L^*) and the color indexes a^* (green to red, green being negative and red positive) and b^* (blue to yellow, blue being negative and yellow positive). The ratio a^*/b^* was also calculated for all boreholes, as it can be used as a better proxy to identify changes in sediment characteristics than the independent values of a^* and b^* .

Measurements were taken in the most uniform color zones in a unit. This is shown by the data in the sense that massive corals sampled in several points present a consistent pattern of color. In these situations, the data obtained show a main value with a small deviation for the three parameters (L^* , a^* , b^*). In the locations where *Tubipora* sp. was found, a strong signal in the red spectrum (a^*) was found. In most of the boreholes, slightly higher values of reflectance are present just below the seafloor where modern reef sediment was recovered.

Along the HYD-01C transect, Holes M0031A, M0032A, and M0033A are located in similar water depths and can be correlated. No significant trends were found in these cores, but the reflectance for all of these boreholes shows similar values. This is also true for Holes M0035A and M0036A. Discrete measurements of reflectance values for all boreholes along the HYD-01C transect are represented in Figure F19. Boreholes are represented in landward to seaward order. All cores are presented in core depth below seafloor in meters.

Downhole measurements

Downhole geophysical logs provide continuous information on physical, chemical, textural, and structural properties of geological formations penetrated by a borehole. In intervals of low or disturbed core recovery, downhole geophysical logs provide the only way to characterize the borehole section. This is especially true when recovery is poor and when comparable measurements or observations cannot be obtained from

core, as downhole geophysical logging allows precise depth positioning of core pieces by visual (borehole images) or petrophysical correlation.

The slimline suite deployed at transect HYD-01C comprised the following tools:

- The Spectral Natural Gamma Probe (ASGR) allows identification of the individual elements that emit gamma rays (potassium, uranium, and thorium).
- The Induction Resistivity Probe (DIL 45) provides measurements of electrical conductivity. The output of the tool comprises two logs: induction electrical conductivity of medium investigation depth (ILM; 0.57 m) and induction electrical conductivity of greater investigation depth (ILD; 0.83 m). Measured conductivity is finally converted into electrical resistivity.
- The Full Waveform Sonic Probe (SONIC; 2PSA-1000) measures compressional wave velocities of the formation. In addition, analysis of surface waves in the borehole (i.e., Stoneley waves) can be indicative of formation permeability.
- The Magnetic Susceptibility Probe (EM51) provides measurements of magnetic susceptibility and electrical conductivity. The output of the tool comprises two logs: magnetic susceptibility (MSUS) and electrical conductivity (IL).

Wireline logging operations on the HYD-01C transect provided two sets of comparable through-pipe gamma ray data. Very few open-hole data were acquired in Hole M0036A because of the hole instability. However, it is possible to discern three major logging units at these two sites solely considering the gamma ray data collected through American Petroleum Institute (API) pipe (Fig. F20):

1. The uppermost unit has elevated values of natural radioactivity and is associated with coralgall boundstone.
2. The middle unit is characterized by low values of natural radioactivity and is associated with unconsolidated material (lime sand and pebbles) in Hole M0031A and a coralgall-microbialite boundstone in Hole M0036A.
3. The basal unit has a trend of increasing natural radioactivity to the bottom of the hole. This manifests as unconsolidated material in Hole M0031A, whereas in Hole M0036A a dark-colored, bioeroded boundstone followed by a packstone comprising benthic foraminifers (no corals) is observed. The base of Hole M0036A comprises unconsolidated coarse lime sand and pebbles.

Both total gamma ray (TGR) curves obtained at Holes M0031A and M0036A show a similar trend; therefore, it could be expected that similar formations might be observed. However, there are some significant differences (see Figure F20). It is not certain

whether the large amount of unconsolidated material cored at Hole M0031A is truly representative of the in situ formation or whether the differences between the two holes, which are only ~800 m apart (Hole M0031A at ~90 m water depth and Hole M0036A at ~103 m water depth), are related to low recovery and core quality.

HYD-02A transect: Sites M0040A–M0048A

The southern Hydrographer's Passage transect, HYD-02A, includes (landward to seaward) Holes M0042A, M0048A, M0047A, M0043A, M0045A, M0046A, M0044A, M0040A, and M0041A at depths between 50.8 and 126.1 mbsl. Closely spaced (i.e., <5 m apart) Holes M0045A and M0046A can be seen as a composite hole in the 110 mbsl reef target and Holes M0040A and M0041A form another in the 120 mbsl reef target. Figure F21 summarizes the major lithologic types and their distribution and recovery on the HYD-02A transect.

Sedimentology and biological assemblages

No common pattern appears to link the lithologic successions in the holes along the HYD-02A transect, as is the case along the HYD-01C transect. The following highlights describe shared features observed in the eight holes along the HYD-02A transect rather than exceptions:

- In several holes, the upper sedimentary interval consists of unconsolidated to lithified modern or subrecent seafloor sediment, which is coarser grained in the shallower holes (M0042A and M0044A) and finer grained in the deeper holes (M0040A and M0041A).
- Boundstone lithologies occur below the modern sediments in every one of the eight holes along the transect. Their thickness averages 9–10 m in the deepest (M0040A and M0041A) and shallowest (M0042A) holes and increases to 25 m in the two holes at intermediate depths (Holes M0047A and M0043A).
- In every hole that penetrated below the boundstone, there is an interval of unconsolidated material, usually unconsolidated lime sand, in which *Halimeda* is one of the main components. Recovered thicknesses of this interval ranges from 5 to 10 m.
- The two holes (M0042A and M0043A) that penetrated below the unconsolidated interval encountered a packstone/grainstone interval <1 m thick, which overlies unconsolidated sand in Hole M0043A, and alternating intervals of lithified grainstone to rudstone and unconsolidated sands in Hole M0042A. The lithified inter-

vals in the latter hole contain obvious evidence of subaerial exposure, including calcrete and possible root remains.

The boundstone lithologies contain variable proportions of coral, coralline algae, and microbialite that define several coralgal, coralgal-microbialite, and microbialite boundstones that are also observed in the other GBR transects. The major corals in the boundstones are submassive to massive *Porites*, *Montipora*, branching *Pocilloporidae*, branching *Acropora*, massive *Isopora*, and submassive to massive *Faviidae*.

The common patterns of boundstone distribution spanning most of the holes are

- Coralgal boundstones from 4 to 24 m thick are the uppermost or the only type of boundstone in six of the eight holes (excluding Holes M0040A and M0044A).
- Microbialite-rich boundstones (coralgal-microbialite or microbialite boundstones) lie beneath the coralgal boundstone or are the only boundstone lithology.
- Microbialite boundstone from 4 to 7 m thick occurs only in the two deepest holes (M0040A and M0041A).
- No simple relationship exists between the presence/absence of coralgal and coralgal-microbialite boundstones and the geographic location and/or water depth of holes along the HYD-02A transect.

Physical properties

Recovery for the HYD-02A transect sites averaged ~21%. However, recovery in Holes M0040A and M0041A reached ~50%. Cores were partially saturated and often disturbed, fractured, or contaminated, which affects the quality of physical property data that can be collected. Borehole depths are as follows:

Hole M0040A = 126.07 mbsl, 21.50 m DSF-A.

Hole M0041A = 126.58 mbsl, 22.10 m DSF-A.

Hole M0042A = 50.78 mbsl, 46.40 m DSF-A.

Hole M0043A = 102.93 mbsl, 35 m DSF-A.

Hole M0044A = 105.25 mbsl, 11.00 m DSF-A.

Hole M0045A = 105.25 mbsl, 14.60 m DSF-A.

Hole M0046A = 117.49 mbsl, 20.40 m DSF-A.

Hole M0047A = 99.12 mbsl, 33.20 m DSF-A.

Hole M0048A = 104.57 mbsl, 7.10 m DSF-A.

Plugs and samples taken for discrete *P*-wave and moisture and density (MAD) measurements were obtained from both consolidated and unconsolidated core material.

Density and porosity

Bulk density was measured for the HYD-02A transect using the gamma ray attenuation (GRA) densitometer on the MSCL, providing an estimate of bulk density from whole cores. Discrete MAD measurements were also taken with a pentapycnometer on plugs and/or rock fragments, providing grain density, bulk density (in the case of plug samples), and porosity data. As in the previous transect (HYD-01C), a classical linear correlation was observed between the porosity (ϕ) and the bulk density (ρ) of the discrete samples measured in all boreholes along the HYD-02A transect (Fig. F22). This correlation demonstrates that the average grain density along the HYD-02A transect is 2.77 g/cm³. Grain density varies between 2.7 and 2.85 g/cm³ and may correspond to a value between the grain density of calcite (2.71 g/cm³) and aragonite (2.93 g/cm³). Porosity values for all boreholes in this transect are shown in Figure F23. Similar trends in porosity can be picked out in Holes M0047A and M0043A with a zig-zag step decrease in porosity at 0–12 m CSF-A followed by an increase at ~15 m CSF-A and a gradual decrease to ~25 m CSF-A. Holes M0040A and M0041A have almost identical trends in porosity with ~30% porosity (~0–10 m CSF) increasing to ~50% to the bottom of the drilled holes.

P-wave velocity

A crossplot of velocity versus porosity (both from discrete samples) for all sites shows primarily an inverse relationship (Fig. F24) between acoustic velocity (V_p) and porosity. Whole-core MSCL data (across ~6.6 cm) range from 1508.59 to 1895.75 m/s. As expected, because of the targeted nature of taking discrete samples, much lower V_p values were recorded by the MSCL offshore for coral and microbialite units compared to discrete measurements on core plugs measured during the OSP.

Magnetic susceptibility

Offshore MSCL magnetic susceptibility data are very difficult to interpret for this transect because of limited core recovery in all holes along the transect. Values are generally similar across the holes, with the majority of readings in the -1×10^{-5} to 1×10^{-5} SI range, delineated by short intervals of magnetic susceptibility highs.

Electrical resistivity

Over the entire transect, resistivity is very variable, with the lowest values (0.56 Ωm) measured in Hole M0040A and the highest values (44.84 Ωm) recorded in Hole M0044A. Because of the relatively poor core quality and undersaturated cores, data should be treated with caution.

Color reflectance

In the HYD-02C transect, Holes M0048A, M0047A, M0043A, M0044A, and M0046A are located in similar water depths and can be correlated (with <5 m between the drilled holes). Holes M0047A and M0043A exhibit similar trends, but Hole M0047A presented less scatter in the values of reflectance per section, probably because of the presence of massive corals. Hole M0046A shows a trend in data points similar to the shallower distributed holes; however, there is a smoother distribution of the reflectance measurements. Holes M0048A and M0044A have similar values. However, because of the lack of measurements with depth in Hole M0048A no trend can be compared. Recovery in Hole M0045A was so low that color reflectance was not measured.

Holes M0040A and M0041A are located very close to each other at the same water depth. Both boreholes exhibit less scatter in color reflectance measurements than other boreholes in this transect. Data from these boreholes show a consistent pattern of L^* values of ~50% in the top 2.5 m of the hole, a slight increase at 6–8 m CSF, and a decrease in reflectance after again reaching ~50% at 21 m CSF-A. Color reflectance measurements for all the boreholes in the HYD-02C transect are represented in Figure [F25](#); boreholes have been plotted from landward to seaward (left to right) at the same depth scale. For boreholes found at similar depths, similar trends are present in the color reflectance data, which suggests a possible correlation between them.

Downhole measurements

Wireline logging operations were performed at one API hole (M0042A) along the HYD-02A transect. The priority imaging tools (acoustic borehole image [ABI40] and optical borehole image [OBI40]) were also run to see if quality image data could be obtained in an API hole. However, the standard maximum hole diameter for successful image data acquisition is 15 cm, and API holes tend to have a minimum diameter ~20 cm. Because of this difference, images were not successfully collected.

The slimline suite deployed at transect HYD-02A comprised the following tools:

- The Optical Borehole Televier (OBI40) produces a millimeter-scale, high-resolution image of the borehole wall, similar to a subsurface endoscope.
- The Acoustic Borehole Televier (ABI40) produces millimeter-scale, high-resolution images of the borehole surface using acoustic pulse and echo techniques.
- The Spectral Natural Gamma Probe (ASGR) allows identification of the individual elements that emit gamma rays (potassium, uranium, and thorium).
- The Induction Resistivity Probe (DIL45) provides measurements of electrical conductivity. The output of the tool comprises two logs: ILM (0.57 m) and ILD (0.83 m). Measured conductivity is finally converted into electrical resistivity.
- The Full Waveform Sonic Probe (SONIC; 2PSA-1000) measures compressional wave velocities of the formation. In addition, analysis of surface waves in the borehole (i.e., Stoneley waves) can be indicative of formation permeability.
- The Magnetic Susceptibility Probe (EM51) provides measurements of magnetic susceptibility and electrical conductivity. The output of the tool comprises two logs: MSUS and IL.
- The Caliper Probe (CAL; 2PCA-100) is a three-arm (mechanical) caliper tool that measures the borehole diameter.

Four main logging units were identified from the downhole data from Hole M0042A:

1. The uppermost unit is characterized by low TGR counts (through-pipe and open hole), high conductivity, and very low magnetic susceptibility. Borehole diameter is extremely large in Unit I (>40 cm in places), which may be a consequence of the API bottom-hole assembly (BHA) moving and eroding the top of the open hole. Four main lithologies are associated with the uppermost unit: lime sand and algal bindstone, coralgal boundstone, coralgal-microbialite boundstone, and unconsolidated sediment (lime granules and pebbles).
2. The second unit is associated with a sequence of grainstone to unconsolidated sediment (lime granules and pebbles) to grainstone with rhodoliths downsection. These lithological variations are most mirrored by the conductivity data, which exhibit some minor fluctuations downhole. TGR has intermediate values, and conductivity does not vary. Magnetic susceptibility is extremely low and constant, and the borehole diameter is in gauge.
3. The third unit is characterized by increasing values of TGR downhole and relatively high conductivity and stable borehole diameter figures. Lithologies associated with this logging unit are (from upper to lower downsection): grainstone

with rhodoliths, unconsolidated sediment (lime granules and pebbles), and gray rudstone and rudstone with brown staining.

4. The fourth unit represents a zone of reduced TGR counts. A decline in conductivity is present at the very top of the fourth unit, and then values gradually increase to the base of the hole. Magnetic susceptibility remains very low and only fluctuates slightly, and the caliper registers the hole to be in gauge. Only one lithology is associated with this logging unit: rudstone with brown staining.

RIB-02C transect: Sites M0049A–M0051A

The RIB-02C transect includes (landward to seaward) Holes M0051A, M0050A, M0049A, and M0049B at depths between 78.1 and 97.6 mbsl. Holes M0050A, M0049A, and M0049B are closely spaced (i.e., <5 m apart) and form a composite hole in the 100 mbsl reef target. Figure F26 summarizes the major lithologic types, lithology, and recovery for all holes in the RIB-02C transect.

Sedimentology and biological assemblages

Only a very rough summary of the lithofacies distribution pattern can be proposed for the RIB-02C transect because of the overall poor recovery in Holes M0049A, M0049B, M0050A, and M0051A. A limited lithological succession can be established only in Holes M0049A, M0049B, and M0050A, in which drilling penetrated below modern and subrecent seafloor. In Hole M0050A, the recovered material likely corresponds to subrecent seafloor sediments mixed with fossil materials. The lithological succession observed is as follows:

- At the top of both holes, the upper sedimentary interval comprises brown-stained fragments of coralgall boundstone in lime sand rich in *Halimeda*, corresponding to lithified and unconsolidated modern or subrecent seafloor sediment.
- Coralgall-microbialite boundstone facies occur below the modern sediments in Holes M0049A, M0049B, and M0050A. The recovered thickness varies from 8 to 16 m, but no underlying lithologic information has been obtained.

Physical properties

Recovery for the RIB-02A transect sites averaged ~16%. However, recovery in Holes M0049A and M0049B reached ~20%. Cores were partially saturated and often disturbed, fractured, or contaminated, which affects the quality of physical property data that can be collected. Borehole depths for the transect are as follows:

Hole M0049A = 97.63 mbsl, 3.50 m DSF-A.

Hole M0049B = 97.63 mbsl, 15.6 m DSF-A.

Hole M0050A = 97.63 mbsl, 10.5 m DSF-A.

Hole M0051A = 79.63 mbsl, 2.50 m DSF-A.

Plugs and samples taken for discrete *P*-wave and MAD measurements were obtained from both consolidated and unconsolidated material.

Density and porosity

Bulk density was measured for RIB-02A transect samples using the GRA densitometer on the MSCL, providing an estimate of bulk density from whole cores. Discrete MAD measurements were also taken with a pentapycnometer on plugs and/or on rock fragments, providing grain density, bulk density (in the case of plug samples), and porosity data. Data present a classical linear correlation between the porosity (ϕ) and the bulk density (ρ) of the discrete samples measured in all boreholes along the RIB-02A transect (Fig. F27). The average grain density along the RIB-02A transect is 2.78 g/cm³. Grain density varies between 2.75 and 2.79 g/cm³ and may correspond to a value between the grain density of calcite (2.71 g/cm³) and aragonite (2.93 g/cm³). Porosity values for measured boreholes in this transect are shown in Figure F28. Porosity ranges from 17% to 45%; however, the majority of porosity measurements lie around 30%.

P-wave velocity

Only two core plugs were collected from this transect, both from Hole M0049B. A crossplot of velocity versus porosity (both from discrete samples) for all sites shows primarily a negative? inverse relationship (Fig. F29) between acoustic velocity (V_p) and porosity. Whole-core MSCL data (over ~6.5 cm) range from 1504.7 to 1845.36 m/s. As expected, because of the targeted nature of taking discrete samples, much lower V_p values were recorded by the MSCL (offshore) for coral and microbialite units compared to discrete measurements taken on core plugs during the OSP.

Magnetic susceptibility

Magnetic susceptibility (MSCL offshore) data are difficult to interpret for this transect because of low core recovery in all holes along the transect. Very few values were obtained on whole cores, but data range from -0.64×10^{-5} SI (Hole M0049B) to high values of 31.6×10^{-5} SI (Hole M0050A). The most data were collected for Hole M0049B; however, no obvious trends are visible in the data.

Electrical resistivity

Over the entire transect, resistivity is very variable, with the lowest values (0.56 Ωm) measured in Hole M0040A and the highest values (44.84 Ωm) recorded in Hole M0044A. Because of the relatively poor core quality and undersaturated cores, data should be treated with caution.

Color reflectance

Along the RIB-02A transect, recovery for Hole M0051A was very small (<10 cm), and only one value of color reflectance spectrophotometry was taken. Holes M0049A, M0049B, and M0050A were located at the same water depth and are therefore comparable. Discrete measurements of reflectance values for all boreholes in this transect are represented in Fig. F30. No particular trends were observed in these three boreholes, but reflectance values were consistent in all cores where units were recovered at similar depths downhole.

NOG-01B transect: Sites M0052A–M0058A

The NOG-01B transect includes (landward to seaward) Holes M0057A, M0056A, M0055A, M0053A, M0052A–M0052C, M0054A and M0054B, and M0058A (fore reef slope) at depths between 42.3 and 167.1 mbsl. Closely spaced (i.e., <5 m apart) holes M0053A and M0052A–M0052C form a composite hole in the –100 mbsl reef target. Figure F31 summarizes the major lithologic types and their distribution and recovery for all holes along the NOG-01B transect.

Sedimentology and biological assemblages

Mud and muddy sand are found at the top of Holes M0052A–M0052C, M0053A, M0054A, M0054B, and M0055A. Coralgall and coralgall-microbial boundstones occur below the mud interval or from the top of the recovered succession in Holes M0056A and M0057A. The coralgall boundstone reaches thicknesses of 4–15 m. It is dominated by corals encrusted by coralline algae. The algal crusts in many cases contain vermetid gastropods and the encrusting foraminifer *Homotrema rubrum*. The coralgall-microbial boundstone can be as thick as 10–16 m. In this lithology, thick crusts of microbialite, up to several centimeters, are found in addition to corals and coralline algae. The main corals in these boundstones are a diverse assemblage of branching *Acropora*, *Seriatopora*, massive *Isopora*, *Porites*, *Montipora*, *Faviidae*, and *Tubipora*.

Unconsolidated sands as well as grainstone and rudstone lithologies are encountered below the two boundstone facies, except in Holes M0052A–M0052C, in which drilling did not penetrate below the boundstone. Grainstones/rudstones are composed of shell and skeleton fragments of corals, coralline algae, *Halimeda* segments, mollusks, and benthic foraminifers. The consolidated grainstones and rudstones are 4–13 m thick.

In Holes M0053A, M0054A, and M0054B, there is a lime sand interval below the grainstone/rudstone horizon. The downcore succession of unconsolidated and/or modern reef sediment, boundstones, grainstones/rudstones, and lime sand in these two holes is reminiscent of the pattern observed along the HYD-01C transect. No material underlying the grainstone was recovered in Hole M0055A.

In Holes M0056A and M0057A below the uppermost grainstone/rudstone interval, there is a long succession of limestone that includes boundstone, grainstone/rudstone, and packstone facies. Coralgal boundstones, 12 m thick, are the dominant lithologies in Hole M0057A, which includes a thin interval of packstones at the lowest interval of the boundstones. In Hole M0056A, coralgal-microbial boundstones, 8 m thick, overlie a 13 m thick succession of grainstones/packstones. Currently no pattern can be extracted in the succession of facies in these holes. The major corals observed in these deeper, older boundstones are encrusting submassive to massive *Montipora*, massive *Porites*, *Faviidae*, and occasionally *Galaxea* or *Agariciidae*.

In Holes M0055A, M0056A, and M0057A, at the top of the uppermost grainstone/rudstone interval and separating intervals within the underlying boundstone, packstone, and grainstone lithologies, calcrete features including brownish staining, undulated dissolution surfaces, and rhizoliths are observed. Clear dissolution of the constituents, especially aragonitic particles, leave moldic porosity, dissolution, and neomorphism of parts of coral skeletons. These features clearly indicate several phases of immersion and weathering, including paleosol formation, of the recovered deposits.

Hole M0058A, at 167 mbsl (the deepest Expedition 325 hole), was drilled to 41.4 m CSF-A and was mainly composed of unconsolidated green mud with two intercalated sections of fine to medium sand in addition to a few grainstone levels. The three mud sections in Hole M0058A are characterized by a lack of bedding. Scattered within the mud, small fragments of mollusk shells and small benthic foraminifers can be found. Planktonic foraminifers were observed only in Section 325-M0058A-1X-1, Core 7X,

Sections 8X-1 and 11X-3, and Core 12X. Fragments of bryozoan colonies and clypeasteroid burrowing echinoids rarely occur. Cores 325-M0058A-11X and 13X show clear signs of bioturbation. The upper sand/grainstone section is at least 2 m thick and consists of fine to medium sand with fragments of well-cemented grainstone and visible fragments of mollusks, bryozoa, coralline algae, echinoids, larger benthic foraminifers, and serpulids. The grainstone is composed of shells and fragments of calcareous algae, larger benthic foraminifers, and mollusks. The lower sand section, characterized by fine to medium sand, is ~7 m thick and is less distinct than the upper one.

Physical properties

Recovery at NOG-01B transect holes was much greater compared to the other transects visited during Expedition 325, with an average recovery of ~40%. Borehole depths reached at each hole in this transect are as follows:

Hole M0052A = 97.63 mbsl, 1.40 m DSF-A.

Hole M0052B = 97.63 mbsl, 6.90 m DSF-A.

Hole M0052C = 97.63 mbsl, 8.80 m DSF-A.

Hole M0053A = 97.87 mbsl, 37.30 m DSF-A.

Hole M0054A = 107.23 mbsl, 18.72 m DSF-A.

Hole M0054B = 107.23 mbsl, 33.20 m DSF-A.

Hole M0055A = 87.33 mbsl, 31.29 m DSF-A.

Hole M0056A = 81.22 mbsl, 41.29 m DSF-A.

Hole M0057A = 42.27 mbsl, 41.78 m DSF-A.

Hole M0058A = 167.14 mbsl, 41.40 m DSF-A.

Density and porosity

Bulk density was measured along the NOG-01B transect using two methods: (1) GRA density measured on the MSCL, providing an estimate of bulk density from whole cores, and (2) discrete MAD samples measured with a pentapycnometer using 20 mm diameter plugs drilled from the working half of core sections and/or rock fragments, providing grain density and porosity data. Because of the higher levels of recovery and core quality in this transect, we have more confidence in the MSCL data than for the previous transects. Bulk density values measured on whole cores range from 1 to 2.52 g/cm³. Bulk densities measured on discrete samples vary between 0.62 and 2.49 g/cm³. Plug porosity varies between 20% and 50% (Fig. F32). These values are to be expected in carbonates, as they are formations known for high heterogeneity. Some

grain density values are $<2.71 \text{ g/cm}^3$; this value is less than the calcite density (2.71 g/cm^3). These low values could be due to an anomalous measurement and/or the presence of clays in the plugs. Data across the transect demonstrate a linear relationship between porosity and bulk density: bulk density increases as porosity decreases (Fig. F33).

P-wave velocity

A crossplot of velocity versus porosity (both from discrete samples) for all sites shows primarily an inverse relationship (Fig. F34) between acoustic velocity (V_p) and porosity. However, there is a secondary group of data with extremely high porosity and relatively low V_p . This group of data relates to the lime mud units recovered in Hole M0058A, where the MSCL data acquired (over $\sim 6.5 \text{ cm}$ crosscore) range from 1502.31 to 1829.983 m/s. In Hole M0058A, because of the high recovery ($\sim 82\%$) and nature of the core, MSCL values and discrete measurements are in accord. For all other holes, much lower values have been recorded for coral and microbialite units compared to discrete measurements on core plugs.

Magnetic susceptibility

Magnetic susceptibility data obtained from the MSCL offshore for the NOG-01A transect can be used with more confidence than at the previous transects. Over this transect, magnetic susceptibility ranges from $-1.6353 \times 10^{-5} \text{ SI}$ (Hole M0053A) to $38.2049 \times 10^{-5} \text{ SI}$ (Hole M0056A). Small variations and trends are clearly visible in Hole M0054B between $\sim 15 \text{ m CSF-A}$ and 22 m CSF-A , and an almost continuous record is available for Hole M0058A.

Electrical resistivity

Obtaining reliable resistivity measurements on whole cores was much easier at this transect with improved recovery. Hole M0058A exhibits the most continuous and convincing record obtained with the MSCL during Expedition 325, with the transect representing the location from where the best resistivity measurements were taken on cores, mainly because of improved recovery and core quality. Over the entire transect, resistivity is very variable, with the lowest values ($0.33 \text{ } \Omega\text{m}$) measured in Hole M0058A and the highest values ($38.20 \text{ } \Omega\text{m}$) recorded in Hole M0056A. Trends in the data are much more visible at this transect, with some small fluctuations in Hole M0055A.

Color reflectance

Along the NOG-01B transect, Holes M0052A, M0052B, M0052C, and M0053A were located in similar water depths and can be correlated. The same applies for Holes M0054A and M0054B. Hole M0058A is located in the fore reef slope area and represents the longest continuous record obtained during Expedition 325. Holes M0052A and M0052B had low recovery, and reflectance measurements exhibited a similar range across both of them. Hole M0052C also had low recovery, and only two measurements of color reflectance were taken for this borehole. Recovery in Hole M0053A was higher (~33%), and the color reflectance values taken in the first few meters are consistent with other boreholes along the NOG-01B transect at the same depth (Holes M0052A, M0052B, and M0052C). Recovery for Hole M0054A was low but relates well to values obtained for Hole M0054B, the neighboring borehole. Discrete measurements of reflectance values for all boreholes along the NOG-01B transect are represented in Figure [F35](#); boreholes are plotted from landward to seaward (left to right) at the same depth scale. Reflectance shows consistent trends for holes located at the same water depth, indicating a possible correlation between them.

Downhole measurements

Wireline logging operations for the NOG-01B transect were performed in one HQ hole (M0054B). This provided the only opportunity to run both of the high-priority imaging tools in a “logging” hole. After completion of coring, ASGR logging through-pipe was performed, and then the HQ drill string was pulled and the coring bit exchanged for an open shoe casing to provide borehole stability in unstable sections and a smooth exit and entry of logging tools. In addition, seawater was pumped into the hole in order to try and displace the guar gum drilling mud and condition the hole for open-hole logging. With the exception of the ASGR log through-pipe, logging was obtained over a maximum interval of ~8.5 m. Borehole conditions were relatively hostile, and the lower portion of the hole began to infill. In order to record ultra high-resolution geophysical downhole logging data, the acquisition was done in the rooster box, which is heave compensated.

The slimline suite deployed at transect NOG-01B comprised the following tools:

- The Optical Borehole Televiewer (OBI40) produces a millimeter-scale, high-resolution image of the borehole wall, similar to a subsurface endoscope.
- The Acoustic Borehole Televiewer (ABI40) produces millimeter-scale, high-resolution images of the borehole surface using acoustic pulse and echo techniques.

- The hydrogeological probe (IDRONAUT) measures hydrogeological properties of borehole fluid only.
- The Spectral Natural Gamma Probe (ASGR) allows identification of the individual elements that emit gamma rays (potassium, uranium, and thorium).
- The Induction Resistivity Probe (DIL45) provides measurements of electrical conductivity. The output of the tool comprises two logs: ILM (0.57 m) and ILD (0.83 m). Measured conductivity is finally converted into electrical resistivity.
- The Full Waveform Sonic Probe (SONIC; 2PSA-1000) measures compressional wave velocities of the formation. In addition, analysis of surface waves in the borehole (i.e., Stoneley waves) can be indicative of formation permeability.
- The Magnetic Susceptibility Probe (EM51) provides measurements of magnetic susceptibility and electrical conductivity. The output of the tool comprises two logs: MSUS and IL.
- The Caliper Probe (CAL; 2PCA-100) is a three-arm (mechanical) caliper tool that measures the borehole diameter.

Two main logging units were identified in Hole M0054B (Fig. F36):

1. The first unit is characterized by relatively high TGR and generally low conductivity, although there is a gradual increase in conductivity toward the base of this unit. Magnetic susceptibility wavers around 0.7 mSI throughout, and the caliper shows the borehole to be in gauge. Acoustic images provide a virtual hardness visualization, and within Unit I the large majority of the formation appears “hard.” Lithologies identified within this logging unit include coralgall-microbialite boundstone, lime sand (with *Halimeda*), and a rudstone. Clearly the boundstones lend themselves to providing more stable borehole conditions.
2. The second unit is defined by lower TGR counts compared to the first unit and higher conductivity values. There is a minor decrease in magnetic susceptibility compared to the first unit, and caliper data indicate hole widening compared to the upper unit. Acoustic images clearly show a significant change in “lithology” at a major shallowly dipping boundary. Lithologies observed in this logging unit include a dark gray rudstone which passes downhole into a lime sand (with large benthic foraminifers).

Lithological changes and logging unit boundaries do not perfectly concur; however, coring and wireline operations use different methods to measure depth. Further work will therefore be needed to more fully integrate the log and core data.

Paleomagnetism

Materials acquired during Expedition 325 generally yielded a low concentration of ferromagnetic materials, coupled with a strong drilling overprint. Therefore, it was very difficult to obtain an integration and assessment of the paleomagnetic results from Expedition 325 during the OSP. Several peaks have been detected across some of the holes. However, the nature of these is uncertain, and any possible correlations need to be further investigated through additional rock magnetic studies. Environmental magnetic studies may help refine the climatic origin of these magnetic susceptibility signals and provide information on the volume, composition, and grain size of the magnetic component retained.

However, it was observed that the magnetic susceptibility for the NOG-01B and RIB-02A transects is significantly stronger than for the southern Hydrographer's Passage transects (HYD-01C and HYD-02A); the signal along the RIB-02A transect is stronger than that observed along the NOG-01B transect. One hypothesis is that this may be linked to proximity to a source of magnetic mineral input into the system, suggesting that such a source may exist in the northernmost/north of the Great Barrier Reef.

The majority of results are derived from Holes M0040A, M0041A, and M0058A, which provide longer records because of improved recovery rates. In addition, preliminary results obtained from the paleomagnetic study of a U-channel taken from Section 325-M0041A-12R-1 (HYD-02A transect) are also discussed.

The "noisy" natural remanent magnetization (NRM) demagnetization paths are attributed to the relatively low intensity of magnetizations (1.08×10^{-9} to 2.19×10^{-7} A/m with a mean of 2.02×10^{-8} A/m). Only a few samples are characterized by high NRMs, and these are associated with layers of high values of magnetic susceptibility. Consistency of the NRM inclinations of the discrete cubes measured can also be correlated to the intensity of magnetization results.

The demagnetization method used is not able to remove the magnetization for all core sections. Other methods, such as thermal demagnetization experiments, could be used to remove the overprinting that may be related to the presence of high-coercivity magnetic minerals such as hematite and goethite, and thereby reduce the NRM intensity. However, overprinting cannot be erased with standard alternating-field (AF) demagnetization, and there are still uncertainties regarding how the secondary overprint has been acquired and why some samples do not demagnetize at all whereas others have the potential for demagnetization. The component of any drill-

ing-related overprint that may remain will have a negative effect on both the inclination and declination results. However, samples for which the data analysis suggests no overprinting, or for which much of the drilling overprint has been removed, can be used to conduct further studies, such as paleointensity experiments.

The generally positive and high inclination values obtained for Expedition 325 samples are not what is expected for the low paleolatitude of the sampling sites (latitudes between 17° and 19°S) with the corresponding geomagnetic axial dipole (GAD) values of ~31° to -38°S. One interpretation of the results is that a significant portion of the drilling overprint remains on the majority of the samples studied. Alternatively, there may be a pervasive present-field overprint that was not possible to remove with AF demagnetization experiments.

Geochemistry

Measurements made during the offshore phase of the expedition showed that pH, alkalinity, and ammonium concentrations did not indicate any apparent variation between transects (Tables T3, T4, T5, and T6). The pH values varied from 7.34 to 7.96, which is slightly lower than standard seawater values. Alkalinity ranged from 2.3 to 8.1 mM with an average of 4.1 mM. Ammonium concentrations varied from 0 to 2.2 mM with a mean of 0.3 mM.

Inorganic carbon and inductively coupled plasma–optical emission spectrometry (ICP-OES) measurements conducted during the OSP showed that concentrations of chloride, bromide, sulfate, and most of the characterized major and trace elements vary within the normal range for marine sediments and did not vary significantly between sites and transects (Tables T3, T4, T5, and T6).

Chronology

During the offshore phase of Expedition 325, 68 samples were subsampled from core catcher materials near the base, middle, and top of each hole for preliminary chronology measurements (20 for U-Th and 48 for radiocarbon). These measurements provided approximate age information for each hole before the OSP, thereby aiding the development of targeted sample requests and sampling strategies. U-Th measurements were performed by MC-ICP-MS at the University of Oxford (United Kingdom), and radiocarbon measurements were made by AMS at the Australian National University following sample preparation at the University of Tokyo (Japan). To ensure rapid

sample throughput and presentation of data before the OSP, no sample screening for diagenesis or detrital contamination was performed for either U-Th or radiocarbon measurements. Therefore, age interpretations may be inaccurate and will need to be refined by further measurements after the OSP. Of the 33 holes drilled during Expedition 325, 26 had at least one preliminary dating measurement and 18 had at least three measurements. Of the holes that had more than one preliminary dating measurement, the age interpretations in all but one (Hole M0037A) were in stratigraphic order, adding confidence to the age interpretations and the notion that core catcher material is often broadly representative of in situ stratigraphy.

A total of 60 age interpretations were from 0–30 ka, with eight older ages interpreted from the preliminary data (Fig. F37). The 60 ages from 0 to 30 ka are from core catchers that were drilled from between 51 and 130 mbsl. Preliminary age interpretations therefore demonstrate that Expedition 325 has successfully recovered a complete sequence of material from the LGM interval, through the first half of the last deglaciation up to 10 ka. Therefore, the material recovered will enable investigation of the magnitude and nature of sea level change around the LGM, as well as the rise of sea level out of the glacial period. The rise of sea level during the early stages of deglaciation will also be refined with further chronological and paleoenvironmental analysis. Thus Expedition 325 has recovered material from key periods of interest for sea level change and environmental reconstruction, including MWP1A (and MWP1B), 19ka-MWP, the YD, the Bølling-Allerød, and Heinrich Events 1 and 2. The distribution of ages of the corals recovered during Expedition 325 also fills a gap in the coral record from 14.7 to 16.8 ka (Fig. F37). Paired U-Th:radiocarbon measurements from corals within this gap will be crucial in providing data to refine the radiocarbon calibration, thereby enabling investigation into the carbon cycle during this period of environmental change.

Preliminary scientific assessment

During the Expedition 325 OSP, emphasis was placed on visual description, measurement of physical properties, and sampling of the cores guided by the preliminary chronology provided by the core catcher samples that were dated by U-Th and ^{14}C by AMS prior to the OSP. Thus, the Expedition Reports section of the volume, scheduled to be published in ~July 2011, will contain a descriptive framework for subsequent postcruise research.

The primary objectives of Expedition 325 require the use of specialized geochemical techniques, paleomagnetic analyses, and detailed investigation of lithological and biological assemblages. These types of analyses were not conducted during the OSP but will be conducted over the coming months at the institutions of the expedition scientists as part of their postcruise research.

Fulfillment of the Expedition 325 scientific objectives is as follows:

1. *Establish the course of postglacial sea level change in the Great Barrier Reef (i.e., define the exact shape of the deglaciation curve for the period 20–10 ka).*

During the offshore phase, cores were recovered from a succession of fossil reef features from 42 to 127 mbsl. Therefore, most if not all of the postglacial sequence from the LGM to the present day was recovered. Furthermore, the preliminary chronology provided by the core catcher samples confirm that the recovered cores span this period. During the OSP, high-quality coral samples, consistent with shallow, high-energy settings, were taken for dating and sea level change investigations, the results of which are expected to fulfill the first objective.

2. *Define sea-surface temperature variations for the region over the period 20–10 ka.*

During the offshore phase, massive coral colonies suitable for paleoclimate studies and spanning the LGM and postglacial sequence were recovered in the cores. During the OSP, >200 massive coral colonies, including 17 *Porites*, were slab-sampled for paleoclimate studies, the results of which are expected to fulfil the second objective.

3. *Analyze the impact of sea level changes on reef growth and geometry.*

During the offshore phase, cores were recovered from holes in various water depths and situated on four transects in three different geographic areas along the GBR. Therefore, results of analyses of samples taken during the OSP will be interpreted in a broad temporal and spatial context, which will allow better understanding of the development of the GRB in response to environmental changes.

Additional scientific outcomes from Expedition 325

Preliminary dating information and initial observations of the cores at the OSP indicate that several additional scientific outcomes will be achieved:

1. New sea level and paleoclimate information from recovered corals that likely span the LGM (MIS2), pre-LGM (MIS3), and several earlier Pleistocene periods.

This will also provide new information about the evolution of the GBR during these periods.

2. A 33.3 m record of near continuous sedimentation was recovered in Hole M0058A from the fore reef slope. This will provide a high-resolution record to complement the sea level and paleoclimate records derived from the reef cores collecting on the shelf edge.

Offshore operations

Expedition 325 carried two types of coring tools: an extended nose corer (EXN; equivalent to the extended core barrel [XCB]; core type X) and a standard rotary corer (ALN; equivalent to the rotary core barrel [RCB]; core type R). See Table **T1** for a summary of operations.

Mobilization of the *Greatship Maya*

Mobilization of the drilling platform *Greatship Maya* took place in two stages; the first stage occurred in Singapore (Japan) on 4–13 January 2010 and the second stage took place in Townsville (Australia) on 10–11 February. ESO personnel were also present onboard the *Greatship Maya* during her geotechnical sea trials (18–29 January), assessing operational capability.

Shipping of ESO laboratories, office, database, and refrigerated containers from ESO partners around Europe began in late August 2009 when three containers were dispatched from Germany. This was followed in late November 2009 by four containers from the United Kingdom. Once all the containers had cleared customs, they were delivered to the Keppel Shipyard, Singapore, where they were held until stage one of mobilization in January 2010. Downhole logging tools were air-freighted directly to Townsville in January 2010, where they were held by Westlink Logistics Pty Ltd, who acted as shipping agents, until the second stage of mobilization in February 2010. The staggered shipping of containers and equipment was unusual for a mission-specific platform (MSP) expedition and arose because of a change of vessel by Bluestone Offshore Pte Ltd in late August 2009, which occurred after the containers had left Germany but prior to any other shipment.

The first stage of mobilization was significantly reduced because of delays in the shipyard's schedule of work. Containers were loaded onto the *Greatship Maya* toward the

end of the mobilization period, and power was provided to the containers to enable checking of all equipment. However, an unexpected dock move resulted in power being withdrawn from the two Expedition Drilling Information System (ExpeditionDIS) servers before ESO personnel could shut them down. This resulted in them failing completely. New servers accompanied ESO personnel to the mobilization in Townsville. The second stage of mobilization included installing a shipboard computer network and the new ExpeditionDIS servers, preparing equipment within the laboratories, providing power to the refrigerated container, and loading on and checking all the downhole logging equipment.

Transit to Townsville, Australia

The *Greatship Maya* departed Singapore at 1130 h on 30 January 2010, clearing customs in Singapore at the anchorage at 1330 h, and arrived alongside at Townsville at 1600 h on 9 February. One member of ESO personnel sailed on the transit, continuing to mobilize the containers and equipment where possible en route.

Port call in Townsville

The second stage of mobilization took place in Townsville on 10–11 February 2010. The remaining ESO personnel and members of the science party joined the *Greatship Maya* at 0815 h on 10 February. For this stage of mobilization, the complete ESO team was available. All laboratories and office spaces were networked with computers, the Drilling Information System (DIS) database system was set up, onboard equipment was laid out, and a satellite-based e-mail system was installed in the office containers and the client office inside the vessel's superstructure. New servers supporting the DIS were also installed, having been flown out with the ESO staff following complete failure of both original servers at Singapore during the first stage of mobilization.

At 1200 h on 11 February, the Co-Chief Scientists, Staff Scientist, Operations Superintendent, and ESO Outreach Manager attended a media launch at the Jupiters Hotel, Townsville. Following this, three television teams, local and regional print media, and a number of national radio reporters were invited to visit the *Greatship Maya* for a guided tour of the drilling platform and operational areas; the tour lasted ~1 h.

Transit to HYD-01C transect

The *Greatship Maya* departed for the first site at 2100 h on 11 February 2010 after spending 53 h in port and arrived at Site 5 at the HYD-01C transect, Hole M0030A, at 2315 h on 12 February. For the first 16 h, transit speed was a maximum of 5 kt because

of water coming up through the moonpool door and ingressing into the engine room via a faulty hatch. Once the hatch was repaired, transit speed was slowly increased to 12 kt from 1300 h onward. There was also a problem with the vessels air conditioning system for 24 h after departing from Townsville, which was rectified by the engineering crew onboard.

Site 5

Hole M0030A

The *Greatship Maya* arrived on station over Hole M0030A at 2315 h on 12 February 2010 and proceeded to begin tests on the dynamic positioning (DP) system. The initial spin test revealed an offset of 12 m, as the center of the vessel had not been correctly set to rotate around the drill string in the moonpool. Corrections were made and further spin tests conducted until 0200 h on 13 February. The HiPap seabed transponder was deployed, and at 0223 h the bridge gave the go-ahead to commence coring operations. By 0520 h the API pipe had been run to 5 m above the seabed, and the downpipe camera was deployed for a precoring seabed survey to check that the position was devoid of live coral. It was noted that there were very strong currents present pushing the end of the API pipe.

At 0610 h the camera became stuck on recovery when the cable wrapped around the camera frame. By 0625 h the camera was at the top of the string but again caught, so the cable was cut and the camera recovered. By 0700 h API pipe was being run to tag the seabed, and the first core was on deck at 0945 h. Core Runs 1 and 2 were conducted using the ALN barrel and Run 3 using the EXN. However, during the EXN run the shoe became blocked with loose carbonate sand, so the coring strategy was altered, pumping the ALN barrel back down with seawater and coring with seawater flushing. However, at 1345 h the overshot wire became slack and entangled when deployed to recover the ALN barrel and had to be cut. By 1700 h the wireline had been recovered but the overshot had been left inside the API pipe, as the shackle had broken. This required tripping of the string to recover the barrel and overshot, thereby terminating the hole at 6 m CSF-A with an average recovery of 4%. Recovery of the barrel and overshot was completed by 1730 h, and it was found that the chaser on the overshot had jammed in the first API pipe. Repairs were conducted on the overshot chaser and the wireline between 1730 h and 2005 h. It was decided to core the same location (Hole M0030B).

Hole M0030B

By 2015 h on 13 February 2010 API pipe was being run, and the seabed was tagged at 2215 h. The first ALN core was recovered at 2240 h. At 0030 h on 14 February the vessel has to reposition to compensate for the strong current, bringing the API pipe back to vertical. Two more ALN cores were run, but on recovering the third at 0100 h, the barrel became stuck and the wireline winch cable snapped. This again required tripping the API pipe, so Hole M0030B was terminated at 9 m CSF-A with an average recovery of 6.1%. Between 0200 and 0250 h, operations were suspended while repairs to the roughneck jaw grips were undertaken, but by 0520 h the BHA was up at the drill floor. The barrel was still stuck, but flushing with water finally released it at 0545 h, when it was discovered that the ALN bit was split. The decision was taken to transit slowly to Site 6, Hole M0031A, while repairs to the wireline winch were made. The HiPap beacon was recovered, and the vessel departed for Site 6 at 0550 h.

Site 6

Hole M0031A

The *Greatship Maya* arrived on station at Site 6 at 0730 h on 14 February 2010. While the vessel established DP mode, the overshot tools were tested. Running of the API pipe commenced at 0830 h. The downpipe camera was deployed for the precoring survey at 1030 h but was found not to be working, probably because of a faulty light. The camera was recovered, repaired, and deployed again, but it was found to be sticking ~1 m from the end of the BHA because of a bent lifter loop jamming in the narrowest section of the BHA. The problem was finally rectified and the precoring survey completed by 1755 h.

The first ALN core was recovered at 1825 h on 14 February, and coring operations continued until 0140 h on 16 February. However, problems occurred throughout the operation with strong currents requiring vessel repositioning five times (each move between 2 and 5 m); hole collapse requiring reaming and flushing after Run 5 and during deployment of the barrel in Run 6 (9–12 m CSF-A); the inner barrel becoming stuck inside the outer barrel because of compacted sediment after Runs 6, 11, and 12; 2 h downtime between 0530 h and 0730 h to fix the mud pump; the barrel becoming stuck after Run 9, requiring three attempts to free it and retermination of the overshot wire (1015 h and 1155 h) and reaming prior to core Run 10; and further reaming following a hole collapse after core Run 15 with high pressure indicating a blocked bit during core Run 16, which had very limited recovery.

The hole was terminated after 17 core runs at 43 m CSF-A with an average recovery of 13.2%, and preparations were made to begin downhole through-pipe gamma logging. The through-pipe gamma sonde was deployed at 0230 h and was recovered back onto deck at 0755 h. The API pipe was then tripped to 7 m above the seabed by 0855 h, and a postcoring downpipe camera survey was conducted. The camera was left inside the API pipe for the transit. The *Greatship Maya* departed Hole M0031A at 0945 h on 16 February to transit slowly (under DP) to Hole M0032A, 15 m away.

Hole M0032A

At 0952 h on 16 February 2010 the *Greatship Maya* was settled on station over Hole M0032A and a downpipe camera survey was conducted. At 1050 h an additional API pipe was added, and coring operations commenced at 1115 h using metal splits. The string overpressurized on the first core run, and the ALN had to be tripped to free it. There was also evidence of hole caving and overpressurizing on the second core run. However, coring then progressed steadily until 2355 h, when the bit became heavily blocked with sediment on Run 12 (liner tube for Runs 5–15). Runs 14–16 (metal splits from Run 16) took from 0155 to 0515 h on 17 February to complete. Between 0515 h and 0555 h there was a delay in operations because of refueling the hydraulic powerpacks. Coring then continued to the end of hole at 0925 h at 36.7 m CSF-A (average recovery = 16.3%).

The API pipe was tripped to 5 m above the seabed, and at 1015 h the downpipe camera was deployed for a seabed survey. Once this was completed and the camera recovered at 1110 h, the hydraulic powerpacks were shut down for maintenance until 1330 h, when the vessel departed for Site 6, Hole M0033A.

Hole M0033A

The vessel was on station at 1353 h on 17 February 2010 after an additional 2 m move in a northeast direction from the original location to avoid the presence of live coral. At 1445 h the ALN core barrel and additional API pipe were run, and the first core run commenced at 1510 h after a slight delay because of a Differential Global Positioning System (DGPS) drop-out. Coring operations continued until 0000 h, when refuelling of the compressors and powerpacks took place until 0025 h on 18 February. Coring then restarted until 0530 h, when the barrel became stuck on core Run 16. It was recovered after 30 min but had a broken latch lug on recovery. Core Run 17 was recovered at 0745 h after the water pressure spiked. The liner tube was found to be crushed and stuck inside the barrel, with an extruded lug halfway down the barrel, taking op-

erations to one fully functional core barrel while the liner is removed. Coring continued for another six runs before the hole was terminated at 1335 h at 32.8 m CSF-A with an average recovery of 40.9%.

API pipe was tripped to just above the seabed before the downpipe camera was deployed at 1435 h. However, the camera would not pass through the final 3–4 m of the BHA, and the wireline became twisted. The wireline was quickly untwisted from the top of the derrick, but the camera still could not pass through the BHA, so the camera survey was aborted at 1540 h without running a postcoring survey and recovered to deck by 1600 h. By 1725 h the remainder of the API pipe was tripped, and the vessel began a slow (1 kt) transit to Site 3 in order to allow time for repairs to the roughneck slips.

Site 3

Hole M0034A

The *Greatship Maya* was on station and settled on DP at 1825 h on 18 February 2010. Repairs to the roughneck slips continued while discussions about the best way to hang the HQ pipe were conducted. Between 1925 and 2100 h, the moonpool door was closed. This took longer than expected due to damage sustained during the initial transit out from Townsville. At 1900 h the API started being run to just above the seabed. A downpipe camera survey was conducted, and by 2305 h preparations to run the first core barrel were being made. The first ALN core was recovered at 0020 h on 19 February, and coring continued for another six core runs until 0515 h, when preparations began to change to HQ coring. Running of the HQ rods took from 0900 to 1047 h, when flushing of the hole lasted for 25 min.

The first HQ core (Run 8) was recovered at 1150 h, and HQ coring continued for another four runs until 1500 h, reaching a depth of 18.6 m CSF-A. The bit became blocked on Run 12, and freeing it took 25 min. Flushing then continued until 1525 h. However, currents had been increasing along with wind speed over the course of coring, and at 1525 h the HQ rods twisted off ~2 m below the drill deck. At 1530 h the vessel was moved to straighten the API pipe, and fishing for the end of the broken HQ pipe began using a casing recovery tap. The recovery tool broke off the rod at 1710 h and was manually recovered using a pup joint. At 1915 h an attempt was made to hammer the tap into the broken joint. At 2235 h an additional API was added, connecting to the joint above the moonpool door, and pulled back to the slips. Flushing and reaming continued in an attempt to lower the API pipe slightly in the hole, but

the hole was by this point caving and forcing the API pipe periodically upward. By 0235 h on 20 February the fishing operation could restart, as the top of the API was safely set in the slips at the drill floor. However, another API pipe needed to be added at 0310 h, as the pipe was sinking in a softer lithology.

The HQ pipe was tagged at 0345 h, and recovery began. This was completed at 0734 h, when preparations began to change back to API coring using the ALN core barrel. The hole was open-holed with the API back down to 18.6 m CSF-A. When the ALN barrel was initially deployed, mud pressure spiked and the barrel was recovered without advancing. Two washers were removed from the inner barrel bearing head to increase the shoe/bit air gap, and the barrel was redeployed, with the first core being recovered at 1005 h. Core Run 15 had poor recovery, so a washer was added to the inner barrel bearing head again to reduce the effect of flushing, but this caused the pressure to spike again, so the barrel was tripped and a new impregnated bit was put on. Between 1235 and 1310 h, operations halted because of repairs being made on the mud pumps. Four further attempts were then made to core, all of which resulted in no advance and overpressurizing of the drill string. An infill sample from an unknown depth was recovered on one occasion and was curated as Run 16.

At 1518 h the *Greatship Maya* lost DGPS corrections, and the vessel moved 23 m off station in a water depth of 56 m. GPS was restored at 1520 h and DPGS at 1524 h. Although the vessel was manually moved back onto station within 10 min, the API pipe was bent, requiring a full trip. Once the API pipe was on deck (1810 h), three pipes were found to have been bent and were now unusable. Checks were run with the ALN and BHA in the slips, using both liners and metal splits, and no over pressurizing was noted.

Discussions took place between the Master of the *Greatship Maya*, Chief Engineer, Bluestone Party Chief, ESO Operations Superintendent, European Geophysical Society Surveyor, Chief Mate, and Chief Electrical Engineer as to why the GPS and DGPS signal had been lost. The Master contacted shore-based GC Rieber personnel for advice and stated that no further drilling operations were to take place until the problem had been rectified, thereby terminating Hole M0034A at 23.1 m CSF-A with an average recovery of 29.1%. Another GPS drop-out occurred at 2000 h for 10 min. A passing vessel was contacted, and they had not suffered any loss of signal.

During the early morning of 21 February the *Greatship Maya* suffered three power failures because of the bow thrusters ramping up to 100% without warning and tripping

the generator because of overdemand. At 0945 h, it was decided that a secondary independent positioning system was required before further drilling could take place. This would hold the vessel on DP should a further GPS/DGPS signal drop-out occur. Permission was sought from GBRMPA to use the 3 m × 3 m seabed template with a HiPap beacon installed on it. The Environmental Management Plan (EMP) had previously only allowed a 1 m × 1 m template to be used, which was being pushed off location in the strong currents experienced at Hydrographer's Passage. Notice of permission granted was received from GBRMPA by 1005 h.

It was decided, however, that no coring operations could take place until the secondary power failure issue was rectified. Engine and DP data were downloaded and sent to GC Rieber, Singapore, who passed the information onto ConverTeam, who were responsible for the electrical and DP installation. By 2300 h the vessel crew had identified the problem, run a simulation to ascertain that this was a correct identification, and rectified the issue. At 2330 h the Master informed the drill floor operations team that he was satisfied that changes to the thruster settings had rectified the problem, and that the vessel could move to Site 11, Hole M0035A.

Site 11

Hole M0035A

The *Greatship Maya* arrived at Site 11 over Hole M0035A at 2345 h on 21 February 2010 and settled on DP. At 0045 h the moonpool door was opened, and running of the API pipe commenced at 0100 h on 22 February. Operations halted between 0200 and 0250 h to undertake repairs to the hydraulics on the roughneck. Once the API was just above the seabed, the seabed template was lowered to 20 mbsl to test the Hi-Pap transponder and recovered back to the moonpool. At 0355 h the API was lowered further and the downpipe camera deployed for a precoring survey. The camera was recovered by 0550 h. The API was then run to tag the seabed and pulled back 0.5–1 m, with the aim that the end of the pipe would rest inside the seabed template when deployed but be free to move where the template guided it. The template was lowered onto the seabed at 0635 h. However, because of the template settling into the sediment, the first attempt at ALN coring showed that the API pipe and ALN core barrel were now outside the template entry cone. At 0730 h the ALN barrel and API pipe were tripped, and at 1015 h the seabed template was recovered. The ALN bit was found to be smashed, and the API bit was cracked in three places. Both were repaired, and the API pipe was rerun starting at 1100 h. The API pipe was in position just above

the seabed by 1410 h, and the downpipe camera was deployed. However, at 1445 h the vessel again lost position with the camera still inside the API pipe. As the HiPap transponder was attached to the seabed template, which had not been deployed yet, the vessel started to drift.

At 1451 h the API pipe was raised by 2 m to avoid any obstacles on the seabed while the vessel regained station, and the camera was recovered. The GPS came back online at 1513 h. The Master of the *Greatship Maya* and the DPO Officer stated that they were happy with the DP model at 1555 h and were ready to restart operations, but the ESO Operations Superintendent required that a secondary positioning system was established, henceforth known as the seabed transponder. This was deployed over the side of the vessel prior to any operations beginning at any site from this point on to prevent any further positioning problems occurring during operations. At 2030 h the decision was made to abandon Hole M0035A and return to Townsville, where engineers for both the GPS and DP systems would be waiting. The remainder of the API pipe was tripped, and the drill floor secured for transit.

Port call at Townsville

The *Greatship Maya* departed HYD-01C transect Site 11 (Hole M0035A) at 2240 h on 22 February 2010 and arrived alongside in Townsville at 2050 h on 23 February. Engineers from Veripos (GPS) and ConverTeam (DP) boarded the vessel. Work to identify and rectify problems with both the DP and GPS systems continued overnight. The *Greatship Maya* departed Townsville at 1010 h on 24 February to begin sea trials of the DP and GPS systems. At 2350 h a supply boat arrived alongside the *Greatship Maya*. Additional core liner tubes and a new seabed frame for the HiPap transponder were taken onboard, and one Veripos surveyor and the ConverTeam engineer departed. One Veripos engineer remained onboard.

Transit to HYD-01C transect

The *Greatship Maya* departed for HYD-01C transect Site 11 at 0020 h on 25 February 2010 and arrived at Hole M0035A at 0100 h on 26 February, where she remained waiting on weather until 0405 h on 27 February.

Site 11

Hole M0035A

At 0330 h on 27 February 2010 the HiPap transponder was attached to the seabed frame in readiness for improved weather conditions. Permission was given to begin operations, and at 0430 h the vessel moved 10 m starboard of Site 11, Hole M0035A, under DP to deploy the seabed transponder. The vessel was back on station over Hole M0035A at 0530 h. The bridge confirmed that drilling operations could begin at 0605 h, and work began changing the API bit to a new stepped impregnated bit. Running API commenced at 0715 h, pausing at 0735 h while the seabed template was suspended in the moonpool before continuing until 0930 h. Between 0930 and 1010 h, a downpipe camera survey was conducted. Additional API pipe was then run, and ALN coring commenced at 1110 h.

At 1250 h the second core was recovered to deck. However, there were problems with the hole collapsing, and operations had to cease as power was lost to the drillers console. Coring operations restarted at 1600 h, with the power problem now restricted to the mud pump number 1. The roughneck control box was also found to be leaking hydraulic oil. At 1740 h the bit became blocked. Pumping and reaming was unable to free the bit, so at 1915 h the hammer sampler was deployed, freeing the bit at 2215 h.

At 2325 h the decision was made to switch to HQ coring. Preparations continued until 0205 h on 28 February, including fitting a collar to the API pipe above the seabed template suspended in the moonpool. The API pipe and seabed template were very unstable within the moonpool because of strong currents pushing on the API pipe, and the API pipe was not reacting against the hole. At 0335 h the decision was taken to return to API coring. Repairs were made to the winch cable at 0425 h, which had been damaged during preparations for HQ coring, with coring operations restarting at 0440 h. Between 0800 and 1025 h, operations were halted because of a problem with the mud pumps caused by air entering the suction at the valve in the moonpool. Between 1200 and 1235 h, and again between 1600 and 1620 h, operations halted as repairs were made to the compressor because of it overheating. At 1625 h the bit became blocked on Run 14 but was freed by pumping water.

The bit became blocked again, accompanied by high pressure at 0240 and 0415 h on 1 March. The ALN barrel was recovered on both occasions. Sand was found to be jamming the inner and outer barrel. The barrel was stripped down, fully cleaned, and re-assembled. Coring continued until 0740 h on 1 March, when coring of Hole M0035A

was terminated at 29.9 m CSF-A with an average recovery of 40.9%. The API pipe was tripped to 5 m above the seabed, and a downpipe camera survey was conducted, finishing at 0850 h. The camera was left inside the API pipe for the move to the next coring location. The seabed transponder was recovered and a fully charged beacon attached to the frame.

Hole M0036A

At 0940 h on 1 March 2010 the seabed transponder was redeployed, and the vessel maneuvered under DP to Site 11, Hole M0036A. Between 0940 and 1055 h, the vessel undertook a series of small moves (<5 m) to target the top of a coral high and position the API pipe over an area devoid of live coral using the downpipe camera system to image the seabed. By 1100 h the downpipe camera was recovered and API pipe was being run, tagging the seafloor at 1135 h. The first core (ALN) was recovered at 1150 h, and operations continued until 0600 h on 2 March, with a total of 22 runs reaching 34 m CSF-A and an average recovery of 26.2%. On the penultimate core run at 0445 h, the barrel became blocked with sand, requiring the hammer sampler to free it.

At 0600 h preparations for downhole logging began. Between 0855 and 1115 h, the through-pipe gamma sonde was deployed, logging an interval of 33.26 m wireline log matched depth below seafloor (WMSF). At 1115 h circulation and conditioning of the hole commenced prior to three API pipes being tripped, bringing the pipe to 10 m CSF-A. At 1255 h lowering of the seabed template began, with the template on the seabed at 1400 h. Progress was slow because of strong currents pushing the electrical umbilical around the underside of the template. At 1510, 1630, 1900, and 2050 h, respectively, the resistivity, sonic, open hole gamma, and magnetic susceptibility sondes were deployed downhole, logging the intervals 7.5–25.87, 7.45–16.50, 10.66, and 7.47 m WMSF, respectively. A gradual collapse of the hole during this period was noted, with each successive tool only being able to penetrate to shallower depths. At 2145 h the calliper tool was deployed downhole. However, communication problems with the tool meant that at 2330 h the second caliper was tried downhole. Again, communications problems prevented logging using this instrument, so logging operations were terminated at 2340 h on 2 March. Demobilization of the logging equipment continued until 0040 h on 3 March, when we began to raise the seabed template. At 0130 h two API pipes were tripped, and a downpipe camera survey was conducted. Tripping of the API pipe continued from 0220 h and was completed by 0400 h, when the vessel moved to recover the seabed transponder. The *Greatship Maya* then moved slowly to Site 9, Hole M0037A, while maintenance of the drill floor hydraulics was carried out.

Site 9

Hole M0037A

The seabed transponder was deployed at 0640 h on 3 March 2010, and by 0700 h the vessel was in position above Site 9, Hole M0037A. Running of API pipe commenced at 0745 h; however, repairs to a hydraulic hose on the elevator after a collision with the roughneck halted operations between 0820 and 0950 h. Running of the API restarted at 0950 h and by 1100 h the API was situated 10 m above the seabed and the downpipe camera was being deployed. The camera survey was completed by 1140 h, and preparations to core began. The first ALN core was recovered at 1330 h, and coring continued successfully until 0055 h on 4 March, when the hole was terminated at 21 m CSF-A with an average recovery of 35.8%.

The API pipe was tripped to 10 m above the seabed between 0055 h and 0230 h, when the vessel moved to recover the seabed transponder. At 0250 h the *Greatship Maya* began to move slowly, under DP, to Site 8, Hole M0038A.

Site 8

Hole M0038A

The seabed transponder was deployed at 0320 h on 4 March 2010 prior to moving onto station by 0340 h. However, a mud pump suction failure at 0330 h prevented operations commencing until 1400 h, when API pipe was run to just above the seabed by 1430 h. A downpipe camera survey was completed by 1510 h, and API pipe tagged the seabed at 1535 h. However, on recovery of the first ALN core at 1540 h, the bit was found to have been completely destroyed. The decision was taken to lift the drill string, move across 2 m, and begin a new hole to avoid coring any remnants of the ALN bit. As this area was within the field of view from the camera survey for Hole M0038A, no new survey was required prior to coring operations in Hole M0039A.

Hole M0039A

Hole M0039A tagged seabed at 1625 h on 4 March 2010, and the first ALN core was on deck at 1700 h. Coring continued until 2340 h, when the driller noted high mud pressure, suggesting the barrel was blocked. On recovery, the latch head assembly was found to be blocked with sediment. This happened on three consecutive deployments, resulting in there being no advance in the drilled depth. At 0300 h on 5 March the barrel advanced slowly on core Run 10, and coring continued until 1400 h (with

a break between 1130 and 1220 h for repairs to the latch head dog), when the hole was terminated at 28.4 m CSF-A with an average recovery of 36.6%. By 1420 h the API pipe was tripped to just above the seabed in order to run a downpipe camera survey. Tripping the API pipe then continued from 1455 to 1650 h, when the seabed transponder was recovered.

Transit to HYD-02A transect

The *Greatship Maya* transited to the next survey transect under guidance from the pilot. The vessel crossed Hydrographer's Passage in a southeastern direction and reached Site 10, Hole M0040A, by 1830 h on 5 March 2010.

Site 10

Hole M0040A

By 1925 h on 5 March 2010, the seabed transponder had been deployed and the *Greatship Maya* had settled on station over Hole M0040A. API pipe was run to just above the seabed by 2125 h, when the downpipe camera was deployed. The camera survey was completed by 2220 h, and API pipe continued to be run until the seabed was tagged at 2235 h. The first core was on deck at 2250 h, and coring continued until the end of Run 3, when repairs to the driller's shack electrics halted operations between 0030 and 0155 h on 6 March. Operations then restarted for another nine core runs until the hole was terminated at 0825 h at 21.5 m CSF-A with an average recovery of 54.6%.

Three API pipes were tripped to bring the drill string to ~4 m above the seabed. A downpipe camera survey was then conducted between 0850 and 0910 h prior to the vessel moving 10 m to starboard to the next hole.

Hole M0041A

The *Greatship Maya* was on station over hole M0041A by 0915 h on 6 March 2010, and a precoring downpipe camera survey was conducted. The camera was back on deck by 0925 h, and the API pipe tagged the seabed at 0955 h. Coring operations ran smoothly for 12 ALN runs before the hole was terminated at 1650 h at 22.1 m CSF-A with an average recovery of 45.5%.

The API pipe was tripped until it sat ~5 m above the seabed, and the downpipe camera was deployed. However, the camera became stuck in the BHA at 1720 h and could not

be recovered. At 1745 h the decision was taken to cut the camera cable and trip the API pipe, passing the camera cable through each pipe successively in order to retain the camera should it become free while the API pipe was being tripped. At 2110 h the camera became free in the pipe above the collars and was recovered. By 2130 h all API pipe was in the rack/slips and retermination of the camera cable had begun. The seabed transponder was recovered, and the vessel began to transit 6 km landward to Site 2, Hole M0042A, at 2220 h.

Site 2

Hole M0042A

The *Greatship Maya* arrived at Site 2 at 2330 h on 6 March 2010 and began to settle on DP. The seabed template was secured in the moonpool, repairs to the camera cable continued, and the API pipe was run to just above the seabed. At 0145 h on 7 March the downpipe camera was deployed. The first ALN core was recovered at 0330 h, and operations continued until 0500 h, when repairs to a latch head dog stopped coring for 55 min. After ALN Run 5 was recovered at 0715 h, it was decided that the API was spudded into the seabed firmly enough to switch to HQ coring. By 1020 h the seabed template was secured in the moonpool with steel wires, the API pipe was set in the elevators, and the HQ rods were ready to be run. The first HQ core (Run 6) was recovered at 1240 h. However, the API pipe was sinking in the hole (1.5 m), presumably because of soft sediments, and so hole stabilization using a thicker mud continued until 1330 h. During Run 7, the bit became blocked requiring flushing. However, the API started sinking again, now resting on the elevators, and swabbing the hole was believed to be causing further instability. The decision was taken to trip the HQ rods and return to API coring until a harder formation was encountered in which to set the API pipe.

At 1500 h a sample was recovered from the HQ BHA and curated as a wash sample. Between 1540 and 1700 h the API pipe was reconnected and the elevator removed. ALN coring restarted at 1710 h and continued until 0705 h on 8 March, when the hole was terminated at 46.4 m CSF-A with an average recovery of 23.6%.

Downhole logging was conducted following coring operations, and mobilization of the drill floor and logging equipment continued until 1010 h. Between 1010 h and 1150 h the through-pipe gamma log was run. On completion, the API pipe was tripped to 7 m CSF-A, and conditioning of the hole continued until 1340 h. The seabed template was then lowered onto the seabed, and the dual induction logging

sonde was deployed at 1410 h. Following this, the ABI, spectral gamma, magnetic susceptibility, sonic, OBI, and caliper sondes were deployed at 1530, 1710, 1845, 2000, 2125, and 2320 h, respectively. Some hole caving was noted, with the tools logging from 45.07, 43.98, 39.93, 38.49, 33.23, 38.84, and 38.58 m WMSF, respectively. By 0030 h on 9 March all downhole logging had been completed and demobilization of the equipment and securing of the drill floor for transit had begun. At 0130 h the seabed template was recovered, and by 0345 h all API pipe had been tripped. The seabed transponder was onboard and secured by 0400 h, and the vessel began the 6.5 km transit seaward to Site 12, Hole M0044A.

Over the course of coring and logging this hole, three separate remotely operated vehicle (ROV) dives were conducted, viewing the drill string, small entry hole, and the dispersion of drill cuttings.

Site 12

Hole M0043A

The seabed transponder was deployed at 0455 h on 9 March 2010, and by 0515 h the *Greatship Maya* was on station at Site 12 (Hole M0043A). The seabed template was adjusted in the moonpool, and at 0550 h the API was started to run to just above the seabed. A downpipe camera survey was conducted at 0740 h, and coring operations (ALN) started at 0815 h, continuing until 2350 h, when the hole was terminated at 35 m CSF-A with an average recovery of 17.3%. The API pipe was tripped to 7 m above the seabed, and a downhole camera survey was completed by 0115 h on 10 March. The camera remained inside the pipe for the vessel move (52 m) to Site 8, Hole M0044A. The seabed transponder was recovered at 0115 h, and the vessel moved slowly under DP to Site 8.

Site 8

Hole M0044A

The seabed transponder was deployed at 0140 h on 10 March 2010, and the vessel was on station over Hole M0044A by 0155 h. The downpipe camera survey was completed by 0225 h, and the barrel was prepared as API pipe was run to tag the seabed. The first core (ALN) was recovered at 0320 h. On recovering the second core at 0415 h, the ALN polycrystalline diamond drill bit (PCD) was found to be damaged and the stabilizer housing was deformed. The bit was changed for a short impregnated ALN bit, and cor-

ing continued. At 0800 h the vessel lost a forward thruster for 5 min without coring operations being affected. At 0905 h the seabed template was lowered in the moon-pool in an attempt to dampen drill string vibration. At 1120 h the ALN barrel became stuck in the BHA during core Run 9. Attempts were made to recover the barrel, but at 1310 h the wireline failed. In order to recover the barrel and overshot, the API pipe had to be tripped, terminating Hole M0044A at 11 m CSF-A with an average recovery of 15.2%. The ALN was recovered from the BHA at 1645 h. The barrel and BHA were checked and the overshot wire repaired.

The API pipe was run in to just above the seabed by 1850 h, and a downpipe camera survey was conducted. The vessel was then moved over ~2.5 m, under DP, to Hole M0045A.

Hole M0045A

The *Greatship Maya* was on station over M0045A in 4 min, with the downpipe camera still deployed. A precoring camera survey was conducted and the camera recovered to deck by 1910 h on 10 March 2010. The seabed was tagged at 1945 h, and coring commenced. However, after initially appearing to core, the drill string then dropped 3 m abruptly. It was believed that the drill string was skipping down the side of a pinnacle, and so the vessel was moved 2 m closer to Hole M0044A before trying another core run. The seabed was again tagged, and the drill string appeared to be compensating at 2115 h. However, the first and second ALN core runs again appeared to “skip” down the side of the pinnacle, with the drill string dropping quickly and with no apparent force. The last 70 cm of the third core run appeared to drill very hard material. However, while recovering the barrel, the drill string fell abruptly 8 m—it was thought that the string had reentered Hole M0044A. If this was so, the drill string should have stopped at the total depth (TD) for Hole M0044A at 11 m CSF-A, but it continued to freefall until 14.6 m CSF-A. As it was not clear whether or not the API string had actually penetrated the target coral pinnacle or was “skipping” down its side, the decision was taken to abandon Hole M0045A and move the vessel. Two API pipes were tripped by 0025 h on 11 March, and the *Greatship Maya* was moved under DP 3 m to the opposite side of Hole M0044A.

Hole M0046A

The *Greatship Maya* was on station above Hole M0046A by 0050 h on 11 March 2010. The first three ALN core runs all appeared to “skip” down a slope, free-falling to 10.8 m CSF-A. However, coring then continued, with seabed corals appearing in the liner

at ~10.8 m CSF-A in Run 4. While recovering Run 10 from a depth of 25.2 m CSF-A, there was a partial hole collapse, so the top 1 m of core from Run 11 represents infill. The hole was terminated after Run 13 at 1040 h at 31.20 m CSF-A with an average recovery of 8.9%. The API pipe was tripped back to joint 11 in preparation for transit to the next site, and the seabed transponder was recovered. The vessel began the move to Site 12, Hole M0047A, at 1145 h.

Core depths were taken from the first indication of the drill string tagging the seabed at the start of Run 1, as it is unknown whether or not the penetration was accurate from this point. It should therefore be noted that all depths may be 10.8 m shallower than recorded if the first presence of corals in the liner tubes at 10.8 m CSF-A represents the actual point of seabed penetration.

Site 12

Hole M0047A

The *Greatship Maya* came onto station over Hole M0047A at 1220 h on 11 March 2010. Retermination of the beacon transponder deployment wire delayed deployment until 1250 h. API pipe was run in to just above the seabed, and a downpipe camera survey was conducted. The camera was back on deck at 1335 h, and the API tagged the seabed at 1410 h. The first ALN core was recovered at 1430 h, and coring continued until 0030 h on 12 March, when the hole was terminated at 33.2 m CSF-A with an average recovery of 11.4%.

The API pipe was tripped to just above the seabed by 0055 h, and a downpipe camera survey was conducted. The seabed transponder was recovered by 0145 h, and the vessel departed for Site 12, Hole M0048A, under DP with the 11 API pipes deployed.

Hole M0048A

The *Greatship Maya* came onto station over Hole M0048A at 0220 h on 12 March 2010. The seabed transponder was deployed, and an additional API pipe was run to take the pipe to just above the seabed by 0305 h. A downpipe camera survey was completed by 0325 h, and the first ALN core was recovered by 0405 h. ALN coring continued until 0610 h, when the decision was made to halt operations at 7.1 m CSF-A after four runs because of winds in excess of 35 kt and heave >2.5 m, with an average recovery of 9.7%.

The API pipe was tripped by 0805 h, and the seabed template was secured by 0850 h. The seabed transponder was then recovered and secured on deck by 0910 h.

Waiting on weather and port call, Townsville

The *Greatship Maya* departed Site 12 (Hole M0048A) at 0910 h on 12 March 2010 to transit to sheltered waters within Hydrographer's Passage in order to conduct a ship to ship transfer of equipment, including a bumper sub, and drilling mud from the *PMG Pride*, which commenced at 1530 h. Because of the failure of previous HQ attempts using the seabed template suspended in the moonpool or water column as a guide for the HQ string and API "casing," a bumper sub was manufactured to facilitate further attempts at recovering HQ cores.

At 1645 h the *Greatship Maya* departed Hydrographer's Passage to transit northward using the inner passage because of deteriorating weather conditions offshore. At 1510 h on 13 March, the *Greatship Maya* dropped anchor at the Townsville Anchorage to wait on weather. Preparations continued to be made in advance of Cyclone Ului; all containers, equipment inside, cables, winches, and banners were securely fastened, and monitoring of the weather continued on a six hourly basis.

At 1916 h on 15 March the *Greatship Maya* weighed anchor, coming alongside in Townsville at 2100 h. Following rebunkering and a GC Rieber marine crew change, the *Greatship Maya* departed Townsville at 2035 h on 16 March and arrived at the Townsville Anchorage at 2205 h to continue waiting on weather. At 1600 h on 17 March a pilot boat came alongside with additional spares. The *Greatship Maya* continued to wait on weather at the Townsville Anchorage until 19 March.

Transit to RIB-02A transect

Following regular assessment of weather conditions at all three geographical drilling locations, the *Greatship Maya* departed Townsville Anchorage and began the transit to Ribbon Reef 3 at 2040 h on 19 March 2001, arriving at 1930 h on 20 March. At 2030 h the *Greatship Maya* began DP trials ~0.3 nmi seaward from RIB-02A transect Site 4. These trials continued to 21 March because of problems with the bow thrusters. At 1530 h on 21 March new DP software was installed, and testing continued until 1645 h, when the *Greatship Maya* began to move onto station at Site 4.

Site 4

Hole M0049A

At 1900 h on 21 March 2010 the *Greatship Maya* arrived on station and the seabed transponder was deployed. The anchor was also made ready for fast deployment as per the EMP for the Ribbon Reef sites. Running of API pipe commenced at 1950. Between 2225 and 2240 h, a downpipe camera survey of the seabed was conducted prior to tagging the seabed at 2300 h.

The first core arrived on deck at 2330 h. However, after two EXN core runs (3.5 m CSF-A), a problem with the water swivel/flush pipe at 0040 h on 22 March necessitated tripping the API pipe to ~7 m above the seabed. The vessel remained on DP and on station during the repairs.

Hole M0049B

Coring recommenced at Site 4, Hole M0049B, at 0400 h on 22 March and continued for 13 core runs (1–3 = EXN cores; 4–13 = ALN cores) until the hole was terminated at 15.6 m CSF-A at 1520 h with an average recovery of 17.9%. The API pipe was tripped to just above the seabed, and a downpipe camera survey was conducted between 1550 and 1610 h.

Hole M0050A

The downpipe camera was retained inside the API pipe while the vessel moved 4 m under DP to Site 4, Hole M0050A. A precoring seabed survey was completed by 1650 h on 22 March 2010, and the first core run (EXN) was started. ALN coring (Core 325-M0050A-2R onward) continued until 2120 h, when the hole was terminated at 10.5 m CSF-A because of entering Pleistocene sequences, with an average recovery of 17.8%. The API pipe was tripped to just above the seabed, and a downpipe camera survey was conducted between 2200 and 2220 h. Between 2220 and 2245 h the API pipe was tripped until there was ~60 m hanging beneath the drill floor. The seabed transponder was then recovered, and at 2305 h the vessel began moving under DP 78 m closer to the modern reef at Site 3.

Site 3

Hole M0051A

The seabed transponder was deployed at 2315 h on 22 March 2010 with the *Greatship Maya* coming onto station at Site 3 (Hole M0051A) at 2320 h. API pipe was run starting at 2330 h. A downpipe camera survey was conducted between 2255 and 0030 h (23 March). The first ALN core was on deck at 0105 h. However, the second core could not be recovered because of a hydraulic failure of the elevator and mud valve at 0230 h, effectively terminating the hole at 2.5 m CSF-A. At 0800 h the vessel was moved into deeper water for safety, having recovered the seabed transponder, while repairs on the hydraulics continued. However, by 0900 h the decision was taken to trip the API pipe using manual elevators. The core barrel was recovered from the BHA once in the slips, between 1315 and 1345 h; however, minimal core remained.

Another prerequisite of the EMP was for a GBRMPA Environmental Site Supervisor (ESS) to be onboard while Sites 1 and 2 at Ribbon Reef 3 were drilled. At 1300 h on 23 March the ESS came alongside in the Reef Charters vessel *Hurricane*. However, after numerous attempts at a boat to boat transfer, it was decided that the sea swell and winds were too high to enable any transfer to be carried out safely. The ESS and the *Hurricane* returned to Cooktown (Australia) at 1400 h, and the *Greatship Maya* began waiting on weather, as conditions prohibited starting a new hole. At 1530 h, following operational discussions regarding the limited drilling options at the Ribbon Reef sites with no ESS available, the seabed transponder was recovered and the drill floor and moonpool secured for transit. The *Greatship Maya* came off DP at 1645 h and departed for Noggin Pass.

Transit to NOG-01B transect and waiting on weather

The *Greatship Maya* departed RIB-02A transect Site 3 (Hole M0051A) at 1645 h on 23 March 2010 and arrived at the NOG-01B transect at 0910 h on 24 March.

Site 6

Hole M0052A

After going onto DP at 0910 h, the vessel moved slowly onto station at Site 6 (Hole M0052A), completing the maneuver at 1120 h on 24 March 2010. Following an assessment of weather conditions at 1145 h, the vessel moved 500 m seaward of Hole

M0052A to wait on weather in deeper water. Operations continued to wait on weather on 25 March.

At 0655 h on 26 March the supply boat *Acheron* arrived alongside. Because of high winds and sea swell, it was not safe to conduct a boat to boat transfer of equipment at the location. At 0745 h both vessels departed NOG-01B Site 6 to transit to calmer waters inside Flora Passage and arrived at 1100 h. Following a successful transfer, the *Greatship Maya* departed Flora Passage at 1120 h, arrived back at NOG-01B Site 6 at 1645 h, and continued waiting on weather. At 1900 h permission was given for coring operations to start, and the seabed transponder was deployed at 1930 h. API pipe was run between 2045 and 2250 h, following which a downpipe camera survey was conducted. At 2355 h the first (EXN) core run commenced.

The core run was halted after 1.4 m because of a very hard lithology, and recovered. However, on recovery the liner was found to be crushed and the bit damaged. During recovery the API drill string came out of the hole because of vessel heave, and Hole M0052A was terminated at 1.4 m CSF-A.

Hole M0052B

Coring (ALN) recommenced at 0115 h on 27 March 2010 at the same location as Hole M0054A. The first core was recovered at 0200 h. The bit was found to be cracked and the hole collapsed back to 1 m. Coring continued for another three runs until 0430 h. However, weather conditions and large sea swells were causing the bit to bounce on the bottom of the hole, as well as DP deviation. At 0430 h the barrel became stuck in the BHA and could not be recovered without tripping the API pipe, so Hole M0052B was terminated at 6.9 m CSF-A. The barrel was recovered at 0745 h, and the bit was found to be bent so that it was catching on the BHA landing ring.

Hole M0052C

At 0815 h on 27 March 2010 API pipe was run in at the same location as Hole M0052B. Open hole coring down to 6.9 m CSF-A commenced at 0915 h. At 1020 h the first ALN core was recovered. On recovering the second core at 1130 h, the bit was found to be missing and the hole had to be terminated at 8.8 m CSF-A. Tripping the API pipe began at 1140 h, completing this operation at 1330 h. The BHA and API ALN systems were checked while the *Greatship Maya* moved to a new location within Site 6.

Hole M0053A

API pipe was run in Hole M0053A starting at 1400 h on 27 March 2010 in preparation for using the HQ coring system. Operations halted between 1510 and 1530 h to make repairs to the elevator. Between 1725 and 1800 h, operations had to stop because of a squall passing through the area. Between 1800 and 1900 h, the dies on the roughneck were checked prior to running the bumper sub and lowering the seabed template to ~10 m below the sea surface. At 2010 h the API string was lowered to the seabed and the bumper sub heave monitored. The heave was not sufficient, possibly because of soft sediment, and a 3 m pup was added. The bumper sub appeared to be compensating, and at 2130 h the seabed template was lowered to the seabed. However, at 2210 h the bumper sub stopped compensating. At 2300 h the decision was taken to abandon HQ coring and return to API.

The seabed template was recovered between 2300 and 0030 h on 28 March and the bumper sub between 0030 and 0110 h. Additional API pipe was run between 0110 and 0120 h. The first EXN core was recovered at 0210 h (all subsequent core runs used the ALN core barrel). Between 0520 and 0550 h on 28 March operations stopped while the latch head assembly was changed, and between 1330 and 1350 h coring operations again stopped because of heavy rain obscuring the driller's view of the derrick. ALN coring then continued for another 17 runs until the hole was terminated at 0250 h on 29 March at 37.3 m CSF-A with an average recovery of 32.7%.

At 0300 h on 29 March the API pipe was tripped to just above the seabed, and a downpipe camera survey was conducted. This operation was completed by 0335 h, with the camera being left in the pipe for the vessel move to the next site, 66 m away. The seabed transponder was recovered at 0355 h and the vessel began the move to Site 7 (Hole M0054A) at 0410 h.

Site 7

Hole M0054A

The *Greatship Maya* was on station over Hole M0054A at 0425 h on 29 March 2010, and the seabed transponder was deployed. The downpipe camera survey began at 0440 h but took until 0530 h to complete because an additional API pipe had to be run in, requiring the recovery and redeployment of the camera system. Time was needed to repair hydraulic fluid leaks on the roughneck and to conduct maintenance on the main power pack. After lowering the seabed template, the seabed was tagged

at 1515 h, followed by washing down to set the API in the hole. HQ coring commenced at 1600 h and continued until 0425 h on 30 March.

The hole was terminated at 0425 h at a depth of 18.72 m after three consecutive core runs recovered no material. It was considered necessary to recover the BHA to deck, where it was discovered that 60 cm of cored material had become wedged in the BHA and was preventing the barrel from latching. The average recovery for Hole M0054A was 23.98%.

Hole M0054B

Operations in Hole M0054B commenced at 0545 h on 30 March 2010 following recovery of the blocked BHA which led to the termination of Hole M0054A. The HQ pipe was run down the API string, tagging the bottom of the borehole at 0830 h. The first core was recovered at 0915 h and consisted of wash material from the caving of Hole M0054A. Coring then continued until 1910 h, when Core 325-M0054A-12R was recovered and a TD of 33.2 m was achieved. The average recovery for Hole M0054B was 29.63%.

Following recovery of this core, the drill floor was prepared for wireline logging operations. Through-pipe gamma logging started at 2330 h and was completed at 0145 h on 1 April. The HQ string was tripped to swap the BHA with a shoe to allow the open-hole logging sondes to be run. At 0315 h a hydraulic fluid leak occurred, delaying the tripping of the HQ string. At 0520 h tripping recommenced, and the HQ BHA was recovered to deck at 0645 h. Following removal of the crossover sub from the top drive, half an API pipe was run in and the crossover reattached. At 0815 h the HQ string was run back into the hole and flushing with mud and water occurred. At 1530 h the HQ string was put into heave compensation. At 1600 h the conductivity sonde was run, followed by the ABI (1745 h), OBI (1900 h), spectral gamma (2145 h), sonic (2330 h), magnetic susceptibility (0110 h on 1 April), idronaut (0155 h), and caliper (0240 h). By 0335 h all wireline tools were recovered to the deck and the logging rooster box was demobilized.

At 0530 h tripping of the HQ string commenced and continued until 0800 h. This was followed by tripping of the HQ pipe to just above the seabed to allow deployment of the downpipe camera for posthole survey. This was interrupted by a further hydraulic fluid leak on the iron roughneck from 0840 to 0855 h, when tripping recommenced. By 0920 h the API pipe was in position just above the seafloor, and the seabed template was lifted to 7 m above the seafloor to allow the camera survey to commence.

At 0940 h the camera was deployed. It is thought that the camera was caught on the steps inside the bumper sub, blowing the bulb and making it impossible to complete the survey.

The camera was recovered to deck by 1000 h. The remaining API pipe was tripped until the bumper sub was level with the drill floor for inspection by 1120 h. By 1140 h the seabed frame had been lifted to 20 mbsl and the seabed transponder recovered to allow transit to the next hole. At 1200 h the vessel commenced transit to Hole M0055A.

Site 5

Hole M0055A

The *Greatship Maya* was on station at Site 5, Hole M0055A, and deploying the seabed transponder at 1230 h on 1 April 2010. Once completed, the seabed template was lowered to ~10 m off the seabed, and API pipe was run to just above the seabed. The downpipe camera survey was conducted by 1530 h, and the API pipe tagged the seabed at 1545 h. By 1620 h the API pipe had been washed down 2 m. The API pipe was then disconnected and set on elevators on the drill floor. Following this, HQ rods were run, tagging the bottom (3.29 m CSF-A) at 1920 h. HQ coring operations continued until 0555 h on 2 April, when the hole was terminated at 31.29 m CSF-A with an average hole recovery of 32%.

The HQ rods were tripped by 0805 h, and the API pipes were clear of the seabed by 0845 h. The seabed template was lifted above the seabed, and the seabed transponder was recovered. The *Greatship Maya* departed Hole M0055A at 0920 h.

Hole M0056A

The *Greatship Maya* transited slowly to Site 5 (Hole M0056A), 66 m away from Hole M0055A, because of the seabed template being suspended in the water column. At 0935 h on 2 April 2010 the seabed transponder was deployed, and at 0945 h the template was lowered over Hole M0056A to 72 mbsl. Between 0955 and 1035 h the API pipe and seabed template were lowered to just above the seabed, at which point the downpipe camera survey was conducted. The seabed template was lowered onto the seabed, and the API pipe tagged bottom at 1120 h. The API was then washed in 1.3 m. At 1230 h the API pipe was broken and the elevators set on the slips prior to running HQ rods.

The HQ rods tagged bottom at 1415 h, at which point coring operations started, continuing until 2100 h when the HQ crossover and saver sub had to be replaced following failure of a weld. Coring restarted at 2140 h and continued until 0635 h on 3 April, when the hole was terminated at 41.29 m CSF-A with an average hole recovery of 30.8%. The HQ rods were tripped by 0840 h and the top drive reconnected to the API pipe. The seabed template and API were lifted to ~9 m above the seabed and a down-pipe camera survey was conducted. At 0935 h the API pipe was tripped back to the bumper sub, and the seabed template was lifted into the moonpool in preparation for transit. At 1040 h the seabed transponder was recovered and the *Greatship Maya* departed Site 5 at 1050 h.

Site 2

Hole M0057A

At 1125 h on 3 April 2010 the seabed transponder was deployed, and by 1140 h the *Greatship Maya* had settled on station at Site 2, Hole M0057A. The transponder on the seabed template was changed prior to lowering the template to ~35 mbsl. At 1135 h API pipe was run to just above the seabed and a downpipe camera survey was conducted. Further API was then run, tagging the seabed at 1400 h. The API pipe was then set on the elevators and disconnected from the top drive at 1430 h in preparation for running HQ pipe. The seabed was tagged with the HQ pipe at 1520 h and coring operations began.

After core Run 3 it was noted that the hole was caving, possibly because of the string swabbing the hole. Coring operations continued after hole conditioning until 2325 h, when there was a twist off between the crossover sub and the top HQ pipe. Between 2325 and 0100 h on 4 April the crossover sub was tripped out for repairs and the core barrel recovered. On the next core run, damage to the threads on two HQ rods was sustained while running a new rod in, resulting in having to trip two rods and replace them. Coring then continued until 0440 h, when it was noted that mud was leaking from the repaired crossover sub/HQ pipe joint. To enable safe working on the joint, three HQ rods were tripped out. During the repair period the hole collapsed. Open hole drilling and flushing back down to the previously reached depth of 32.38 m CSF-A ran from 0610 to 0710 h, at which point coring operations restarted.

Operations were temporarily halted between 1040 and 1100 h because of a fire alarm caused by an oil leak dripping onto the exhaust pipe in the engine room. Operations then continued until 1230 h, when the hole was terminated at 41.78 m CSF-A with

an average hole recovery of 45.5%. Between 1240 and 1520 h, the HQ rods were tripped, followed by the API pipe. A problem with the iron roughneck delayed lifting of the seabed template, which was completed at 1730 h. The seabed transponder was recovered by 1750 h and the template and drill floor secured in preparation for transit to Site 8, Hole M0058A.

Site 8

Hole M0058A

The *Greatship Maya* reached Site 8 at 1950 h on 4 April 2010, and the seabed transponder was deployed prior to the vessel settling on station over Hole M0058A by 2005 h. Between 2010 and 2240 h, repairs on the roughneck and roughneck hydraulics were undertaken prior to running API pipe. The first core run started at 0220 h on 5 April and continued for 15 runs; all runs were EXN with the exception of Run 5, which was ALN. Coring operations were going smoothly until problems with the powerpacks surging and cutting out caused operations to stop between 1035 to 1245 h and again between 1355 and 1425 h. The final hole was terminated after core Run 15 at 41.4 m CSF-A with an average recovery of 82%.

At 1515 h the powerpack stalled, delaying tripping of the API pipe. However, all API pipe was on deck by 1845 h, and the drill floor and template were secured ready for transit by 2105 h. At 2115 h the *Greatship Maya* came off DP, departing Site 8 (Hole M0058A) at 2130 h.

Transit to Townsville

The *Greatship Maya* departed the final site at 2130 h on 5 April 2010 and arrived at the port of Townsville at 1430 h on 6 April 2010. Demobilization of the vessel and clearances of the containers by the Australian Quarantine and Inspection Service (AQIS) and customs officials continued until 1130 h on 7 April, when all ESO personnel and science party members departed the vessel.

Onshore Science Party, Bremen

The cores collected offshore on the GBR were transported under refrigeration to the IODP Bremen Core Repository and Laboratories in the Center for Marine Environmental Sciences (MARUM) building on the campus of Bremen University. Frozen microbiology samples were shipped directly from Australia to scientists' laboratories in

the United States and China by special courier service. Samples from 68 core catchers were also sent to laboratories in Japan and the United Kingdom for U-Th and ^{14}C dating to be carried out in order to produce a preliminary shipboard chronology prior to the OSP. Thermal conductivity measurements and some computed tomography (CT) scans of selected cores were acquired before the start of the OSP.

Further analytical laboratories were accessed by agreement with the Department of Geosciences (geochemistry, paleomagnetism, and mineralogy [X-ray diffraction] laboratories) and MARUM (physical properties, micropaleontology, and nondestructive core logging laboratories) at Bremen University. During the Expedition 325 OSP (2–16 July 2010), the cores were described in detail and sampled, and minimum and some standard measurements were made (Table T2). In addition, sampling for post-cruise scientific work was also undertaken.

References

- Allison, N., Finch, A.A., Tudhope, A.W., Newville, M., Sutton, S.R., and Ellam, R.M., 2005. Reconstruction of deglacial sea surface temperatures in the tropical Pacific from selective analysis of a fossil coral. *Geophys. Res. Lett.*, 32(17):L17609. doi:10.1029/2005GL023183
- Asami, R., Felis, T., Deschamps, P., Hanawa, K., Iryu, Y., Bard, E., Durand, N., and Murayama, M., 2009. Evidence for tropical South Pacific climate change during the Younger Dryas and the Bølling-Allerød from geochemical records of fossil Tahiti corals. *Earth Planet. Sci. Lett.*, 288(1–2):96–107. doi:10.1016/j.epsl.2009.09.011
- Bard, E., Hamelin, B., Arnold, M., Montaggioni, L., Cabioch, G., Faure, G., and Rougerie, F., 1996. Deglacial sea-level record from Tahiti corals and the timing of global meltwater discharge. *Nature (London, U. K.)*, 382(6588):241–244. doi:10.1038/382241a0
- Bard, E., Hamelin, B., and Delanghe-Sabatier, D., 2010. Deglacial meltwater pulse 1B and Younger Dryas sea levels revisited with boreholes at Tahiti. *Science*, 327(5970):1235–1237. doi:10.1126/science.1180557
- Bard, E., Hamelin, B., Fairbanks, R.G., and Zindler, A., 1990. Calibration of the ¹⁴C timescale over the past 30,000 years using mass spectrometric U–Th ages from Barbados corals. *Nature (London, U. K.)*, 345(6274):405–410. doi:10.1038/345405a0
- Bard, E., Hamelin, B., and Fairbanks, R.G., 1990. U–Th ages obtained by mass spectrometry in corals from Barbados: sea level during the past 130,000 years. *Nature (London, U. K.)*, 346(6283):456–458. doi:10.1038/346456a0
- Beaman, R.J., Webster, J.M., and Wust, R.A.J., 2007. New evidence for drowned shelf edge reefs in the Great Barrier Reef, Australia. *Mar. Geol.*, 247(1–2):17–34. doi:10.1016/j.mar-geo.2007.08.001
- Beck, J.W., Récy, J., Taylor, F., Edwards, R.L., and Cabioch, G., 1997. Abrupt changes in early Holocene tropical sea surface temperature derived from coral records. *Nature (London, U. K.)*, 385(6618):705–707. doi:10.1038/385705a0
- Blanchon, P., and Shaw, J., 1995. Reef drowning during the last deglaciation: evidence for catastrophic sea-level rise and ice-sheet collapse. *Geology*, 23(1):4–8. doi:10.1130/0091-7613(1995)023<0004:RDDTLD>2.3.CO;2
- Braga, J.C., and Aguirre, J., 2004. Coralline algae indicate Pleistocene evolution from deep, open platform to outer barrier reef environments in the northern Great Barrier Reef margin. *Coral Reefs*, 23(4):547–558. doi:10.1007/s00338-004-0414-x
- Braithwaite, C.J.R., Dalmaso, H., Gilmour, M.A., Harkness, D.D., Henderson, G.M., Kay, R.L.F., Kroon, D., Montaggioni, L.F., and Wilson, P.A., 2004. The Great Barrier Reef: the chronological record from a new borehole. *J. Sediment. Res.*, 74(2):298–310. doi:10.1306/091603740298
- Broecker, W.S., 1990. Salinity history of the Northern Atlantic during the last deglaciation. *Paleoceanography*, 5(4):459–467. doi:10.1029/PA005i004p00459
- Broecker, W.S., 1992. Defining the boundaries of the late-glacial isotope episodes. *Quat. Res.*, 38(1):135–138. doi:10.1016/0033-5894(92)90036-I
- Brown, J., Collins, M., Tudhope, A.W., and Toniazzo, T., 2008. Modelling mid-Holocene tropical climate and ENSO variability: towards constraining predictions of future change with palaeo-data. *Clim. Dyn.*, 30(1):19–36. doi:10.1007/s00382-007-0270-9
- Cabioch, G., Banks-Cutler, K.A., Beck, W.J., Burr, G.S., Corrège, T., Edwards, R.L., and Taylor, F.W., 2003. Continuous reef growth during the last 23 cal kyr BP in a tectonically active

- zone (Vanuatu, southwest Pacific). *Quat. Sci. Rev.*, 22(15–17):1771–1786. doi:10.1016/S0277-3791(03)00170-7
- Camoin, G.F., Colonna, M., Montaggioni, L.F., Casanova, J., Faure, G., and Thomassin, B.A., 1997. Holocene sea level changes and reef development in the southwestern Indian Ocean. *Coral Reefs*, 16(4):247–259. doi:10.1007/s003380050080
- Camoin, G.F., Iryu, Y., McInroy, D.B., and the Expedition 310 Scientists, 2007. *Proc. IODP, 310*: Washington, DC (Integrated Ocean Drilling Program Management International, Inc.). doi:10.2204/iodp.proc.310.2007
- Carter, R.M., and Johnson, D.P., 1986. Sea-level controls on the post-glacial development of the Great Barrier Reef, Queensland. *Mar. Geol.*, 71(1–2):137–164. doi:10.1016/0025-3227(86)90036-8
- Chappell, J., and Polach, H., 1991. Post-glacial sea-level rise from a coral record at Huon Peninsula, Papua New Guinea. *Nature (London, U. K.)*, 349(6305):147–149. doi:10.1038/349147a0
- Clark, P.U., McCabe, A.M., Mix, A.C., and Weaver, A.J., 2004. Rapid rise of sea level 19,000 years ago and its global implications. *Science*, 304(5674):1141–1144. doi:10.1126/science.1094449
- Corrège, T., Gagan, M.K., Beck, J.W., Burr, G.S., Cabioch, G., and Le Cornec, F., 2004. Interdecadal variation in the extent of South Pacific tropical waters during the Younger Dryas event. *Nature (London, U. K.)*, 428(6986):927–929. doi:10.1038/nature02506
- Cutler, K.B., Edwards, R.L., Taylor, F.W., Cheng, H., Adkins, J., Gallup, C.D., Cutler, P.M., Burr, G.S., and Bloom, A.L., 2003. Rapid sea-level fall and deep-ocean temperature change since the last interglacial period. *Earth Planet. Sci. Lett.*, 206(3–4):253–271. doi:10.1016/S0012-821X(02)01107-X
- Davies, P.J., and Peerdeman, F.M., 1998. The origin of the Great Barrier Reef: the impact of Leg 133 drilling. In Camoin, G.F., and Davies, P.J. (Eds.), *Reefs and Carbonate Platforms in the Pacific and Indian Oceans*. Spec. Publ. Int. Assoc. Sedimentol., 25:23–38.
- Davies, P.J., Symonds, P.A., Feary, D.A., and Pigram, C.J., 1989. The evolution of the carbonate platforms of northeast Australia. In Crevello, P.D., Wilson, J.L., Sarg, J.F., and Read, J.F. (Eds.), *Controls on Carbonate Platform and Basin Development*. Spec. Publ.—Soc. Econ. Paleontol. Mineral., 44:233–258.
- De Deckker, P., and Yokoyama, Y., 2009. Micropalaeontological evidence for late Quaternary sea-level changes in Bonaparte Gulf, Australia. *Global Planet. Change*, 66(1–2):85–92. doi:10.1016/j.gloplacha.2008.03.012
- DeLong, K.L., Quinn, T.M., Shen, C.-C., and Lin, K., 2010. A snapshot of climate variability at Tathiti at 9.5 ka using a fossil coral from IODP Expedition 310. *Geochem., Geophys., Geosyst.*, 11(6):Q06005. doi:10.1029/2009GC002758
- Denton, G.H., Anderson, R.F., Toggweiler, J.R., Edwards, R.L., Shafer, J.M., and Putnam, A.E., 2010. The last glacial termination. *Science*, 328(5986):1652–1656. doi:10.1126/science.1184119
- Dubois, N., Kindler, P., Spezzaferri, S., and Coric, S., 2008. The initiation of the southern central Great Barrier Reef: new multiproxy data from Pleistocene distal sediments from the Marion Plateau (NE Australia). *Mar. Geol.*, 250(3–4):223–233. doi:10.1016/j.mar-geo.2008.01.007
- Dullo, W.C., Camoin, G.F., Blomeier, D., Colonna, M., Eisenhauer, A., Faure, G., Casanova, J., and Thomassin, B.A., 1998. Morphology and sediments of the fore-slopes of Mayotte, Comoro Islands: direct observations from a submersible. In Camoin, G.F., and Davies, P.J.,

- Reefs and Carbonate Platforms in the Pacific and Indian Oceans*. Spec. Publ. Int. Assoc. Sedimentol., 25:219–236.
- Edwards, R.L., Beck, J.W., Burr, G.S., Donahue, D.J., Chappell, J.M.A., Bloom, A.L., Druffel, E.R.M., and Taylor, F.W., 1993. A large drop in atmospheric $^{14}\text{C}/^{12}\text{C}$ and reduced melting in the Younger Dryas, documented with ^{230}Th ages of coral. *Science*, 260(5110):962–968. [doi:10.1126/science.260.5110.962](https://doi.org/10.1126/science.260.5110.962)
- Fairbanks, R.G., 1989. A 17,000-year glacio-eustatic sea level record: influence of glacial melting rates on the Younger Dryas event and deep-ocean circulation. *Nature (London, U. K.)*, 342(6250):637–642. [doi:10.1038/342637a0](https://doi.org/10.1038/342637a0)
- Feary, D.A., Symonds, P.A., Davies, P.J., Pigram, C.J., and Jarrard, R.D., 1993. Geometry of Pleistocene facies on the Great Barrier Reef outer shelf and upper slope—seismic stratigraphy of Sites 819, 820, and 821. In McKenzie, J.A., Davies, P.J., Palmer-Julson, A., et al., *Proc. ODP, Sci. Results*, 133: College Station, TX (Ocean Drilling Program), 327–351. [doi:10.2973/odp.proc.sr.133.250.1993](https://doi.org/10.2973/odp.proc.sr.133.250.1993)
- Fujita, K., Omori, A., Yokoyama, Y., Sakai, S., and Iryu, Y., 2010. Sea-level rise during Termination II inferred from large benthic foraminifers: IODP Expedition 310, Tahiti Sea Level. *Mar. Geol.*, 271(1–2):149–155. [doi:10.1016/j.margeo.2010.01.019](https://doi.org/10.1016/j.margeo.2010.01.019)
- Gagan, M.K., Ayliffe, L.K., Beck, J.W., Cole, J.E., Druffel, E.R.M., Dunbar, R.B., and Schrag, D.P., 2000. New views of tropical paleoclimates from corals. *Quat. Sci. Rev.*, 19(1–5):45–64. [doi:10.1016/S0277-3791\(99\)00054-2](https://doi.org/10.1016/S0277-3791(99)00054-2)
- Gagan, M.K., Ayliffe, L.K., Hopley, D., Cali, J.A., Mortimer, G.E., Chappell, J., McCulloch, M.T., and Head, M.J., 1998. Temperature and surface-ocean water balance of the mid-Holocene tropical western Pacific. *Science*, 279(5353):1014–1018. [doi:10.1126/science.279.5353.1014](https://doi.org/10.1126/science.279.5353.1014)
- Gagan, M.K., Hendy, E.J., Haberle, S.G., and Hantoro, W.S., 2004. Post-glacial evolution of the Indo-Pacific Warm Pool and El Niño–Southern Oscillation. *Quat. Int.*, 118–119:127–143. [doi:10.1016/S1040-6182\(03\)00134-4](https://doi.org/10.1016/S1040-6182(03)00134-4)
- Grammer, G.M., and Ginsburg, R.N., 1992. Highstand versus lowstand deposition on carbonate platform margins: insight from Quaternary foreslopes in the Bahamas. *Mar. Geol.*, 103(1–3):125–136. [doi:10.1016/0025-3227\(92\)90012-7](https://doi.org/10.1016/0025-3227(92)90012-7)
- Griffiths, M.L., Drysdale, R.N., Gagan, M.K., Zhao, J.-X., Ayliffe, L.K., Hellstrom, J.C., Hantoro, W.S., Frisia, S., Feng, Y.-X., Cartwright, I., St. Pierre, E., Fischer, M.J., and Suwargadi, B.W., 2009. Increasing Australian–Indonesian monsoon rainfall linked to early Holocene sea-level rise. *Nat. Geosci.*, 2(9):636–639. [doi:10.1038/ngeo605](https://doi.org/10.1038/ngeo605)
- Griffiths, M.L., Drysdale, R.N., Vohnof, H.B., Gagan, M.K., Zhao, J.-X., Ayliffe, L.K., Hantoro, W.S., Hellstrom, J.C., Cartwright, I., Frisia, S., and Suwargadi, B.W., 2010. Younger Dryas–Holocene temperature and rainfall history of southern Indonesia from $\delta^{18}\text{O}$ in speleothem calcite and fluid inclusions. *Earth Planet. Sci. Lett.*, 295(1–2):30–36. [doi:10.1016/j.epsl.2010.03.018](https://doi.org/10.1016/j.epsl.2010.03.018)
- Guilderson, T.P., Fairbanks, R.G., and Rubenstone, J.L., 1994. Tropical temperature variations since 20,000 years ago: modulating interhemispheric climate change. *Science*, 263(5147):663–665. [doi:10.1126/science.263.5147.663](https://doi.org/10.1126/science.263.5147.663)
- Hanebuth, T., Statterger, K., and Grootes, P.M., 2000. Rapid flooding of the Sunda Shelf: a late-glacial sea-level record. *Science*, 288(5468):1033–1035. [doi:10.1126/science.288.5468.1033](https://doi.org/10.1126/science.288.5468.1033)
- Hanebuth, T.J.J., Statterger, K., and Bojanowski, A. 2009. Termination of the Last Glacial Maximum sea-level lowstand: the Sunda-Shelf data revisited. *Global Planet. Change*, 66(1–2):76–84. [doi:10.1016/j.gloplacha.2008.03.011](https://doi.org/10.1016/j.gloplacha.2008.03.011)

- Harris, P.T., and Davies, P.J., Submerged reefs and terraces on the shelf edge of the Great Barrier Reef, Australia. *Coral Reefs*, 8(2):87–98. doi:10.1007/BF00301807
- Hopley, D., 2006. Coral reef growth on the shelf margin of the Great Barrier Reef with special reference to the Pompey Complex. *J. Coastal Res.*, 22(1):150–158. doi:10.2112/05A-0012.1
- Inoue, M., Yokoyama, Y., Harada, M., Suzuki, A., Kawahata, H., Matsuzaki, H., and Iryu, Y., 2010. Trace element variations in fossil corals from Tahiti collected by IODP Expedition 310: reconstruction of marine environments during the last deglaciation (15 to 9 ka). *Mar. Geol.*, 271(3–4):303–306. doi:10.1016/j.margeo.2010.02.016
- International Consortium for Great Barrier Reef Drilling, 2001. New constraints on the origin of the Australian Great Barrier Reef: results from an international project of deep coring. *Geology*, 29(6):483–486. doi:10.1130/0091-7613(2001)029<0483:NCOTOO>2.0.CO;2
- Lambeck, K., 1993. Glacial rebound and sea-level change: an example of a relationship between mantle and surface processes. In Wortel, M.J.R., Hansen, U., and Sabadini, R. (Eds.), *Relationships Between Mantle Processes and Geologic Processes at or near the Earth's Surface*. Tectonophysics, 223(1–2):15–37. doi:10.1016/0040-1951(93)90155-D
- Lambeck, K., Purcell, A., Funder, S., Kjær, K., Larsen, E., and Møller, P., 2006. Constraints on the late Saalian to early middle Weichselian ice sheet of Eurasia from field data and rebound modelling. *Boreas*, 35(3):539–575. doi:10.1080/03009480600781875
- Lambeck, K., Purcell, A., Johnston, P., Nakada, M., and Yokoyama, Y., 2003. Water-load definition in the glacio-hydro-isostatic sea level equation. *Quat. Sci. Rev.*, 22(2–4):309–318. doi:10.1016/S0277-3791(02)00142-7
- Lambeck, K., Yokoyama, Y., and Purcell, T., 2002. Into and out of the Last Glacial Maximum: sea-level change during oxygen isotope Stages 3 and 2. *Quat. Sci. Rev.*, 21(1–3):343–360. doi:10.1016/S0277-3791(01)00071-3
- Larcombe, P., Carter, R.M., Dye, J., Gagan, M.K., and Johnson, D.P., 1995. New evidence for episodic post-glacial sea-level rise, central Great Barrier Reef, Australia. *Mar. Geol.*, 127(1–4):1–44. doi:10.1016/0025-3227(95)00059-8
- Lindstrom, D.R., and MacAyeal, D.R., 1993. Death of an ice sheet. *Nature (London, U. K.)*, 365(6443):214–215. doi:10.1038/365214a0
- Linsley, B., Rosenthal, Y., and Oppo, D.W., in press. Evolution of the Indonesian throughflow and Western Pacific Warm Pool During the Holocene. *Nat. Geosci.*
- Liu, Z., Kutzbach, J., and Wu, L., 2000. Modeling climate shift of El Niño variability in the Holocene. *Geophys. Res. Lett.*, 27(15):2265–2268. doi:10.1029/2000GL011452
- Locker, S.D., Hine, A.C., Tedesco, L.P., and Shinn, E.A., 1996. Magnitude and timing of episodic sea-level rise during the last deglaciation. *Geology*, 24(9):827–830. doi:10.1130/0091-7613(1996)024<0827:MATOES>2.3.CO;2
- Macintyre, I.G., Rützler, K., Norris, J.N., Smith, K.P., Cairns, S.D., Bucher, K.E., and Steneck, R.S., 1991. An early Holocene reef in the western Atlantic: submersible investigations of a deep relict reef off the west coast of Barbados, W.I. *Coral Reefs*, 10(3):167–174. doi:10.1007/BF00572177
- MARGO Project Members, 2009. Constraints on the magnitude and patterns of ocean cooling at the Last Glacial Maximum. *Nat. Geosci.*, 2(2):127–132. doi:10.1038/ngeo411
- Martin, P.A., Lea, D.W., Mashiotto, T.A., Papenfuss, T., and Sarnthein, M., 1999. Variation of foraminiferal Sr/Ca over Quaternary glacial-interglacial cycles: evidence for changes in mean ocean Sr/Ca? *Geochem., Geophys., Geosyst.*, 1(12):1004–1023. doi:10.1029/1999GC000006

- McCulloch, M., Mortimer, G., Esat, T., Xianhua, L., Pillans, B., and Chappell, J., 1996. High resolution windows into early Holocene climate: Sr/Ca coral records from the Huon Peninsula. *Earth Planet. Sci. Lett.*, 138(1–4):169–178. doi:10.1016/0012-821X(95)00230-A
- McGregor, H.V. and Gagan, M.K., 2004. Western Pacific coral $\delta^{18}\text{O}$ records of anomalous Holocene variability in the El Niño–Southern Oscillation. *Geophys. Res. Lett.*, 31(11):L11204. doi:10.1029/2004GL019972
- McKenzie, J.A., Davies, P.J., Palmer-Julson, A., et al., 1993. *Proc. ODP, Sci. Results*, 133: College Station, TX (Ocean Drilling Program). doi:10.2973/odp.proc.sr.133.1993
- Milne, G.A., Gehrels, W.R., Hughes, C.W., and Tamisiea, M.E., 2009. Identifying the causes of sea-level change. *Nat. Geosci.*, 2(7):471–478. doi:10.1038/ngeo544
- Mix, A.C., Bard, E., and Schneider, R., 2001. Environmental processes of the ice age: land, oceans, glaciers (EPILOG). *Quat. Sci. Rev.*, 20(4):627–657. doi:10.1016/S0277-3791(00)00145-1
- Moy, C.M., Seltzer, G.O., Rodbell, D.T., and Anderson, D.M., 2002. Variability of El Niño/southern oscillation activity at millennial timescales during the Holocene epoch. *Nature (London, U. K.)*, 420(6912):162–165. doi:10.1038/nature01194
- Nakada, M., 1986. Holocene sea levels in oceanic islands: implications for the rheological structure of the Earth's mantle. *Tectonophysics*, 121(2–4):263–276. doi:10.1016/0040-1951(86)90047-8
- Nakada, M., and Lambeck, K., 1987. Glacial rebound and relative sea-level variations: a new appraisal. *Geophys. J. R. Astron. Soc.*, 90(1):171–224.
- Oppo, D.W., Rosenthal, Y., and Linsley, B.K., 2009. 2000-year-long temperature and hydrology reconstructions from the Indo-Pacific Warm Pool. *Nature (London, U. K.)*, 460(7259):1113–1116. doi:10.1038/nature08233
- Otto-Bleisner, B.L., Brady, E.C., Shin, S.-I., Liu, Z., and Shields, C., 2003. Modeling El Niño and its tropical teleconnections during the last glacial–interglacial cycle. *Geophys. Res. Lett.*, 30(23):2198–2201. doi:10.1029/2003GL018553
- Otto-Bleisner, B.L., Schneider, R., Brady, E.C., Kucera, M., Abe-Ouchi, A., Bard, E., Braconnot, P., Crucifix, M., Hewitt, C.D., Kageyama, M., Marti, O., Paul, A., Rosell-Melé, A., Waelbroeck, C., Weber, S.L., Weinelt, M., and Yu, Y., 2009. A comparison of PMIP2 model simulations and the MARGO proxy reconstruction for tropical sea surface temperatures at Last Glacial Maximum. *Clim. Dyn.*, 32(6):799–815. doi:10.1007/s00382-008-0509-0
- Peltier, W.R., 1994. Ice age paleotopography. *Science*, 265(5169):195–201. doi:10.1126/science.265.5169.195
- Peltier, W.R., and Fairbanks, R.G., 2006. Global glacial ice volume and Last Glacial Maximum duration from an extended Barbados sea level record. In Rose, J., Tzedakis, C., and Elderfield, H. (Eds.), *Critical Quaternary Stratigraphy*. *Quat. Sci. Rev.*, 25(23–24):3322–3337. doi:10.1016/j.quascirev.2006.04.010
- Rodbell, D.T., Seltzer, G.O., Anderson, D.M., Abbott, M.B., Enfield, D.B., and Newman J.H., 1999. An ~15,000-year record of El Niño-driven alluviation in southwestern Ecuador. *Science*, 283(5401):516–520. doi:10.1126/science.283.5401.516
- Sandweiss, D.H., Richardson, J.B., III, Reitz, E.J., Rollins, H.B., and Maasch, K.A., 1996. Geochronological evidence from Peru for a 5000 years B.P. onset of El Niño. *Science*, 273(5281):1531–1533. doi:10.1126/science.273.5281.1531
- Stocker, T.F., and Wright, D.G., 1991. Rapid transitions of the ocean's deep circulation induced by changes in surface water fluxes. *Nature (London, U. K.)*, 351(6329):729–732. doi:10.1038/351729a0

- Stoll, H.M., and Schrag, D.P., 1998. Effects of Quaternary sea level cycles on strontium in seawater. *Geochim. Cosmochim. Acta*, 62(7):1107–1118. doi:10.1016/S0016-7037(98)00042-8
- Stott, L., Cannariato, K., Thunell, R., Haug, G.H., Koutavas, A., and Lund, S., 2004. Decline of surface temperature and salinity in the western tropical Pacific Ocean in the Holocene epoch. *Nature (London, U. K.)*, 431(7004):56–59. doi:10.1038/nature02903
- Stuiver, M., and Grootes, P.M., 2000. GISP2 oxygen isotope ratios. *Quat. Res.*, 53(3):277–284. doi:10.1006/qres.2000.2127
- Thomas, A.L., Henderson, G.M., Deschamps, P., Yokoyama, Y., Mason, A.J., Bard, E., Hamelin, B., Durand, N., and Camoin, G., 2009. Penultimate deglacial sea-level timing from Uranium/Thorium dating of Tahitian corals. *Science*, 324(5931):1186–1189. doi:10.1126/science.1168754
- Tudhope, A.W., Chilcott, C.P., McCulloch, M.T., Cook, E.R., Chappell, J., Ellan, R.M., Lea, D.W., Lough, J.M., and Shimmield, G.B., 2001. Variability in the El Niño–Southern Oscillation through a glacial-interglacial cycle. *Science*, 291(5508):1511–1517. doi:10.1126/science.1057969
- Wang, Y.J., Cheng, H., Edwards, R.L., An, Z.S., Wu, J.Y., Shen, C.-C., and Dorale, J.A., 2001. A high-resolution absolute-dated late Pleistocene monsoon record from Hulu Cave, China. *Science*, 294(5580):2345–2348. doi:10.1126/science.1064618
- Webster, J.M., Beaman, R.J., Bridge, T., Davies, P.J., Byrne, M., Williams, S., Manning, P., Pizarro, O., Thornborough, K., Woolsey, E., Thomas, A., and Tudhope, S., 2008a. From corals to canyons: the Great Barrier Reef margin. *Eos, Trans. Am. Geophys. Union*, 89(24):217–218. doi:10.1029/2008EO240002
- Webster, J.M., Davies, P., Beaman, R., Williams, S., and Byrne, M., 2008b. Evolution of drowned shelf edge reefs in the GBR; implications for understanding abrupt climate change, coral reef response and modern deep water benthic habitats. *Marine National Facility RV Southern Surveyor 2007 Program: Voyage Summary SS07/2007*: Victoria, Australia (CSIRO). <http://www.marine.csiro.au/nationalfacility/voyagedocs/2007/summarySS07-2007.pdf>
- Webster, J.M., Clague, D.A., Riker-Coleman, K., Gallup, C., Braga, J.C., Potts, D., Moore, J.G., Winterer, E.L., and Paull, C.K., 2004. Drowning of the –150 m reef off Hawaii: a casualty of global meltwater pulse 1A? *Geology*, 32(3):249–252. doi:10.1130/G20170.1
- Webster, J.M., and Davies, P.J., 2003. Coral variation in two deep drill cores: significance for the Pleistocene development of the Great Barrier Reef. In Blanchon, P., and Montaggioni, L. (Eds.), *Late Quaternary Reef Development*. *Sediment. Geol.*, 159(1–2):61–80. doi:10.1016/S0037-0738(03)00095-2
- Wolanski, E., 1982. Aspects of physical oceanography of the Great Barrier Reef lagoon. *Proc. Int. Coral Reef Symp.*, 8:375–381.
- Yokoyama, Y., Esat, T.M., and Lambeck, K., 2001a. Coupled climate and sea-level changes deduced from Huon Peninsula coral terraces of the last ice age. *Earth Planet. Sci. Lett.*, 193(3–4):579–587. doi:10.1016/S0012-821X(01)00515-5
- Yokoyama, Y., Esat, T.M., and Lambeck, K., 2001b. Last glacial sea-level change deduced from uplifted coral terraces of Huon Peninsula, Papua New Guinea. *Quat. Int.*, 83–85:275–283. doi:10.1016/S1040-6182(01)00045-3
- Yokoyama, Y., Lambeck, K., De Deckker, P., Johnston, P., and Fifield, L.K., 2000. Timing of the Last Glacial Maximum from observed sea level minima. *Nature (London, U. K.)*, 406(6797):713–716. doi:10.1038/35021035

- Yokoyama, Y., Nakada, M., Maeda, Y., Nagaoka, S., Okuno, J., Matsumoto, E., Matsushima, Y., and Sato, H., 1996. Holocene sea-level change and hydro-isostasy along the west coast of Kyushu, Japan. *Palaeogeogr., Palaeoclimatol., Palaeoecol.*, 123(1–4):29–47. [doi:10.1016/0031-0182\(95\)00112-3](https://doi.org/10.1016/0031-0182(95)00112-3)
- Yokoyama, Y., Naruse, T., Ogawa, N.O., Tada, R., Kitazato, H., and Ohkouchi, N., 2006a. Dust influx reconstruction during the last 26,000 years inferred from a sedimentary leaf wax record from the Japan Sea. *Global Planet. Change*, 54(3–4):239–250. [doi:10.1016/j.gloplacha.2006.06.022](https://doi.org/10.1016/j.gloplacha.2006.06.022)
- Yokoyama, Y., Purcell, A., Lambeck, K., and Johnston, P., 2001c. Shore-line reconstruction around Australia during the Last Glacial Maximum and Late Glacial Stage. *Quat. Int.*, 83–85:9–18. [doi:10.1016/S1040-6182\(01\)00028-3](https://doi.org/10.1016/S1040-6182(01)00028-3)
- Yokoyama, Y., Purcell, A., Marshall, J.F., and Lambeck, K., 2006b. Sea-level during the early deglaciation period in the Great Barrier Reef, Australia. *Global Planet. Change*, 53(1–2):147–153. [doi:10.1016/j.gloplacha.2006.01.014](https://doi.org/10.1016/j.gloplacha.2006.01.014)
- Yuan, D., Cheng, H., Edwards, R.L., Dykoski, C.A., Kelly, M.J., Zhang, M., Qing, J., Lin, Y., Wang, Y., Wu, J., Dorale, J.A., An, Z., and Cai, Y., 2004. Timing, duration, and transitions of the last interglacial Asian monsoon. *Science*, 304(5670):575–578. [doi:10.1126/science.1091220](https://doi.org/10.1126/science.1091220)

Expedition 325 Preliminary Report

Table T1. Coring summary, Expedition 325. (See table notes.)

Hole	Latitude	Longitude	Water depth (m)		Number of core runs	Interval cored (m)	Core recovered (m)	Core recovery (%)	Penetration depth DSF-A (m)	Hole recovery (%)	Time on site (days)
			EM300	Drill string							
325-											
M0030A	19.6819°S	150.2379°E	83.47	85.00	2	6.00	0.24	4.00	6.00	4.00	0.85
M0030B	19.68188°S	150.23791°E	83.47	85.00	3	9.00	0.55	6.11	9.00	6.11	0.40
M0031A	19.67895°S	150.23961°E	90.05	92.00	17	43.00	5.68	13.21	43.00	13.21	2.09
M0032A	19.678836°S	150.239666°E	91.58	93.00	20	36.70	5.99	16.32	36.70	16.32	1.15
M0033A	19.678886°S	150.239862°E	91.32	91.50	23	32.80	13.41	40.88	32.80	40.88	1.15
M0034A	19.69226°S	150.230254°E	51.00	55.00	16	23.10	6.71	29.05	23.10	29.05	3.19
M0035A	19.672637°S	150.243834°E	100.05	103.00	23	29.90	12.23	40.90	29.90	40.90	2.98
M0036A	19.672398°S	150.243964°E	103.21	103.00	22	34.00	8.91	26.21	34.00	26.21	1.77
M0037A	19.670749°S	150.246265°E	122.29	129.17	14	21.00	7.52	35.81	21.00	35.81	0.83
M0038A	19.671602°S	150.244904°E	107.04	108.58	1	1.50	0.18	12.00	1.50	12.00	0.53
M0039A	19.671595°S	150.244888°E	107.04	108.58	21	28.40	10.39	36.58	28.40	36.58	1.02
M0040A	19.796286°S	150.481417°E	126.07	132.67	12	21.50	11.73	54.56	21.50	54.56	0.61
M0041A	19.796324°S	150.481503°E	126.58	132.67	12	22.10	10.06	45.52	22.10	45.52	0.55
M0042A	19.84398°S	150.44803°E	50.78	56.32	29	46.40	10.94	23.58	46.40	23.58	2.19
M0043A	19.798851°S	150.479365°E	102.93	107.88	23	35.00	6.04	17.26	35.00	17.26	0.85
M0044A	19.798453°S	150.479617°E	105.25	104.31	9	11.00	1.67	15.18	11.00	15.18	0.72
M0045A	19.798421°S	150.479609°E	105.25	105.01	4	14.60	0.00	0.00	14.60	0.00	0.24
M0046A	19.798468°S	150.479625°E	117.49*	120.41*	11	20.40	2.52	12.35	20.40	12.35	0.45
M0047A	19.799752°S	150.478853°E	99.12	100.51	14	33.20	3.79	11.42	33.20	11.42	0.56
M0048A	19.801176°S	150.477653°E	97.47	102.31	4	7.10	0.69	9.72	7.10	9.72	0.28
M0049A	15.472375°S	145.823698°E	97.63	98.61	2	3.50	0.77	22.00	3.50	22.00	0.24
M0049B	15.472372°S	145.823694°E	97.63	100.00	13	15.60	2.79	17.88	15.60	17.88	0.52
M0050A	15.472337°S	145.823697°E	97.63	98.20	6	10.50	1.87	17.81	10.50	17.81	0.27
M0051A	15.472138°S	145.823013°E	78.13	80.90	2	2.50	0.15	6.00	2.50	6.00	0.35
M0052A	17.101109°S	146.576317°E	97.63	103.70	1	1.40	1.30	92.86	1.40	92.86	0.25
M0052B	17.101109°S	146.576333°E	97.63	103.70	4	6.90	0.46	6.67	6.90	6.67	0.30
M0052C	17.101115°S	146.576327°E	97.63	106.80	2	1.90	0.10	5.26	8.80	5.26	0.22
M0053A	17.101173°S	146.576328°E	97.87	104.60	33	37.30	12.18	32.65	37.30	32.65	1.59
M0054A	17.1007°S	146.576743°E	107.23	110.33	6	9.30	2.23	23.98	18.72	11.91	1.06
M0054B	17.1007°S	146.576743°E	107.23	110.33	12	27.84	8.25	29.63	33.20	24.85	2.26
M0055A	17.101888°S	146.5747°E	87.33	93.06	10	28.50	10.00	35.09	31.29	31.96	0.89
M0056A	17.102243°S	146.574162°E	81.22	85.56	16	40.20	12.73	31.67	41.29	30.83	1.05
M0057A	17.105021°S	146.563991°E	42.27	47.67	16	40.60	19.00	46.80	41.78	45.48	1.30
M0058A	17.097269°S	146.58928°E	167.14	172.41	15	41.40	33.94	81.98	41.40	81.98	1.06

Notes: * = depth correction made because of drill pipe “skipping” down a pinnacle side for 10.8 m before finally penetrating the seafloor; applying the same correction gives 117.49 m instead of the previously expected 106.69 m. EM300 = corrected EM300 echo sounder data, drill string = drill string tagging seabed including predicted tidal variations.

Expedition 325 Preliminary Report

Table T2. Summary of descriptions and measurements made during Expedition 325. (See [table notes](#).)

<i>Greatship Maya</i> , offshore GBR	Onshore Science Party, Bremen
Core description: Core catcher description	Core description: Split-core visual core description
Core photography: Core catcher photography	Discrete sample moisture and density properties: Compressional <i>P</i> -wave velocity Bulk, dry, and grain density
Whole-core multisensor logging: Density Velocity Magnetic susceptibility Electrical resistivity	Water content Porosity Core photography: Photography of massive corals and their specialized splitting
Geochemistry: pH by ion-specific electrode Alkalinity by single-point titration to pH Ammonium by flow injection method Salinity by refractometer	Geochemistry: IW analysis by ICP-OES (major and trace elements) IC (chloride, bromide, sulfate, and nitrate) Sediment TOC, TC, and TS by LECO (carbon-sulfur analyzer) Sediment mineralogy by XRD
Downhole logging: Spectral natural gamma ray Total natural gamma ray Full waveform sonic Optical imaging Acoustic imaging Caliper Magnetic susceptibility Electrical conductivity	Micropaleontology: Benthic foraminifers Planktonic foraminifers Other: Thermal conductivity Color reflectance of split-core surface at discrete points Continuous digital line scanning of split-core surface CT scanning (selected cores only) Discrete paleomagnetic measurements Discrete magnetic susceptibility measurements

Notes: IW = interstitial water, ICP-OAES = inductively coupled plasma–optical emission spectroscopy. IC = ion chromatography. TOC = total organic carbon, TC = total carbon, TS = total sulfur. XRD = X-ray diffraction. CT = computed tomography.

Table T3. Geochemical data relating to interstitial water collected from the HYD-01C transect, Expedition 325. (Continued on next page.) (See table note.)

Core, section, interval (cm)	Depth (CSF-A)	Sample ID	pH	Alk (mM)	NH ₄ (mM)	Ca (mM)	Si (μM)	Sr (μM)	Mg (mM)	B (mM)	K (mM)	S (mM)	Na (mM)	Ba (μM)	Li (μM)	Al (μM)	As (μM)	Be (μM)
325-M0031A-10R-1, 15	20.65	S1	7.660	6.575	0.114	11.2684	73.2376	90.5740	49.7081	0.4441	9.6136	26.2746	437.2559	0.1319	24.4739	46.2161	0.0000	0.1909
325-M0033A-21R-1, 38	27.18	S3	7.634	3.173	0.030	9.8019	60.4224	91.9498	51.7301	0.4538	10.0606	27.0513	463.5383	0.0712	27.6947	55.3696	0.3503	0.1064
22R-1, 42	28.72	S4	7.543	2.668	0.013	10.5207	46.4216	100.5966	53.3171	0.4361	10.2384	28.9109	478.2124	0.0927	24.2419	48.4290	0.3492	0.1187
325-M0035A-13R-1, 30–35	16.78	S6	7.649	4.667	0.028	—	—	—	—	—	—	—	—	—	—	—	—	—
325-M0036A-4R-1, 76	4.26	S7	7.436	7.474	0.005	—	—	—	—	—	—	—	—	—	—	—	—	—
14R-1, 25	18.75	S8	7.603	5.985	0.000	10.4934	66.2492	94.5942	46.9639	0.3995	9.1419	25.1453	435.7008	0.1016	21.3060	59.4057	0.0000	0.1250
21R-2, 6	29.9	S9	7.892	5.481	0.705	8.9722	155.3092	136.6600	48.0593	0.5949	9.8599	24.8596	451.6778	0.1067	39.8089	50.6086	0.2372	0.1021
325-M0037A-1R-1, 30	0.3	S10	7.609	2.326	0.008	10.1792	55.7373	89.7069	52.7886	0.4266	10.3715	28.6486	475.7374	0.0638	25.1570	46.2647	0.0000	0.0837
1R-2, 15	1.65	S11	7.771	2.300	0.010	10.0156	48.5527	87.8958	52.8316	0.4204	10.9513	28.7289	472.1911	0.0493	26.9581	41.0125	0.1334	0.1437
7R-1, 8	9.58	S12	7.591	3.106	0.040	—	—	—	—	—	—	—	—	—	—	—	—	—
9R-1, 30	12.8	S13	7.680	3.427	0.038	10.2585	67.4373	102.6599	52.4902	0.4429	10.1925	27.8488	453.9781	0.0571	26.6202	40.5371	0.0990	0.1007
10R-1, 126	15.26	S14	7.661	3.088	0.063	10.3093	85.7664	117.9545	53.0022	0.4489	10.1937	28.5889	469.9897	0.0763	27.1897	46.8438	0.0000	0.1310
13R-1, 27	18.27	S15	7.664	3.021	0.112	10.4348	102.5683	133.1171	52.9769	0.4465	10.2070	28.6883	460.4748	0.0694	27.5248	45.6267	0.3850	0.1248
325-M0039A-5R-1, 28	6.28	S16	7.722	3.762	0.017	9.1096	53.3462	72.1539	50.2965	0.4085	9.6703	26.0278	404.3193	0.0919	26.4080	46.9404	0.0000	0.0984
20R-1, 19	25.59	S17	7.542	5.249	0.017	10.0419	43.7029	76.5696	44.3400	0.3547	8.6521	23.5549	381.5826	0.1126	21.8232	35.9847	0.3502	0.1112
21R-1, 18	27.08	S18	7.660	3.337	0.014	10.5320	52.5293	96.2851	52.8849	0.4373	10.2598	28.4540	446.8340	0.0997	24.2092	45.7782	0.0509	0.0741

Note: — = no result.

Table T3 (continued).

Core, section, interval (cm)	Depth (CSF-A)	Sample ID	Cd (μM)	Co (μM)	Cr (μM)	Cu (μM)	Fe (μM)	Mn (μM)	Mo (μM)	Ni (μM)	P (μM)	Pb (μM)	Ti (μM)	V (μM)	Zn (μM)	Zr (μM)	Cl (mM)	Br (mM)	SO ₄ (mM)
325-M0031A-10R-1, 15	20.65	S1	0.0254	0.0414	0.0316	0.0000	13.1251	1.4496	0.1433	0.4432	2.9749	0.0227	0.0000	0.2097	5.6026	0.7163	516.841	0.802	26.931
325-M0033A-21R-1, 38	27.18	S3	0.0000	0.0000	0.0000	0.0000	1.5934	0.0221	0.0000	0.0303	4.7105	0.0000	0.0000	0.1366	3.9739	0.4324	557.238	0.855	28.131
22R-1, 42	28.72	S4	0.0000	0.0000	0.0000	0.0000	0.9344	0.0000	0.0000	0.0000	2.0588	0.0000	0.0000	0.2674	3.7950	0.3432	567.230	0.879	29.525
325-M0035A-13R-1, 30-35	16.78	S6	—	—	—	—	—	—	—	—	—	—	—	—	—	—	—	—	—
325-M0036A-4R-1, 76	4.26	S7	—	—	—	—	—	—	—	—	—	—	—	—	—	—	—	—	—
14R-1, 25	18.75	S8	0.0000	0.0265	0.0000	0.0000	3.6786	0.1288	0.0000	0.0450	13.9705	0.0419	0.0000	0.1226	4.1171	0.2015	544.336	0.845	28.300
21R-2, 6	29.9	S9	-0.0000	0.0000	0.0584	0.0863	0.9644	0.0562	0.0000	0.0447	3.4828	0.0000	0.0000	0.1978	3.7370	0.3226	553.760	0.861	25.621
325-M0037A-1R-1, 30	0.3	S10	0.0000	0.0490	0.0000	0.0000	7.9513	0.3620	0.0000	0.0000	1.1133	0.0000	0.0000	0.0000	3.5477	0.2446	568.674	0.889	29.775
1R-2, 15	1.65	S11	0.0000	0.0000	0.0000	0.0000	1.0256	0.5249	0.0000	0.0606	1.8867	0.0075	0.0000	0.1397	3.5819	0.2537	561.597	0.878	29.425
7R-1, 8	9.58	S12	—	—	—	—	—	—	—	—	—	—	—	—	—	—	—	—	—
9R-1, 30	12.8	S13	0.0000	0.0000	0.0000	0.0000	1.3782	0.0058	0.0000	0.0000	1.8158	0.0000	0.0000	0.4868	4.1695	0.2971	553.196	0.862	28.554
10R-1, 126	15.26	S14	0.0007	0.0000	0.0000	0.0000	1.0996	0.0118	0.0000	0.0318	2.6406	0.0000	0.0027	0.0970	4.5060	0.2823	570.161	0.888	29.366
13R-1, 27	18.27	S15	0.0037	0.0000	0.0000	0.0000	1.3279	0.0120	0.0000	0.0000	2.0483	0.0135	0.0000	0.4078	3.6653	0.3281	568.973	0.892	29.583
325-M0039A-5R-1, 28	6.28	S16	0.0000	0.0368	0.0000	0.2761	0.9737	0.1028	0.0000	0.0660	5.4778	0.0000	0.0000	0.3776	4.0520	0.3940	518.296	0.804	26.666
20R-1, 19	25.59	S17	0.0000	0.0000	0.0000	0.2059	1.3051	0.4451	1.7756	0.1326	12.3202	0.0000	0.0993	0.1275	4.1397	0.2868	—	—	—
21R-1, 18	27.08	S18	0.0000	0.0000	0.0000	0.0000	0.8836	0.0449	0.4917	0.0006	3.0915	0.0000	0.0000	0.3701	3.6850	0.2909	546.753	0.853	28.752

Table T4. Geochemical data relating to interstitial water collected from the HYD-02A transect, Expedition 325. (Continued on next page.) (See table note.)

Core, section, interval (cm)	Depth (CSF-A)	Sample ID	pH	Alk (mM)	NH ₄ (mM)	Ca (mM)	Si (μM)	Sr (μM)	Mg (mM)	B (mM)	K (mM)	S (mM)	Na (mM)	Ba (μM)	Li (μM)	Al (μM)	As (μM)	Be (μM)
325-M0040A-																		
1R-1, 75	0.75	S19	7.768	2.652	0.045	10.5814	103.3102	105.2575	53.0810	0.4268	10.3297	28.7083	466.7886	0.0762	25.5719	41.8549	0.0681	0.1670
1R-2, 21	1.72	S20	7.708	3.043	0.042	10.5983	107.1337	108.4624	53.3623	0.4328	10.4080	28.7980	470.0387	0.0736	26.2760	40.4366	0.0000	0.0543
10R-1, 36	14.36	S21	7.806	3.436	0.061	9.8397	81.2545	96.6237	51.5216	0.4553	10.1272	26.3788	442.1514	0.0742	28.8150	40.4363	0.0000	0.0943
12R-1, 92	19.42	S22	7.696	2.787	0.030	10.5511	91.8760	114.1451	53.3527	0.4432	10.2806	29.2198	446.4632	0.0742	25.3116	47.2273	0.0000	0.1353
325-M0041A-																		
1R-1, 27	0.27	S23	7.637	2.745	0.027	10.2558	97.5419	98.5440	52.8028	0.4514	10.4782	28.7009	465.3980	0.0706	24.7575	44.1129	0.0000	0.1022
8R-1, 42	13.32	S24	7.760	2.936	0.030	10.4657	69.1398	110.1113	53.4591	0.4512	10.2860	28.8220	465.8233	0.0821	26.2101	42.2941	0.0000	0.1413
10R-1, 72	16.82	S25	7.723	2.838	0.034	10.5299	72.8010	111.9237	53.5546	0.4464	10.2791	29.4385	472.0512	0.0700	27.3837	42.1953	0.1384	0.0712
11R-1, 60	18.2	S26	7.712	2.607	0.032	10.5660	69.5859	115.1079	53.8051	0.4407	10.2690	29.6715	456.6070	0.0745	25.1990	39.3609	0.0000	0.0928
12R-1, 29	19.39	S27	7.667	2.805	0.029	10.6179	76.4194	116.2952	53.7578	0.4424	10.3108	29.1098	468.9157	0.0738	25.3284	44.0197	0.0281	0.1079
12R-1, 130	20.4	S28	7.665	2.556	0.030	10.5807	80.9219	116.8019	53.7830	0.4446	10.3158	28.8864	471.7450	0.0797	26.0274	43.9958	0.0000	0.1028
325-M0042A-																		
13R-1, 36	17.86	S29	7.699	4.416	0.002	11.4577	29.1000	102.9404	49.4554	0.4214	9.8714	26.0665	424.2975	0.0942	24.6351	—	—	—
29R-1, 29	44.65	S30	7.635	5.246	0.000	14.5557	57.5074	103.7072	39.9085	0.4208	9.6910	18.5233	427.2207	0.1271	24.5292	46.0565	0.0000	0.0797
325-M0043A-																		
2R-1, 33	2.53	S31	7.838	3.109	0.000	9.9839	42.0191	81.7836	53.3539	0.4548	10.2530	28.3628	459.3678	0.0747	25.4365	50.3305	0.0000	0.0576
10R-1, 26	14.26	S32	7.612	5.045	0.040	—	—	—	—	—	—	—	—	—	—	—	—	—
18R-1, 7	26.07	S33	7.947	7.058	0.000	—	—	—	—	—	—	—	—	—	—	—	—	—
18R-1, 15	26.15	S34	7.788	3.343	0.032	10.4307	41.1054	97.4683	52.4109	0.4319	10.0330	27.2991	440.9500	0.0713	24.0719	43.9634	0.1832	0.0988
325-M0046A-																		
13R-2, 3	29.34	S36	7.705	4.977	0.039	—	—	—	—	—	—	—	—	—	—	—	—	—
13R-2, 6	29.37	S35	7.726	6.591	0.010	9.0566	38.4786	65.3275	53.8782	0.4472	10.0058	26.8378	449.0131	0.0623	26.8714	37.1363	0.0698	0.1233
325-M0047A-																		
8R-1, 14	18.34	S37	7.774	5.171	0.014	—	—	—	—	—	—	—	—	—	—	—	—	—
8R-1, 20	18.4	S38	7.694	4.007	0.030	10.0468	38.9004	96.8789	52.0754	0.4316	9.9225	27.3476	438.4033	0.0668	24.4646	48.8829	0.0000	0.0775

Note: — = no result.

Table T4 (continued).

Core, section, interval (cm)	Depth (CSF-A)	Sample ID	Cd (μM)	Co (μM)	Cr (μM)	Cu (μM)	Fe (μM)	Mn (μM)	Mo (μM)	Ni (μM)	P (μM)	Pb (μM)	Ti (μM)	V (μM)	Zn (μM)	Zr (μM)	Br (mM)	SO ₄ (mM)
325-M0040A-																		
1R-1, 75	0.75	S19	0.0000	0.0000	0.0000	0.0000	0.9816	0.2901	0.0000	0.0000	2.6510	0.0000	0.0504	0.0067	3.8744	0.2562	0.890	29.795
1R-2, 21	1.72	S20	0.0000	0.0000	0.0000	0.0000	1.2384	0.2769	0.0000	0.0000	1.5459	0.0000	0.0000	0.0000	3.3718	0.2622	0.907	29.808
10R-1, 36	14.36	S21	0.0000	0.0000	0.0000	0.0000	1.0346	0.0120	0.0000	0.0384	4.0918	0.0000	0.0000	0.5308	3.7416	0.2216	0.871	27.143
12R-1, 92	19.42	S22	0.0000	0.0000	0.0000	0.0000	1.8694	0.0629	0.0000	0.0124	2.3713	0.0000	0.0045	0.0000	5.3669	0.3081	0.899	29.803
325-M0041A-																		
1R-1, 27	0.27	S23	0.0108	0.0227	0.0000	0.0000	1.1763	0.2500	0.0000	0.0000	3.9473	0.0000	0.0000	0.0000	3.3571	0.2947	0.897	29.763
8R-1, 42	13.32	S24	0.0000	0.0000	0.0000	0.0000	0.9379	0.0162	0.0000	0.0023	1.1490	0.0000	0.0000	0.1333	3.9585	0.2566	0.901	29.626
10R-1, 72	16.82	S25	0.0000	0.0000	0.0000	0.0000	0.9581	0.0480	0.0000	0.0000	32.9156	0.0000	0.0000	0.1526	3.2650	0.2376	0.903	29.648
11R-1, 60	18.2	S26	0.0000	0.0000	0.0000	0.0000	1.6393	0.0250	0.0000	0.0000	1.1896	0.0000	0.0000	0.0651	3.5304	0.2624	0.908	29.653
12R-1, 29	19.39	S27	0.0000	0.0000	0.0000	0.0000	1.3198	0.0229	0.0000	0.0362	1.8632	0.0020	0.0000	0.0000	3.8698	0.3266	0.890	29.090
12R-1, 130	20.4	S28	0.0000	0.0000	0.0000	0.0000	2.2412	0.0370	0.0000	0.0357	0.7824	0.0000	0.0005	0.0867	3.6578	0.2280	0.920	30.052
325-M0042A-																		
13R-1, 36	17.86	S29	—	—	—	—	—	—	—	—	—	—	—	—	—	—	0.867	26.663
29R-1, 29	44.65	S30	0.0000	0.0000	0.0000	0.0000	1.3981	0.1201	0.1894	0.1005	7.4072	0.0000	0.0000	0.0000	3.8354	0.3081	0.835	19.187
325-M0043A-																		
2R-1, 33	2.53	S31	0.0000	0.1207	0.0000	0.0000	1.0275	0.0971	0.0000	0.1328	1.3298	0.0000	0.0000	0.1498	3.5513	0.3413	0.914	29.324
10R-1, 26	14.26	S32	—	—	—	—	—	—	—	—	—	—	—	—	—	—	—	—
18R-1, 7	26.07	S33	—	—	—	—	—	—	—	—	—	—	—	—	—	—	—	—
18R-1, 15	26.15	S34	0.0000	0.0465	0.0000	0.0000	1.1008	0.0540	0.0000	0.1607	2.9706	0.0000	0.0000	0.0000	4.4414	0.3298	0.890	29.019
325-M0046A-																		
13R-2, 3	29.34	S36	—	—	—	—	—	—	—	—	—	—	—	—	—	—	—	—
13R-2, 6	29.37	S35	0.0000	0.0216	0.0000	0.0000	0.8742	0.0121	0.3063	0.0363	8.2073	0.0000	0.0000	1.5283	2.9166	0.4115	—	—
325-M0047A-																		
8R-1, 14	18.34	S37	—	—	—	—	—	—	—	—	—	—	—	—	—	—	—	—
8R-1, 20	18.4	S38	0.0000	0.0000	0.0000	0.0000	0.8282	0.0035	0.0000	0.0000	3.2428	0.0000	0.0000	0.5368	3.6112	0.3469	0.891	28.609

Table T5. Geochemical data relating to interstitial water collected from the RIB-02A transect, Expedition 325.

Core, section, interval (cm)	Depth (CSF-A)	Sample ID	pH	Alk (mM)	NH ₄ (mM)	Ca (mM)	Si (μM)	Sr (μM)	Mg (mM)	B (mM)	K (mM)	S (mM)	Na (mM)	Ba (μM)	Li (μM)	Al (μM)	As (μM)	Be (μM)
325-M0049A-1R-1, 35	0.35	S39	7.760	2.852	0.022	10.4571	47.8592	87.0969	52.9869	0.4331	10.2871	28.7845	457.4910	1.9327	25.9453	42.5232	0.6025	0.1527
325-M0050A-1X-1, 45	0.45	S40	7.704	3.830	0.023	10.7760	29.4716	90.0604	52.4300	0.4318	9.9958	28.1172	463.2583	0.0902	23.8118	42.8577	0.2236	0.1909

Core, section, interval (cm)	Depth (CSF-A)	Sample ID	Cd (μM)	Co (μM)	Cr (μM)	Cu (μM)	Fe (μM)	Mn (μM)	Mo (μM)	Ni (μM)	P (μM)	Pb (μM)	Ti (μM)	V (μM)	Zn (μM)	Zr (μM)	Cl (mM)	Br (mM)	SO ₄ (mM)
325-M0049A-1R-1, 35	0.35	S39	0.0000	0.0000	0.0011	0.0000	0.9292	1.0020	0.0000	0.2238	19.2720	0.0000	0.0000	0.1218	35.0625	0.3146	553.664	0.895	29.152
325-M0050A-1X-1, 45	0.45	S40	0.0000	0.1014	0.0031	0.0000	1.0867	2.5552	0.0000	0.0000	4.5743	0.0097	0.0000	0.3121	3.6688	0.7336	559.408	0.897	29.469

Table T6. Geochemical data relating to interstitial water collected from the NOG-01B transect, Expedition 325. This table is available in an [oversized format](#).

Figure F1. A. Previously published data on relative sea level from 20 cal. y BP through present (upper symbols) plotted with GISP2 $\delta^{18}\text{O}$ (proxy for temperature over Greenland; black line) for comparison, Expedition 325. Meltwater pulse 1A (MWP-1A) refers to an interval of particularly rapid sea level rise during the last deglaciation. MWP-1B = meltwater pulse 1B. YD = Younger Dryas, B/A = Bölling Alleröd, LGM = last glacial maximum. Source of data: Tahiti = Bard et al., 1996, 2010. Huon Peninsula = Chappell and Polach 1991; Edwards et al., 1993. Huon drill core = Cutler et al., 2003. Sunda shelf = Hanebuth et al., 2000. Barbados = Fairbanks, 1989; Bard et al., 1990. GISP2 = Stuiver and Grootes, 2000). **B.** Planktonic foraminifer Mg/Ca records of mixed-layer temperatures in the western sector of the Western Pacific Warm Pool (WPWP). Comparison of Indonesian and WPWP *Globigerinoides ruber* Mg/Ca-based sea-surface temperature (SST) anomaly records modified from Linsley et al. (in press). Anomalies calculated as departures relative to average of last 2,000 y. Data shown are 200 y nonoverlapping binned averages of eight cores throughout the western sector of the WPWP (black) and average of only four southern Makassar region cores (green) (see Linsley et al., in press). Orange SST data are from Oppo et al. (2009) for only the southern Makassar Strait. Light green and dashed bounding lines show the standard error (SE) of all measurements in each 200 y bin. The LGM, Holocene Climatic Optimum, and Medieval Warm Period (MWP) are indicated. Composite reconstruction indicates that SSTs in this broad region of the WPWP warmed $\sim 3^\circ\text{C}$ after the LGM and reached a maximum 0.5°C higher than in preindustrial times from $\sim 10,000$ to $7,000$ y cal. BP during the Holocene Climatic Optimum. (Figure shown on next page.)

Figure F1. (Caption shown on previous page.)

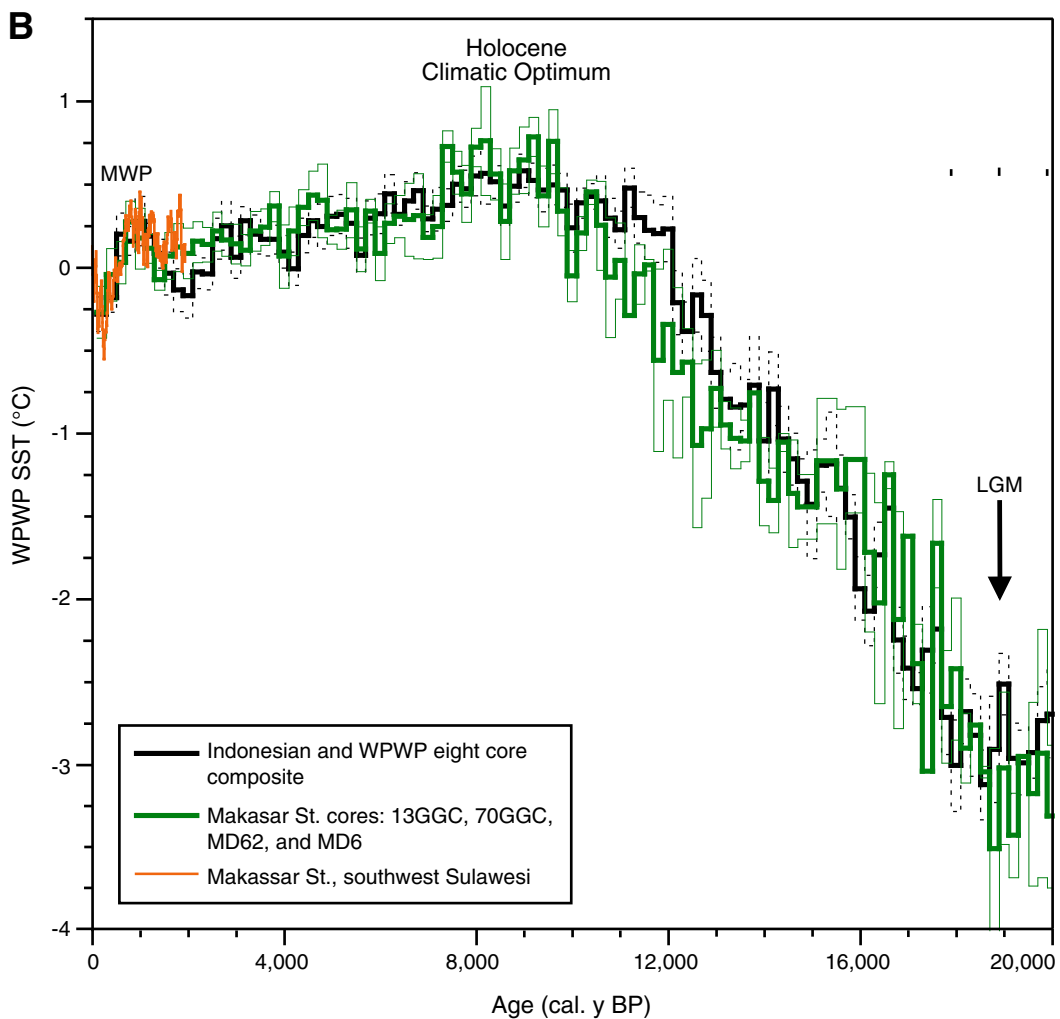
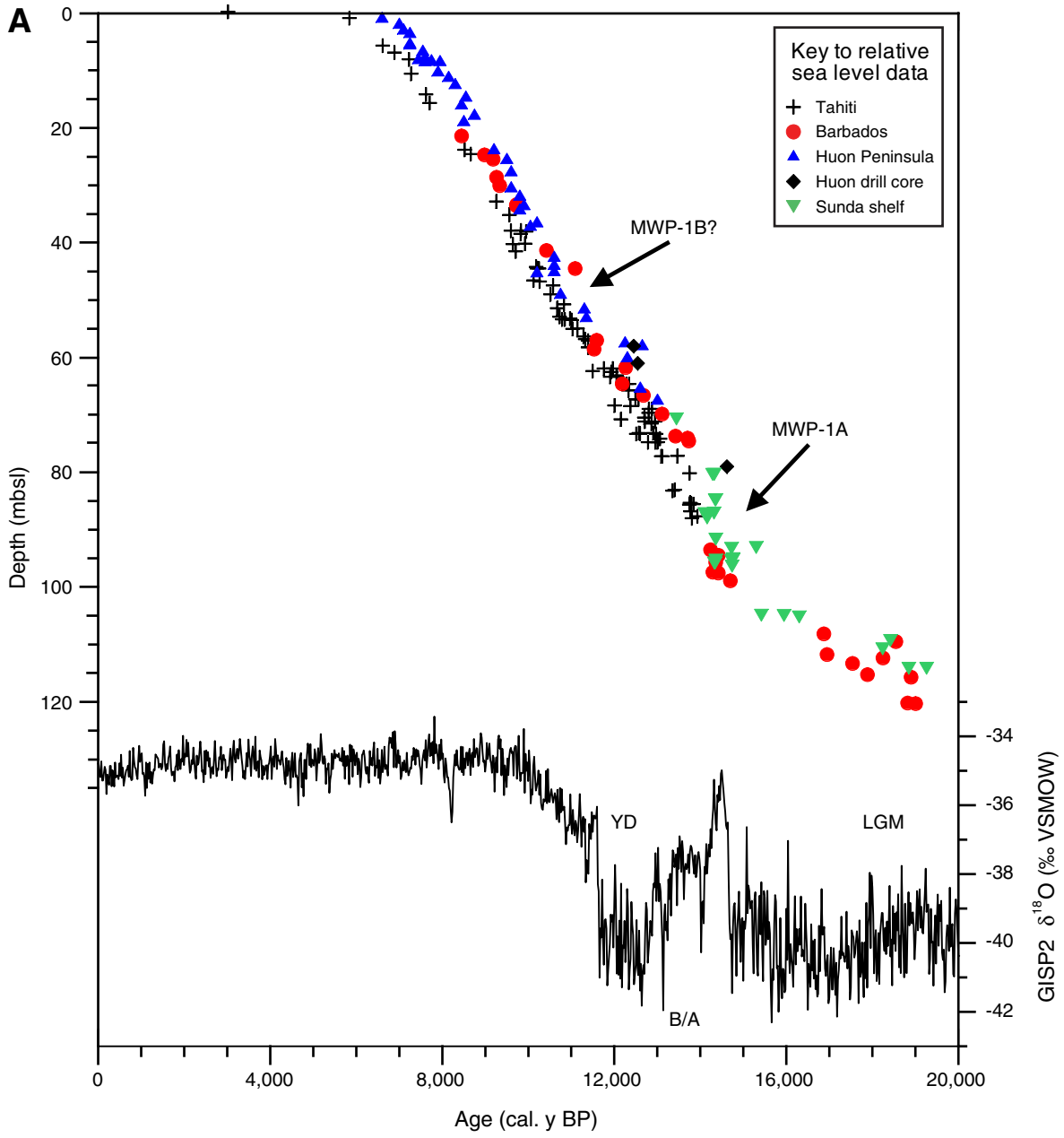


Figure F2. Regional map showing locations of the five proposed drill sites at the following regions: Ribbon Reef 3 and 5 (RIB-02A and RIB-01C, respectively), Noggin Pass (NOG-01B), and Hydrographer's Passage (HYD-01C and HYD-02A). During the offshore phase, Expedition 325 drilled sites at HYD-01C, HYD-02A, NOG-01B, and RIB-02A.

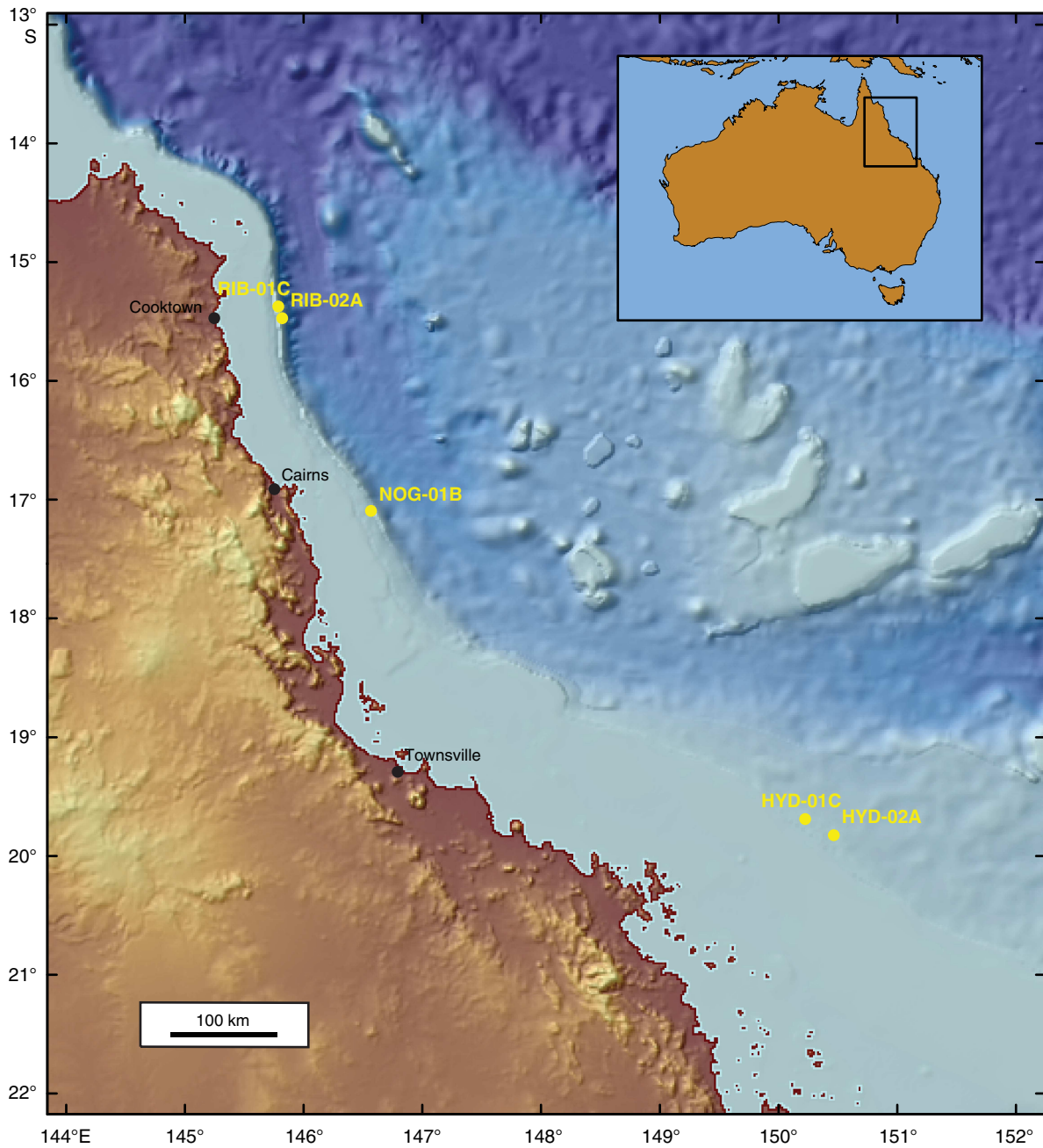


Figure F3. Contour plot showing location HYD-01C (Hydrographer's Passage), Expedition 325. Sites 1–11 and Holes M0030A–M0039A are indicated. See Figure F2 for general location.

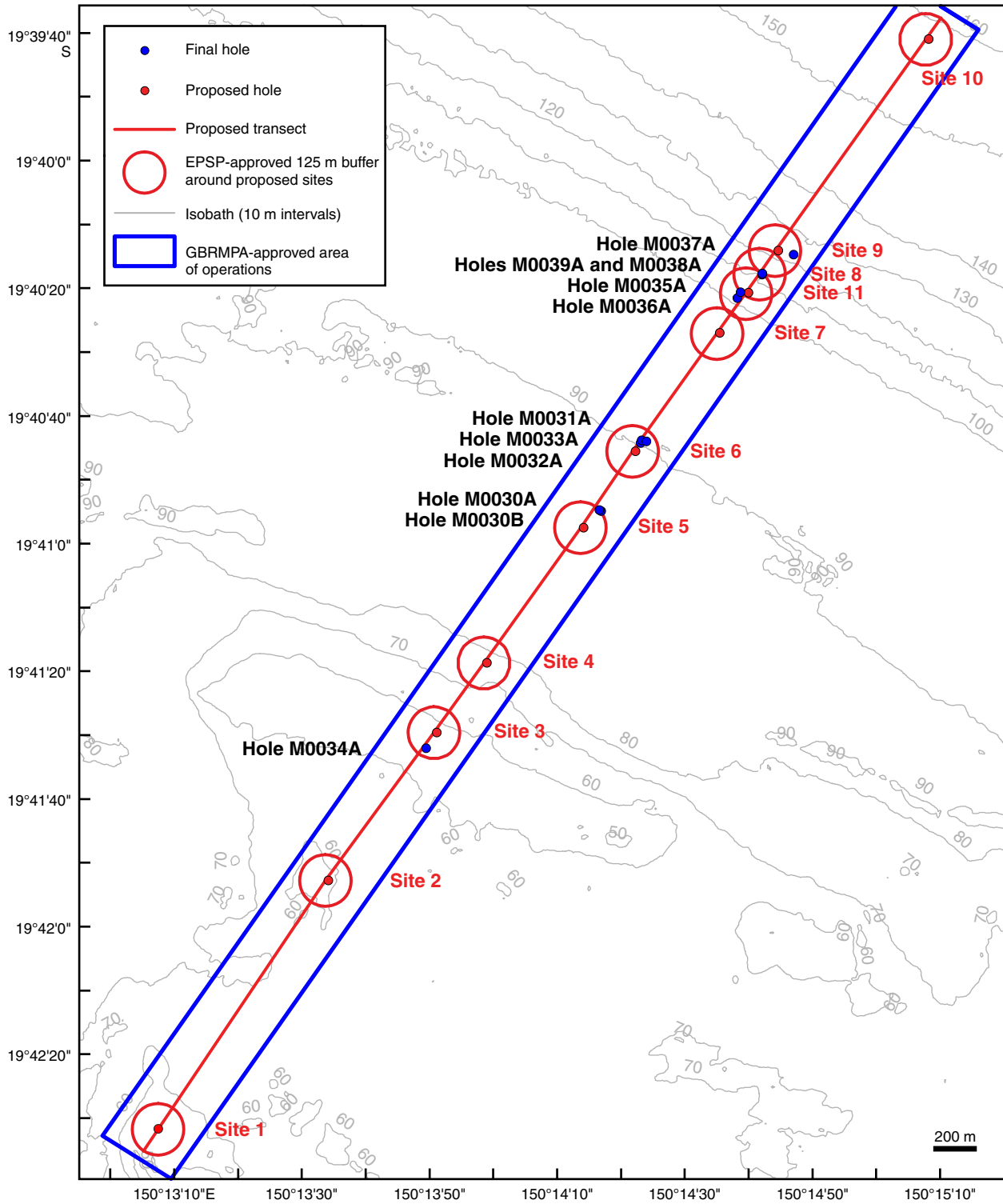


Figure F4. Topas PS18 seismic Profile SEG_SS072007_026_006 showing location of proposed drill sites at HYD-01C, Expedition 325. Approximate location of seismic profile is shown in Figure F3 (proposed transect). Red lines = actual drill locations, solid lines = holes drilled on the seismic profile transect, dashed lines = holes drilled off the seismic profile transect.

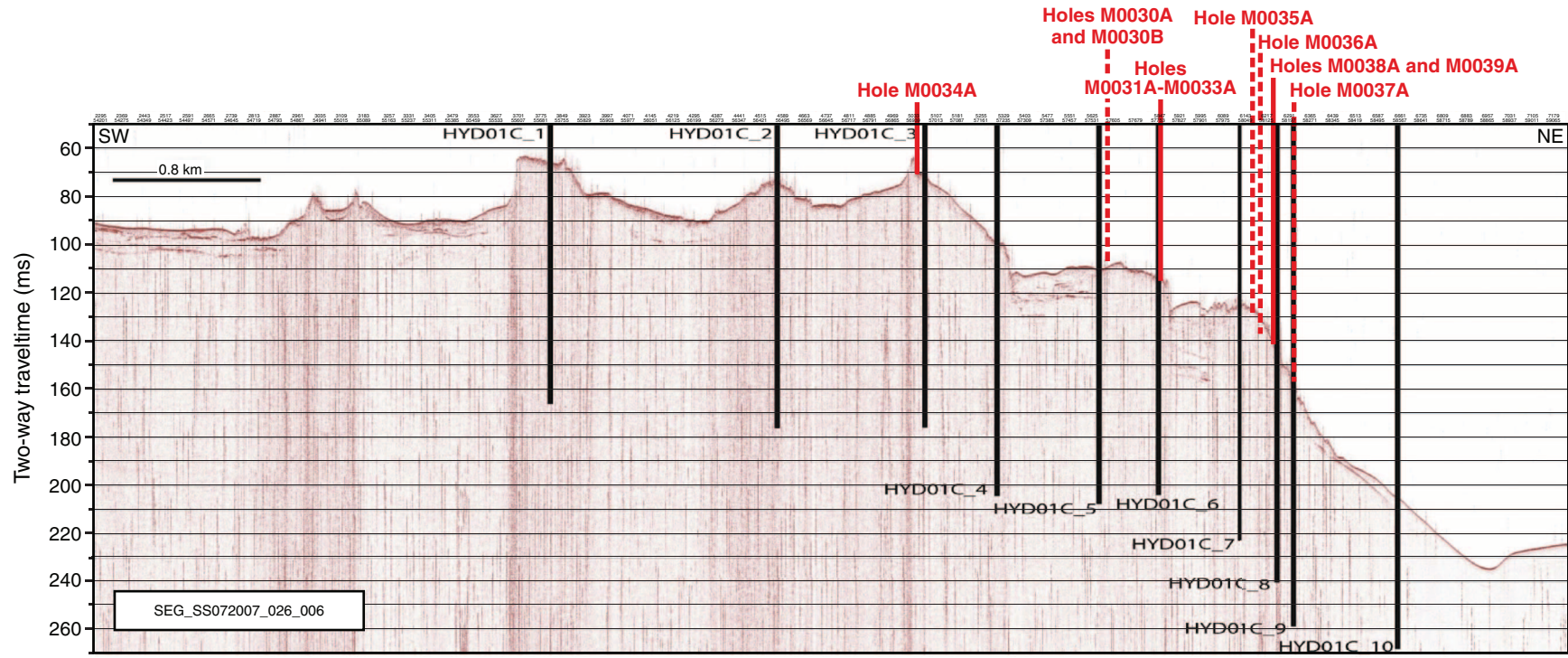


Figure F5. Contour plot showing location HYD-02A (Hydrographer’s Passage), Expedition 325. Sites 1–12 and Holes M0040A–M0048A are indicated. See Figure F2 for general location.

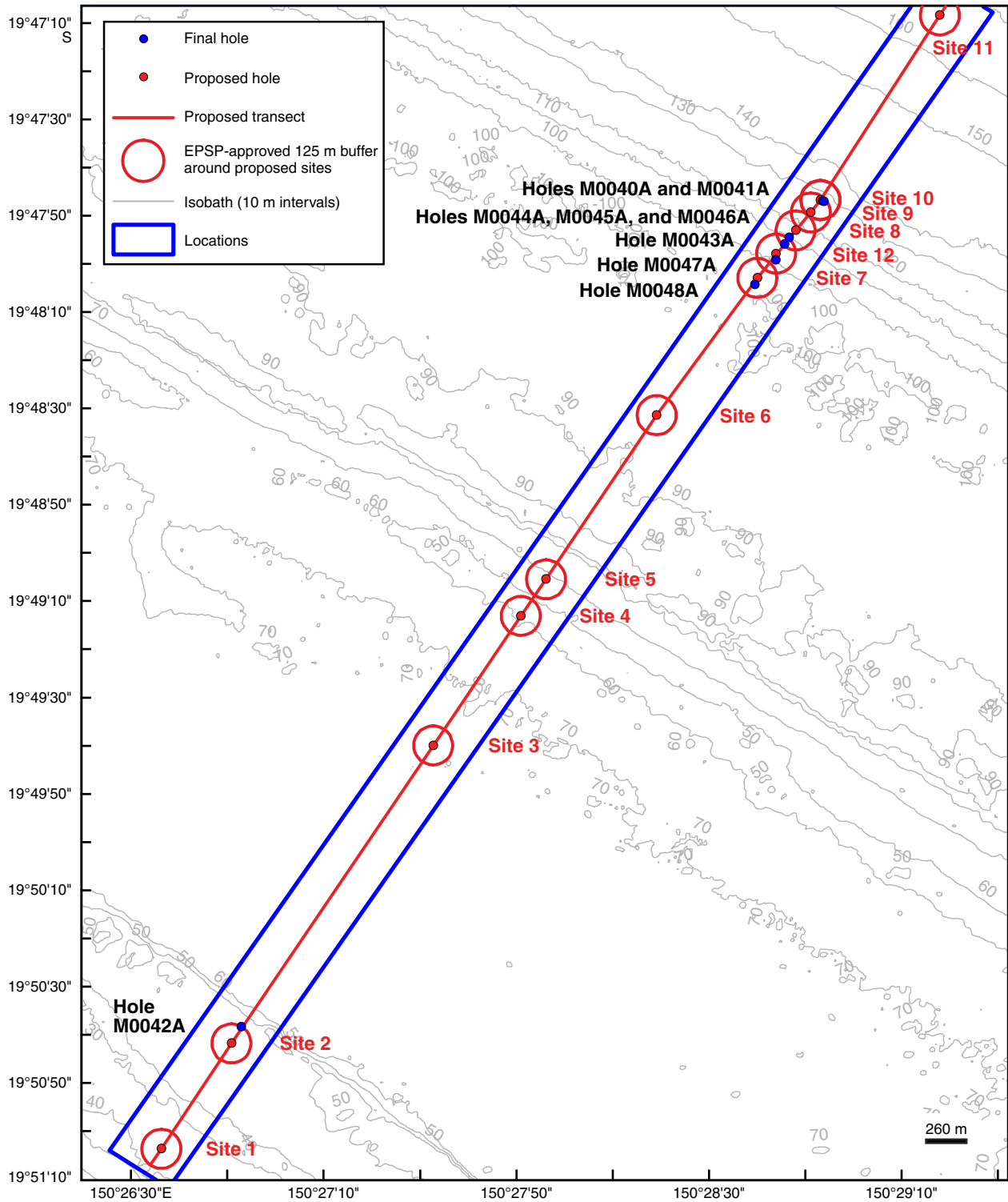


Figure F6. Topas PS18 seismic Profile SEG_SS072007_024_030 showing location of proposed drill sites at HYD-02A, Expedition 325. Approximate location of seismic profile is shown in Figure F5 (proposed transect). Red lines = actual drill locations, solid lines = holes drilled on the seismic profile transect, dashed lines = holes drilled off the seismic profile transect.

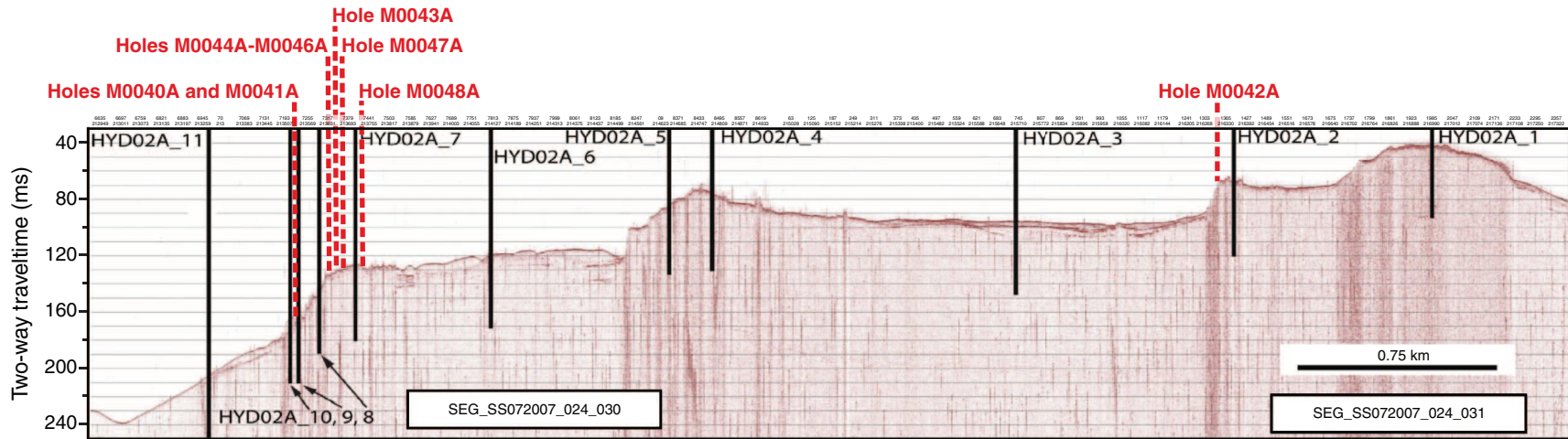


Figure F7. Contour plot showing location RIB-02A (Ribbon Reef 3), Expedition 325. Sites 1–4 and Holes M0049A–M0051A) are indicated. See Figure F2 for general location.

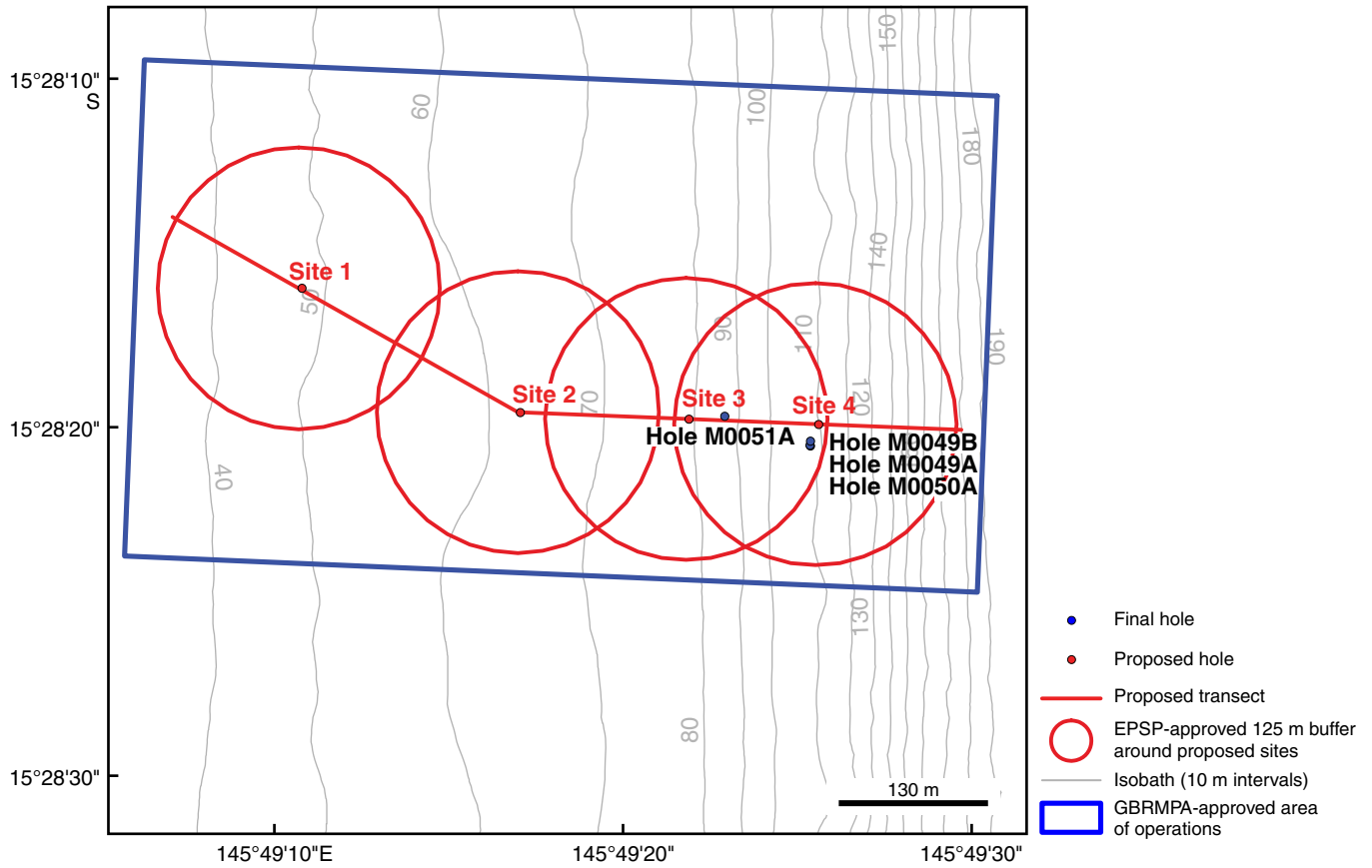


Figure F8. Topas PS18 seismic profile SEG_SS072007_006_003 showing location of proposed drill sites at RIB-02A, Expedition 325. Approximate location of seismic profile is shown in Figure F7 (proposed transect). Red lines = actual drill locations, solid lines = holes drilled on the seismic profile transect, dashed lines = holes drilled off the seismic profile transect.

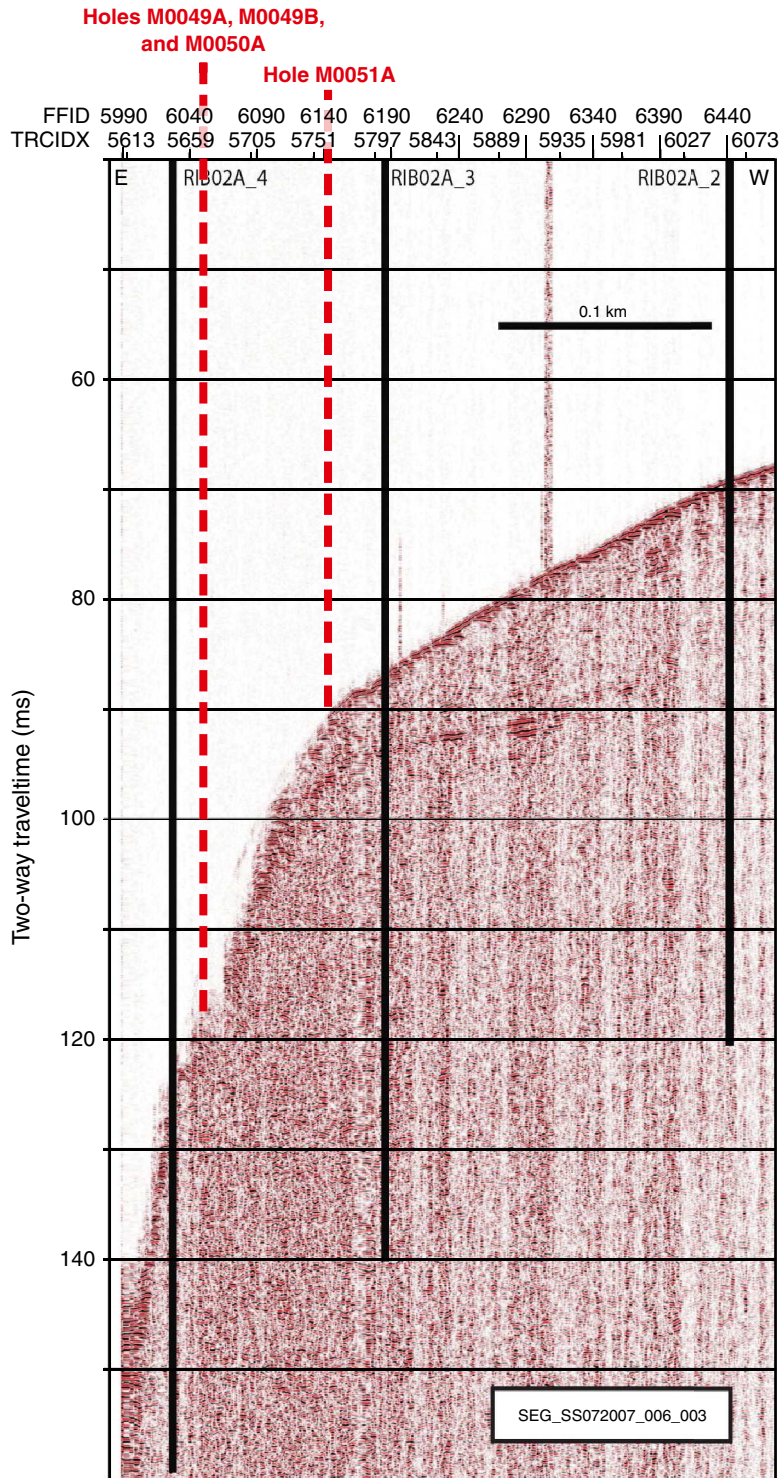


Figure F9. Contour plot showing location NOG-01B (Noggin Pass), Expedition 325. Sites 1–8 and Holes M0052A–M0058A) are indicated. See Figure F2 for general location.

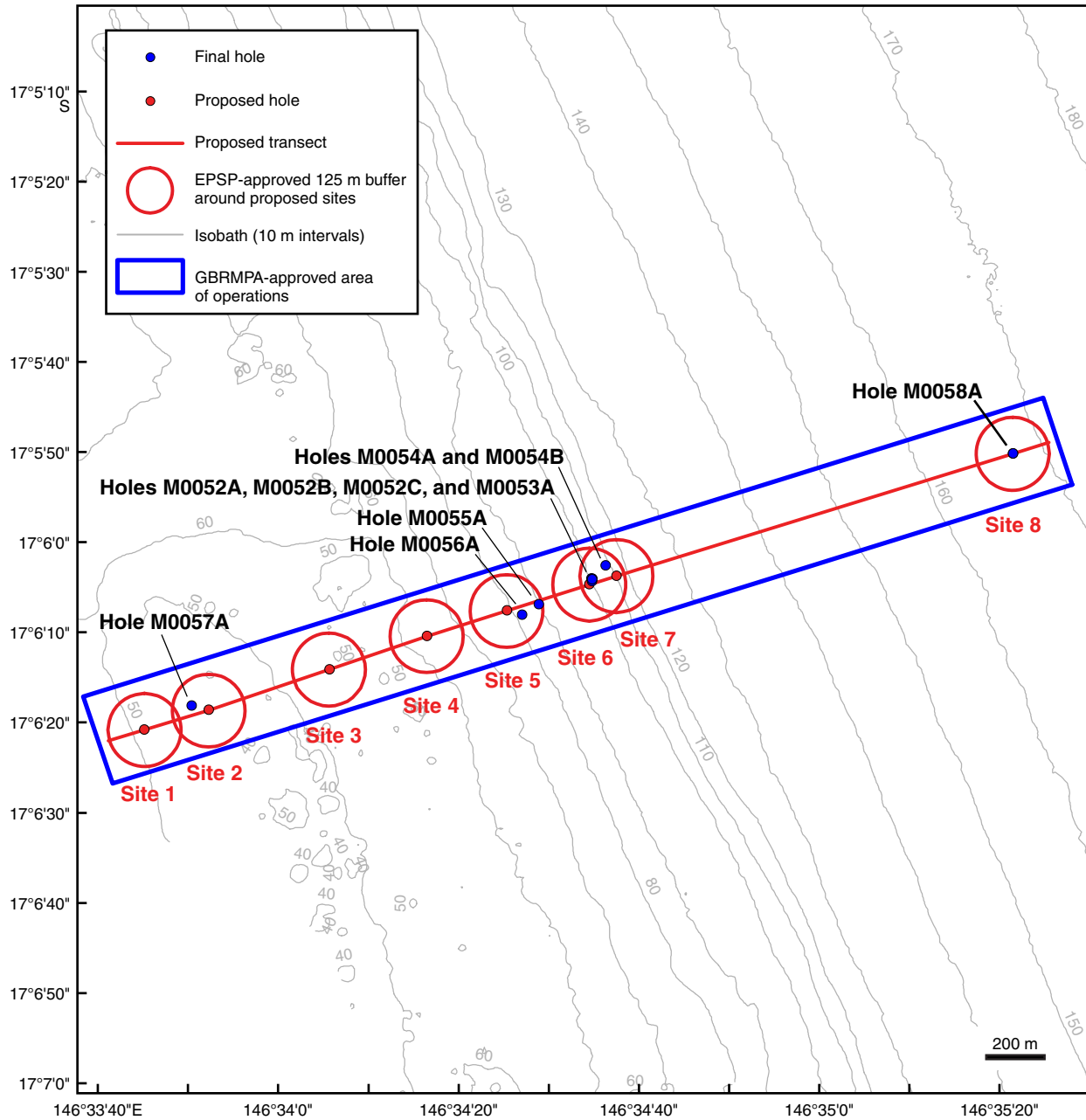


Figure F10. Topas PS18 seismic profile SEG_SS072007_012_012 showing location of proposed drill sites at NOG-01B, Expedition 325. Approximate location of seismic profile is shown in Figure F9 (proposed transect). Red lines = actual drill locations, solid lines = holes drilled on the seismic profile transect, dashed lines = holes drilled off the seismic profile transect.

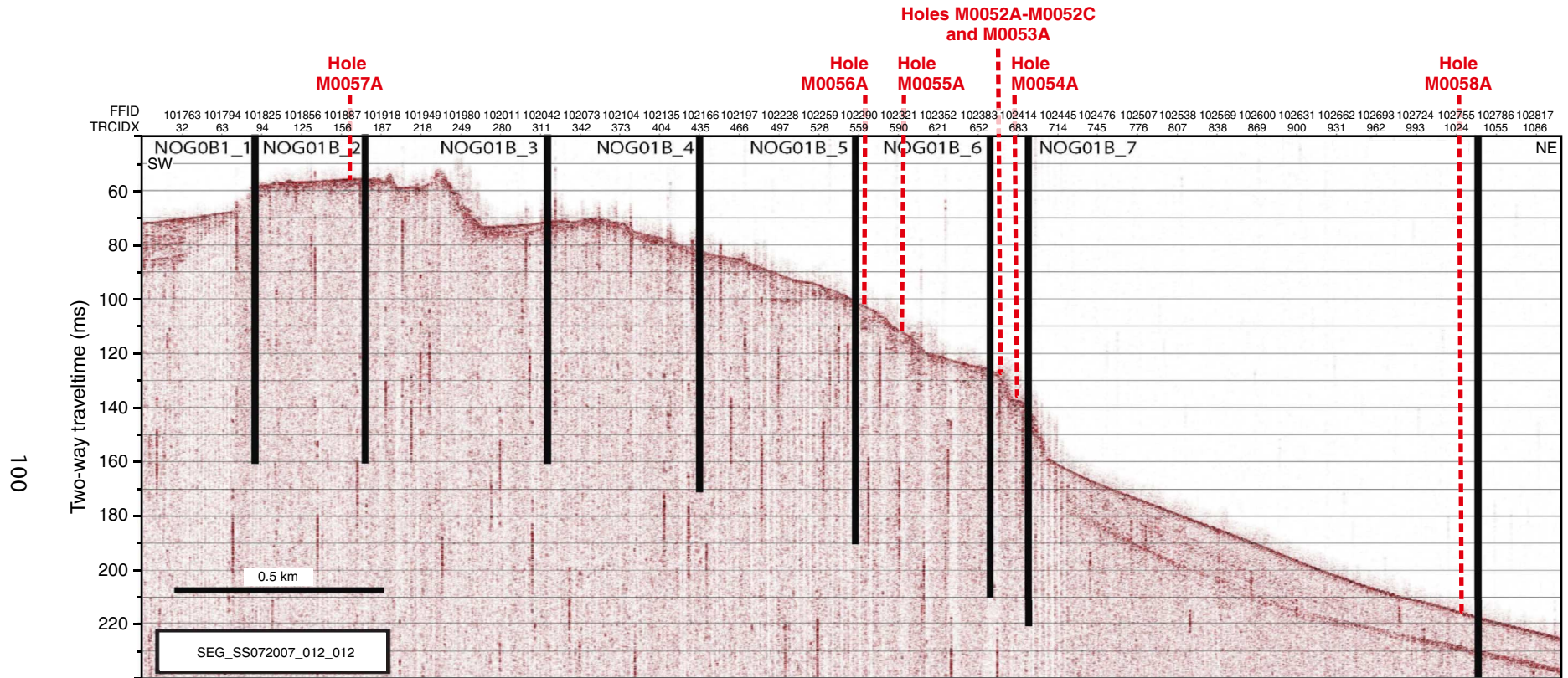


Figure F11. Enlargement of Figure F3 showing holes along the HYD-01C transect, Expedition 325. **A.** Holes M0030A–M0033A. **B.** Holes M0035A–M0039A.

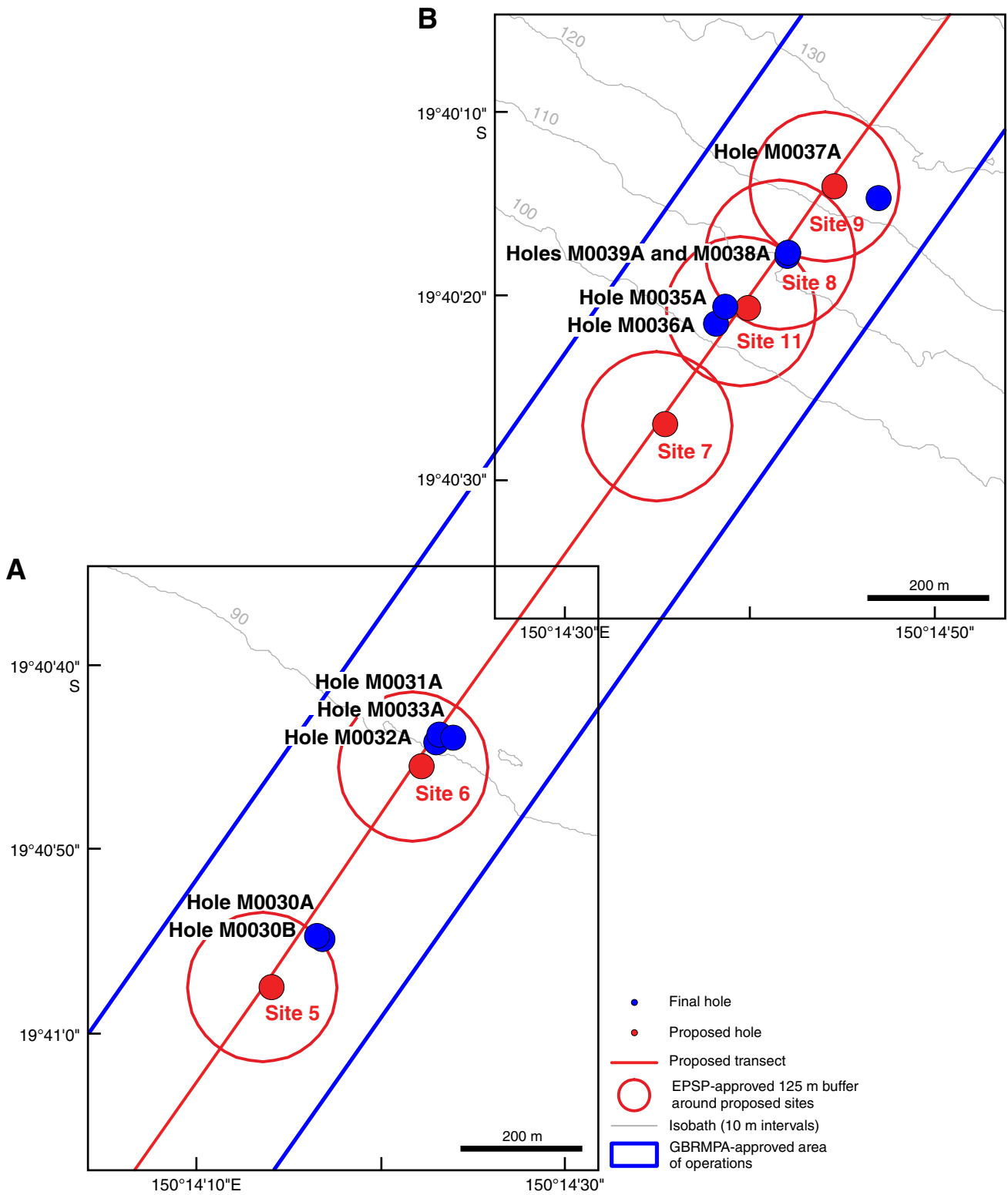


Figure F12. Enlargement of Figure F5 showing Holes M0040A, M0041A and M0043A–M0048A at HYD-02A, Expedition 325.

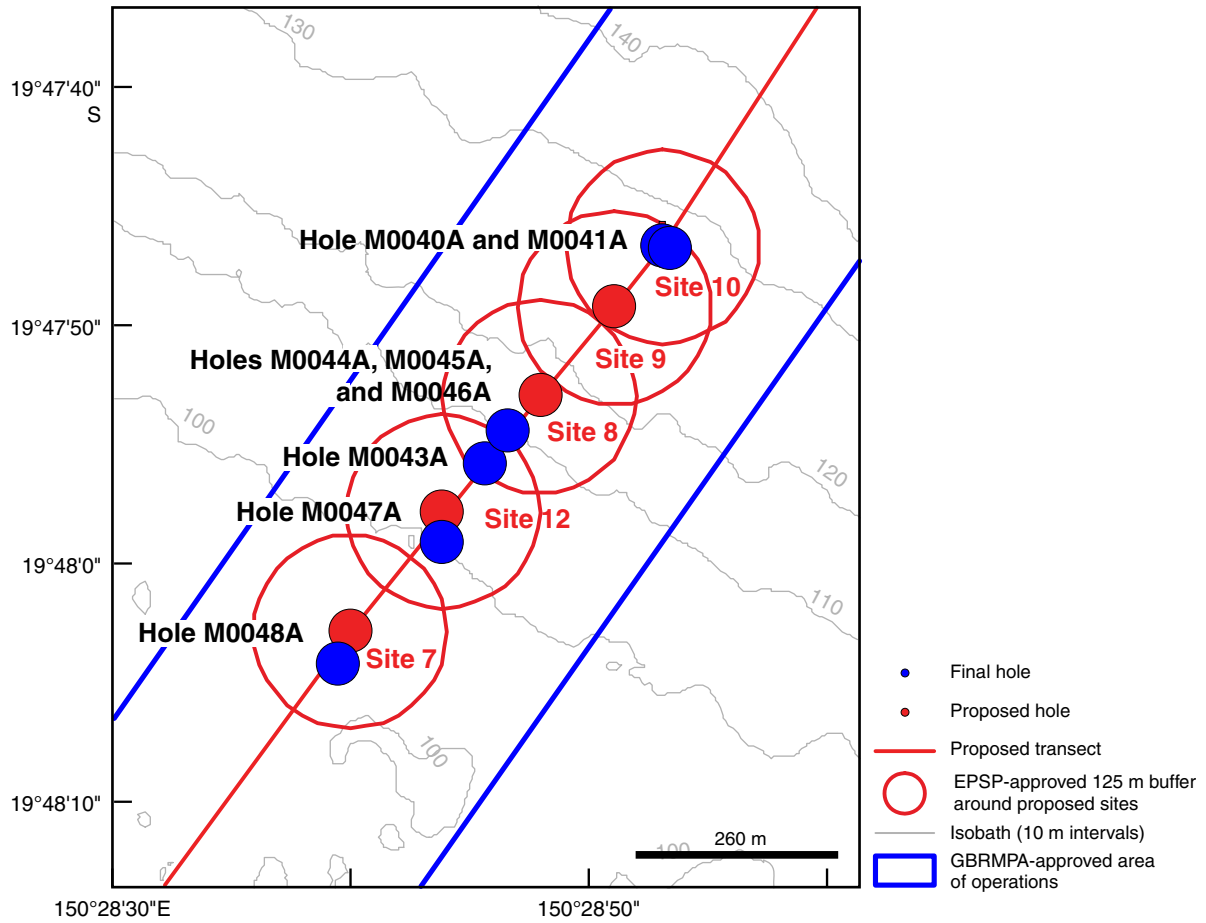


Figure F13. Enlargement of Figure F7 showing Holes M0049A–M0051A at RIB-02A, Expedition 325.

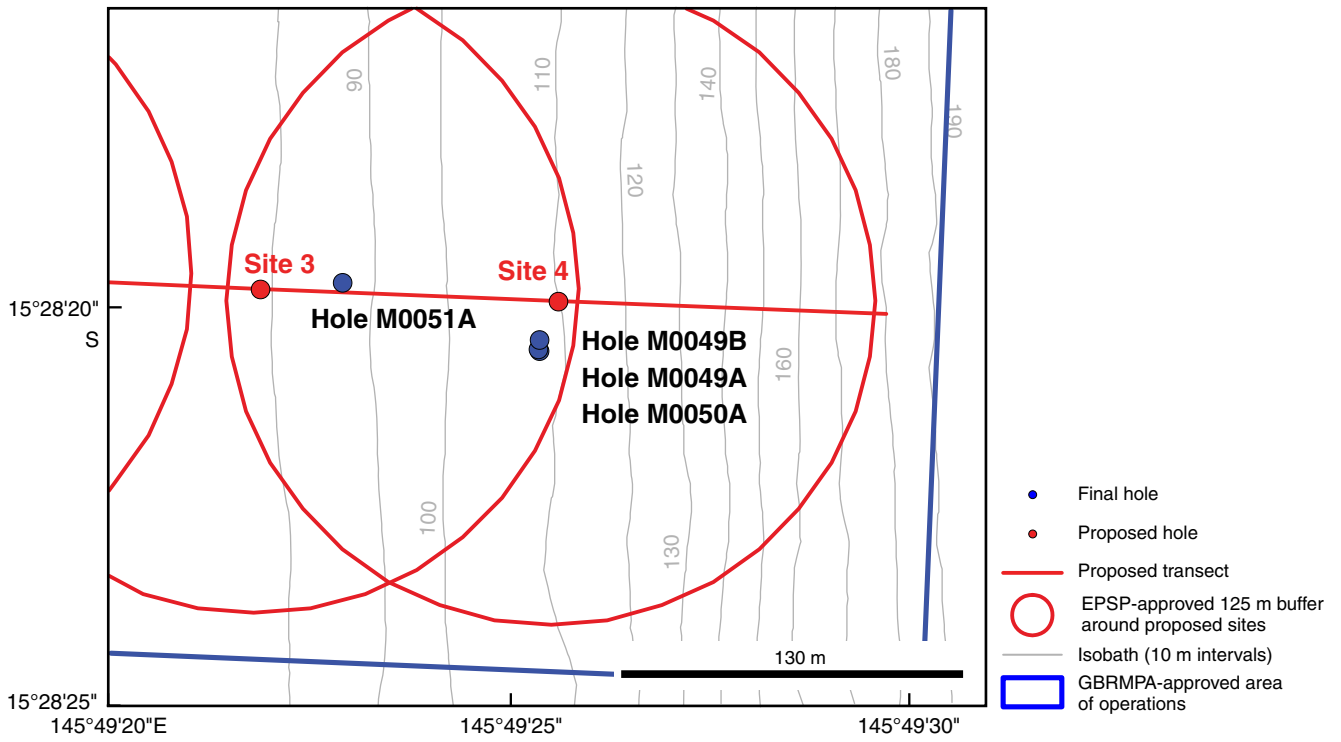


Figure F14. Enlargement of Figure F9 showing Holes M0052A–M0056A at NOG-01B, Expedition 325.

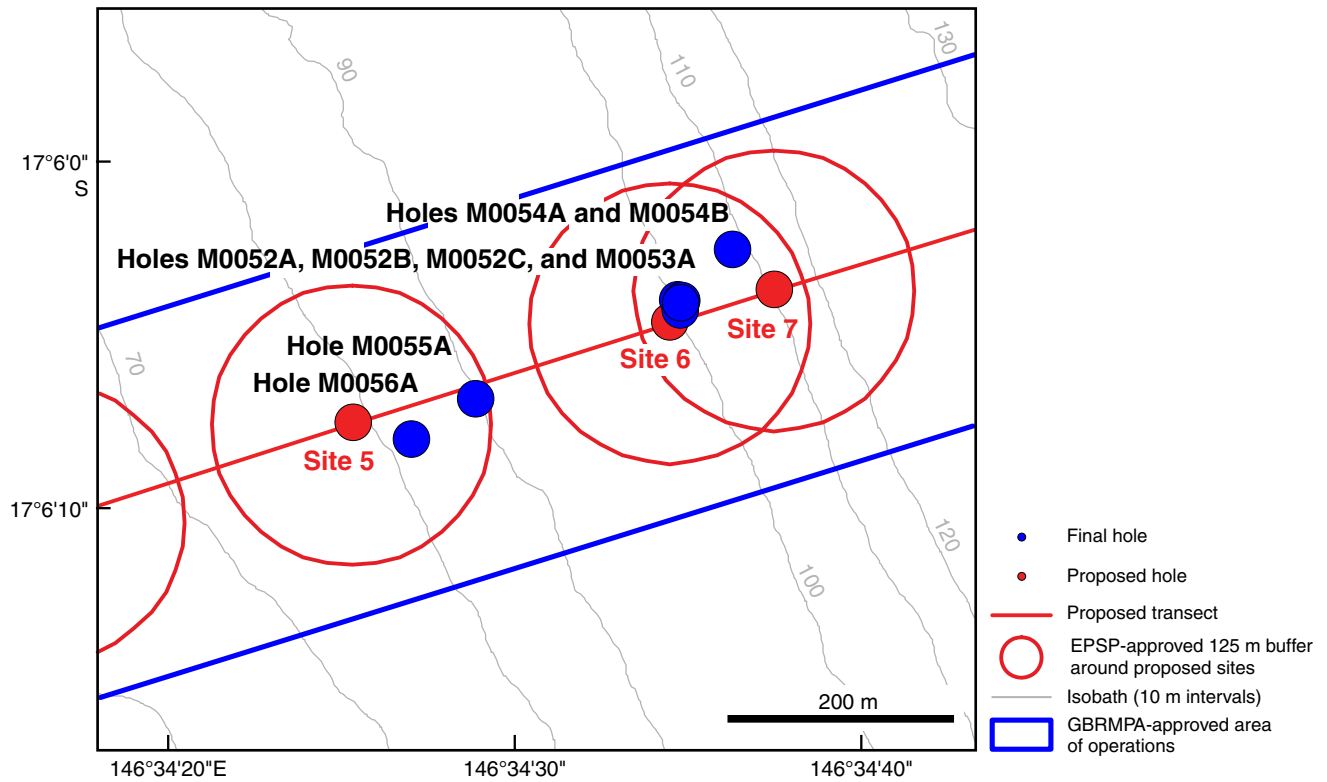


Figure F15. Transect summary of the holes forming the HYD-01C transect showing recovery, facies units, location within each hole of core catcher samples taken for preliminary dating, and distance between each hole/group of holes, Expedition 325. Depth shown in meters below present-day sea level (LAT taken from corrected EM300 multibeam bathymetry).

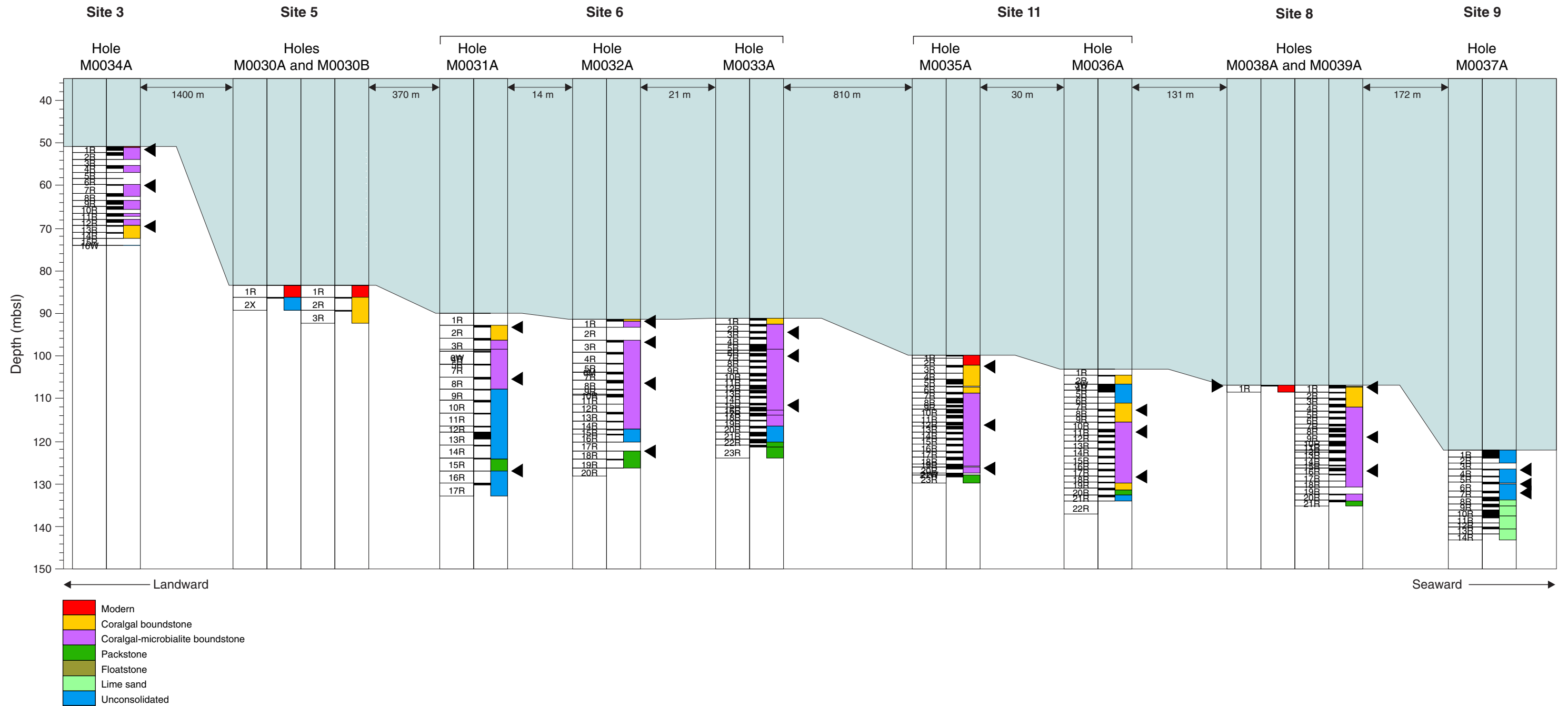


Figure F16. Porosity of discrete samples for all holes measured along the HYD-01C transect in order from shallow water to deep water (left to right), Expedition 325.

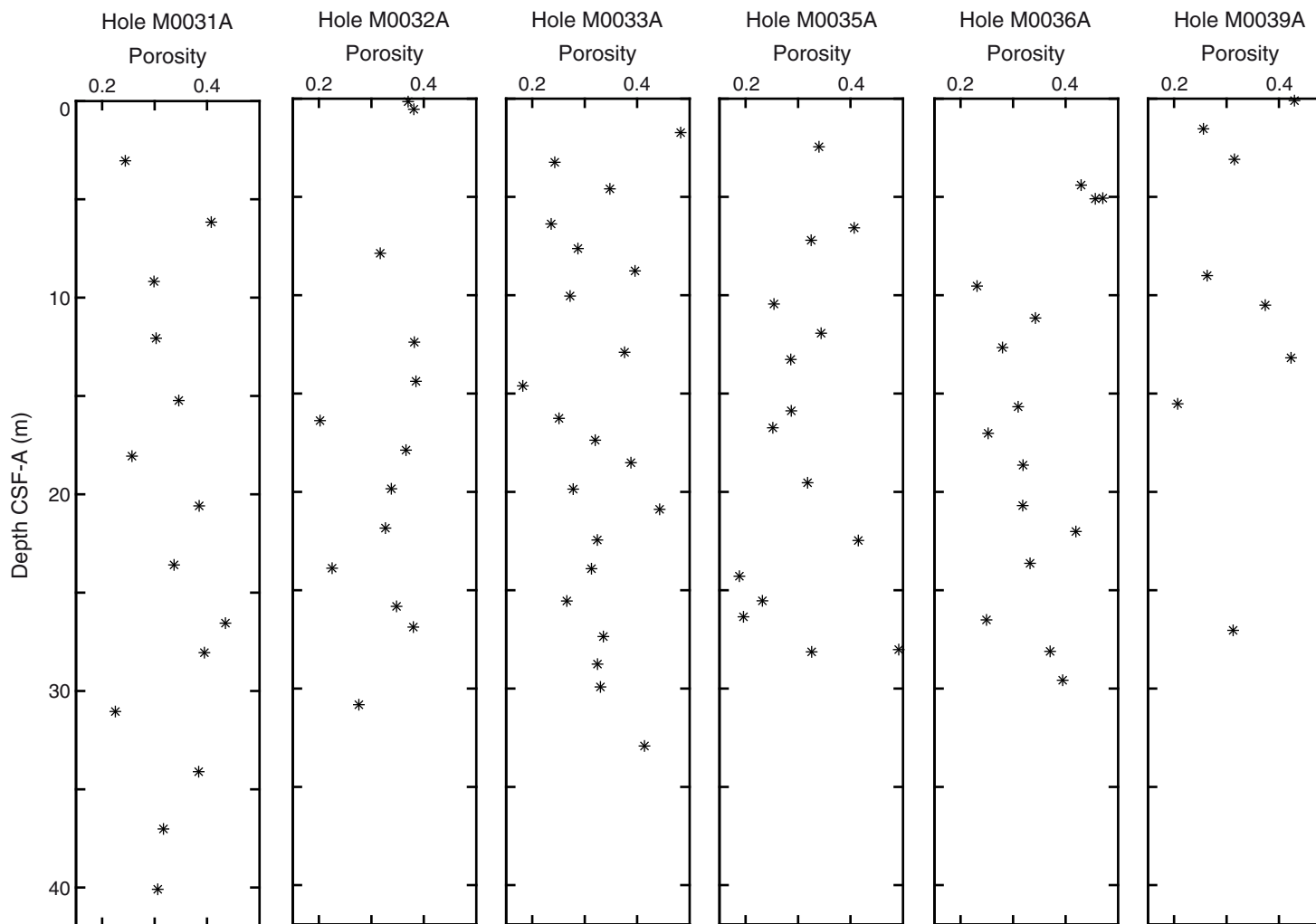


Figure F17. Crossplot showing porosity against bulk density measured in discrete samples from the HYD-01C transect, Expedition 325.

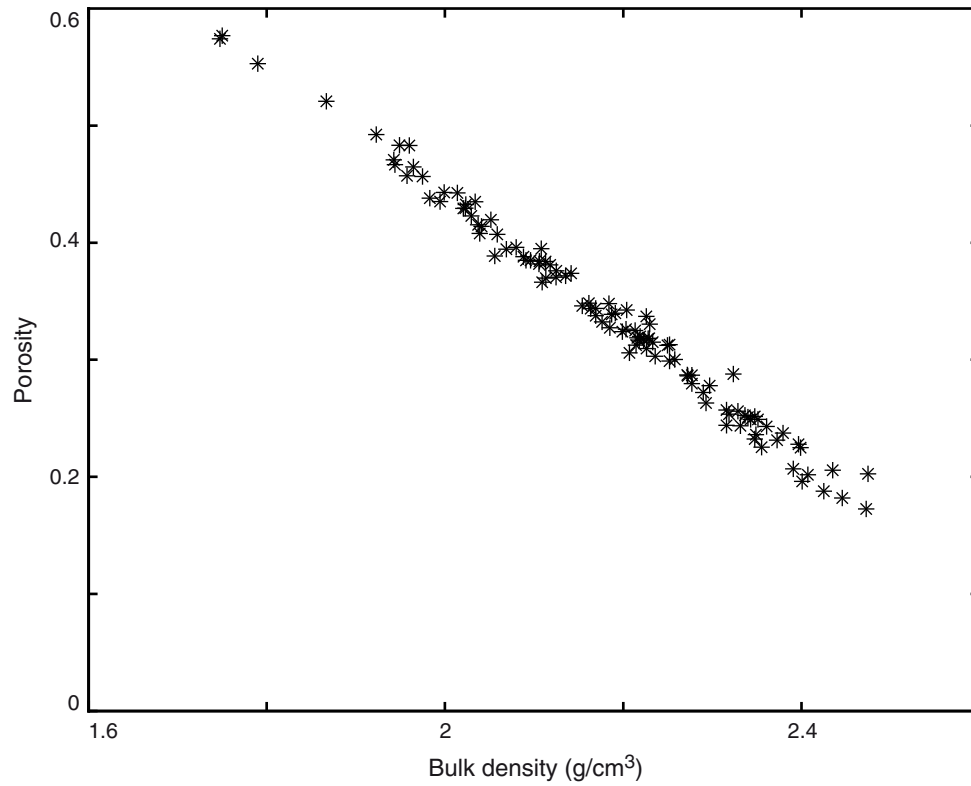


Figure F18. Crossplot of all porosity and V_p measurements from discrete sample analysis from all holes in the HYD-01C transect, Expedition 325.

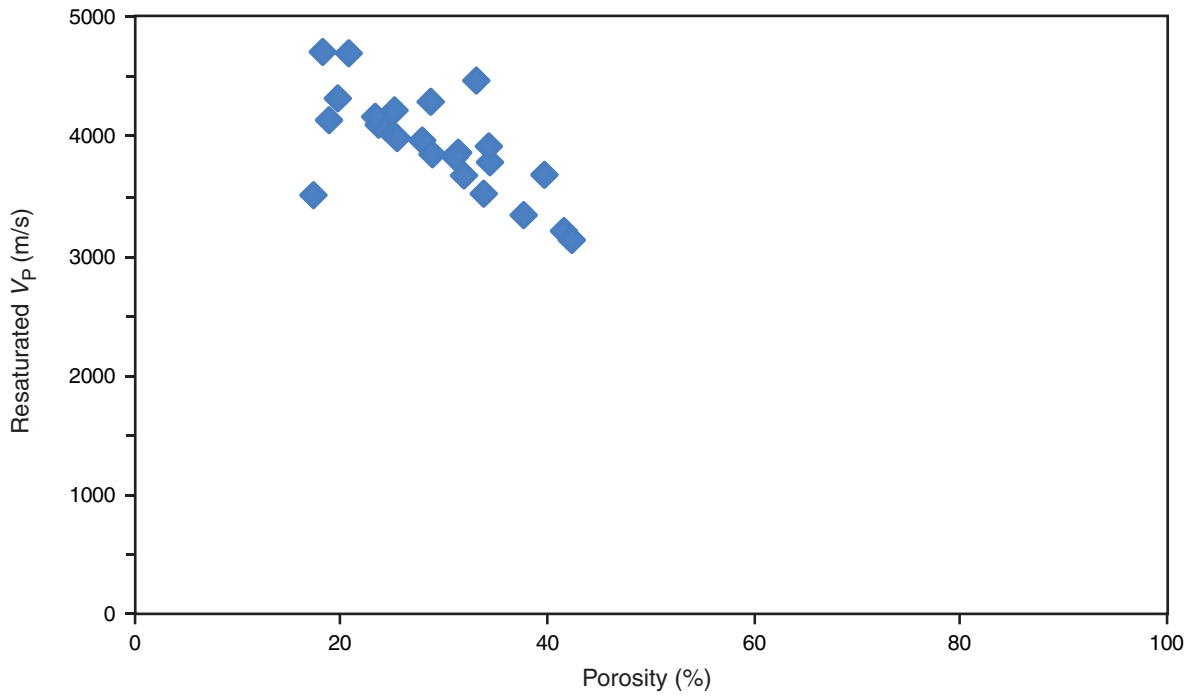
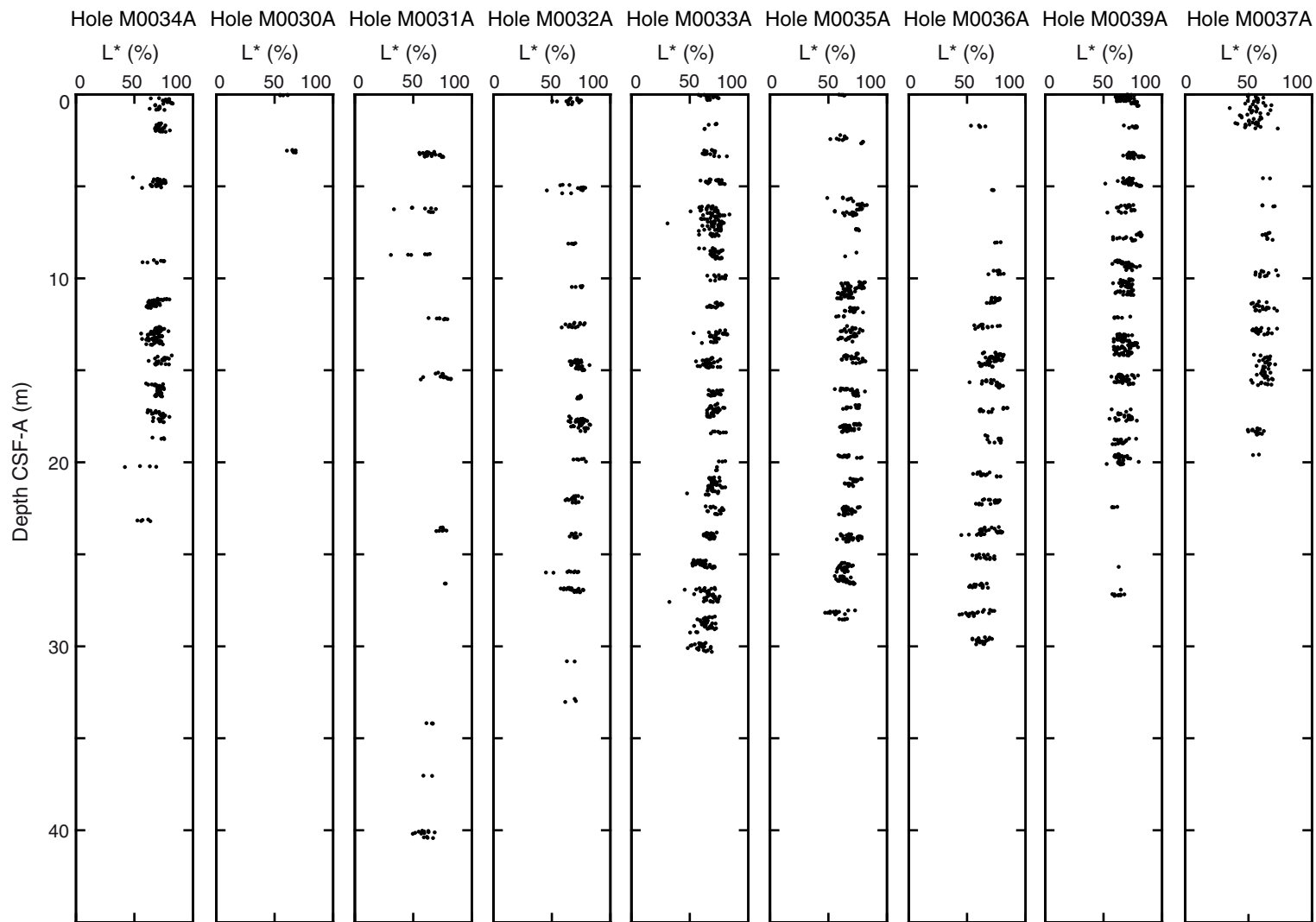


Figure F19. Color reflectance, L^* (%), for all holes along the HYD-01C transect in order from shallow water to deep water (left to right), Expedition 325.



Expedition 325 Preliminary Report

Figure F20. Composite comparing the total gamma ray (TGR) curve measured through pipe (TP) in Hole M0031A to the TGR (TP) log acquired in Hole M0036A. Negative concentration values removed are overlain by an interpolation line. Dashed grey lines denote possible correlations between the two logs.

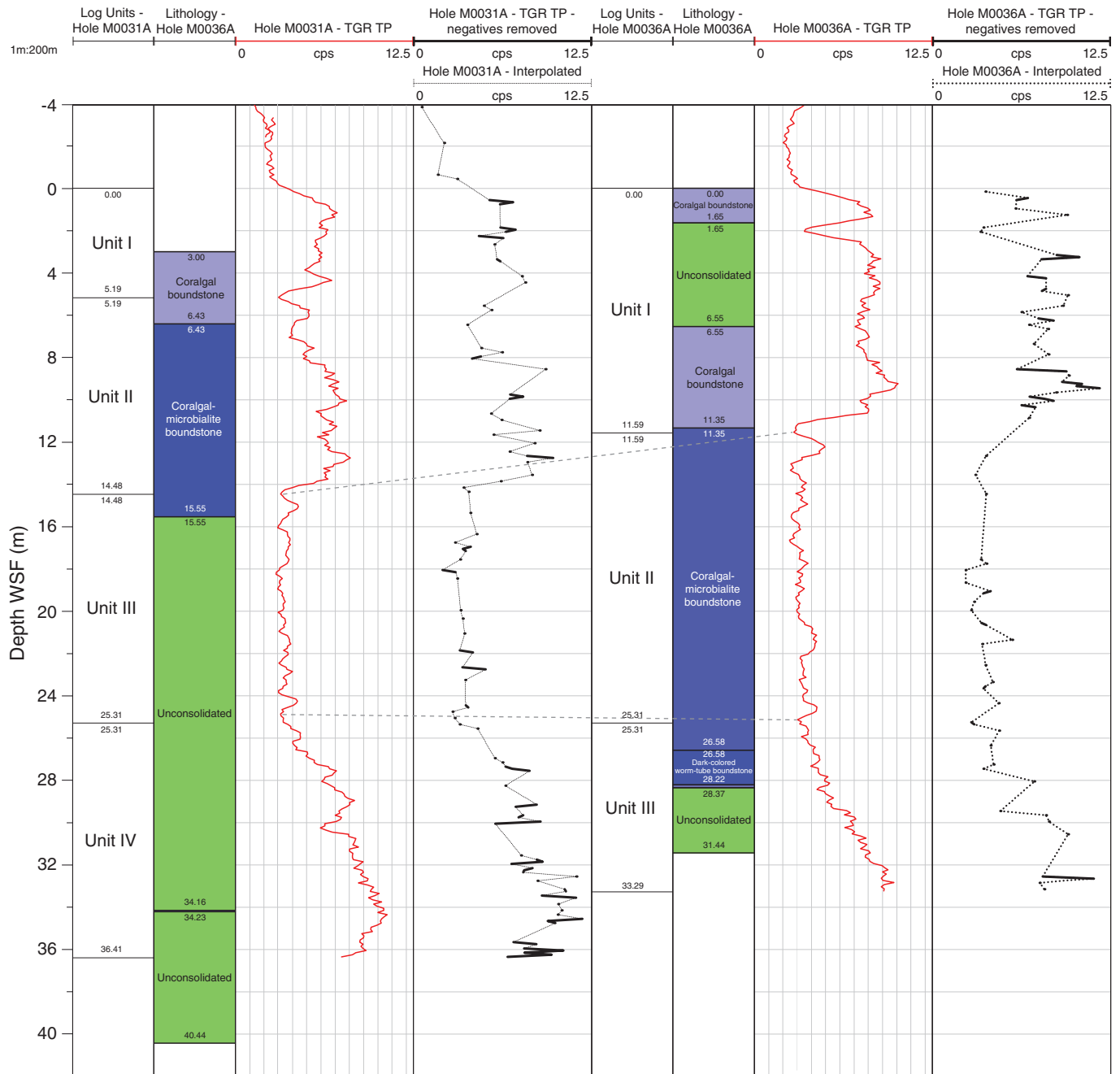


Figure F21. Transect summary of holes forming the HYD-02A transect showing recovery, facies units, location within each hole of core catcher samples taken for preliminary dating, and distance between each hole/group of holes, Expedition 325. Depth shown in meters below present-day sea level (LAT taken from corrected EM300 multibeam bathymetry).

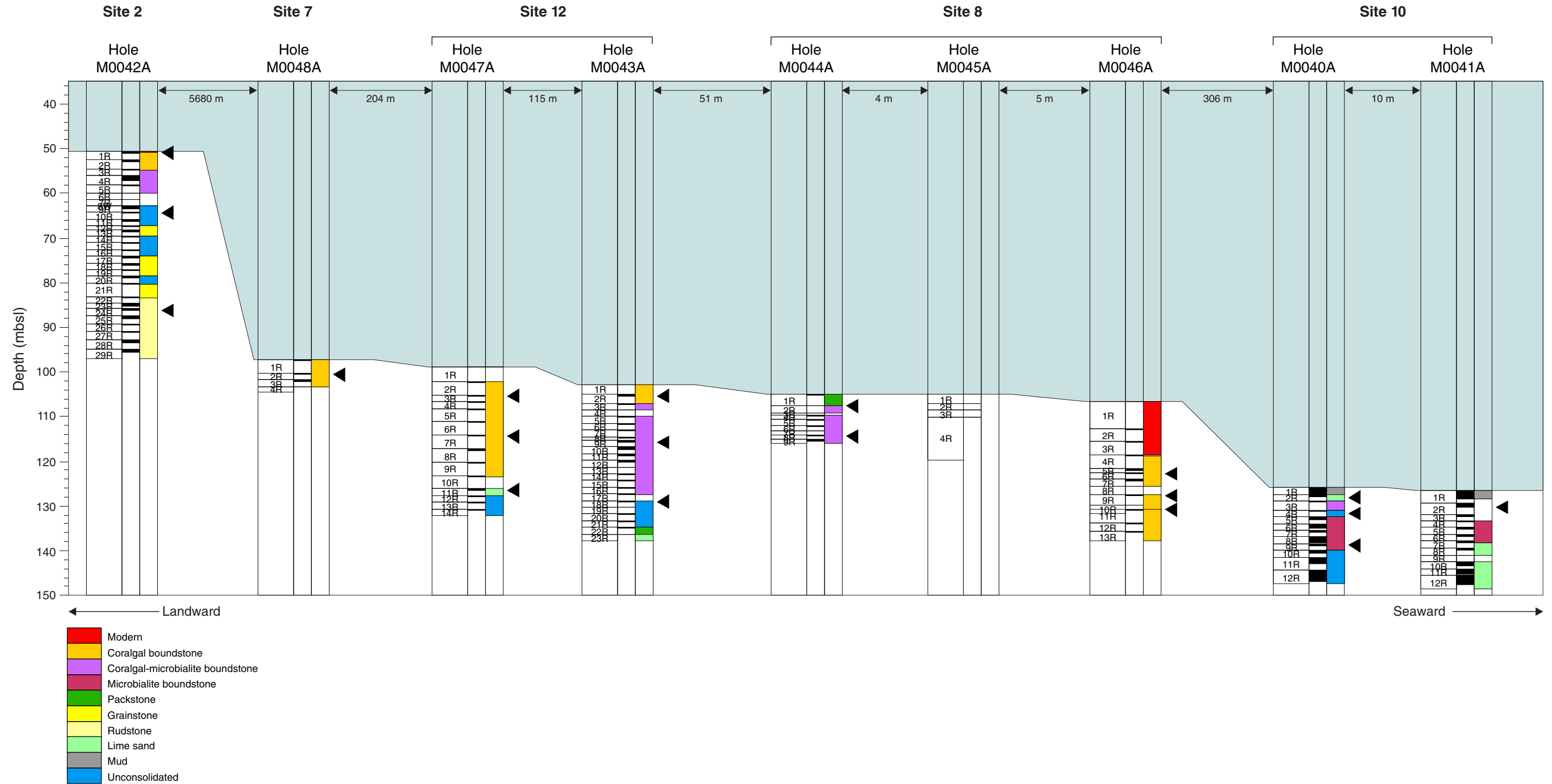


Figure F22. Porosity of discrete samples for all holes measured along the HYD-02A transect in order from shallow water to deep water (left to right), Expedition 325.

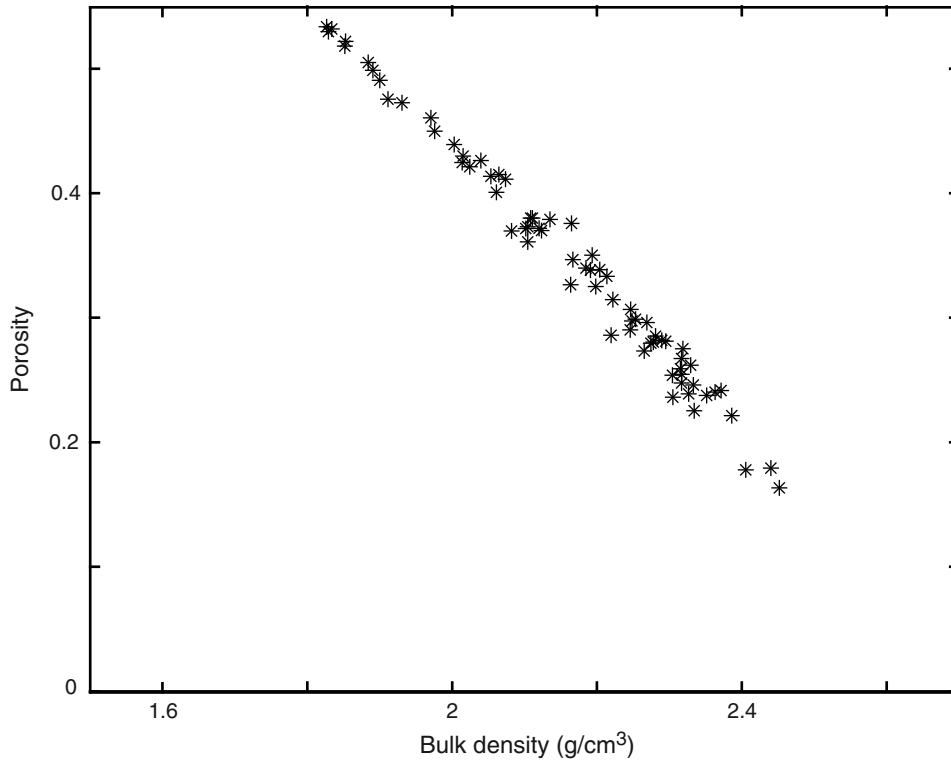


Figure F23. Crossplot showing porosity against bulk density measured in discrete samples from the HYD-02A transect, Expedition 325.

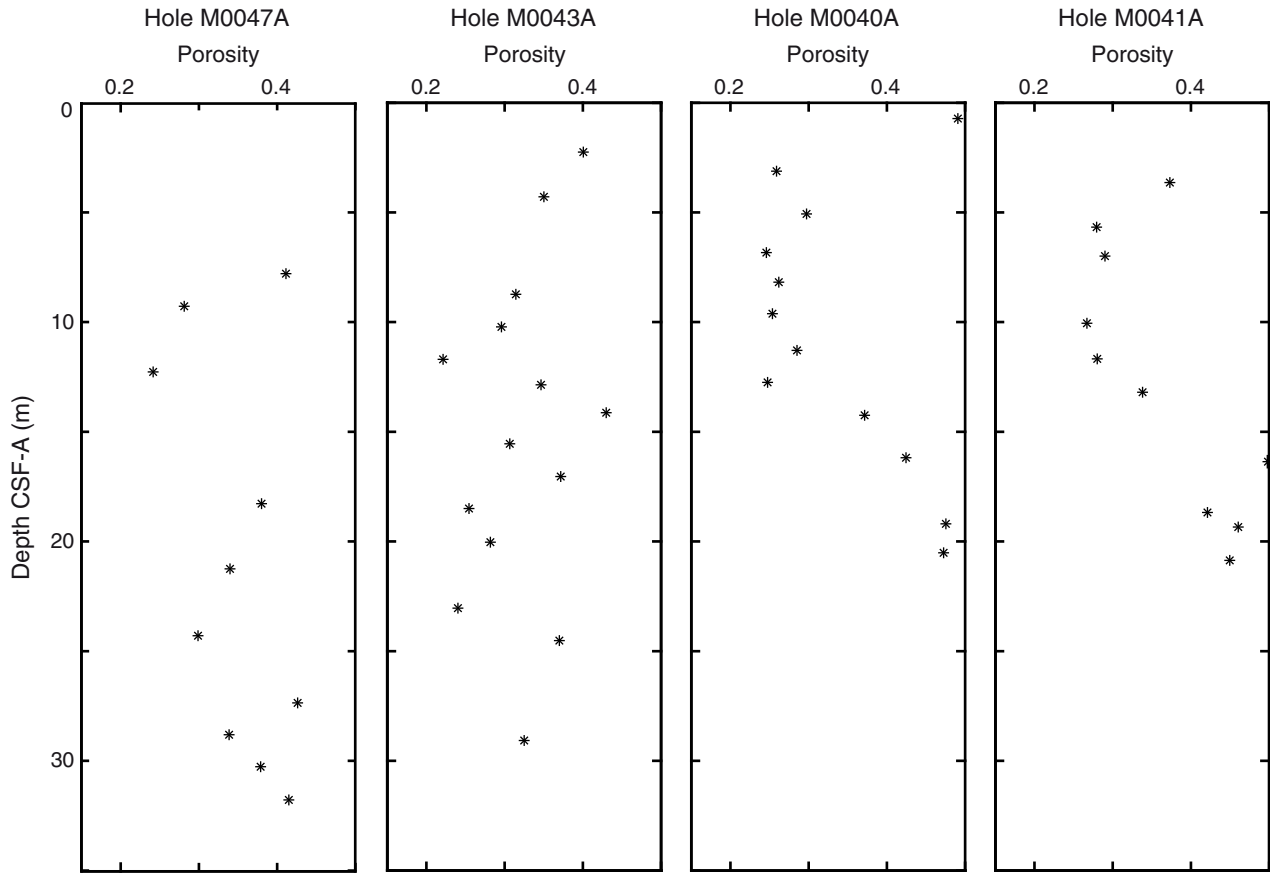


Figure F24. Crossplot of all porosity and V_p measurements from discrete sample analysis from all holes in the HYD-02A transect, Expedition 325.

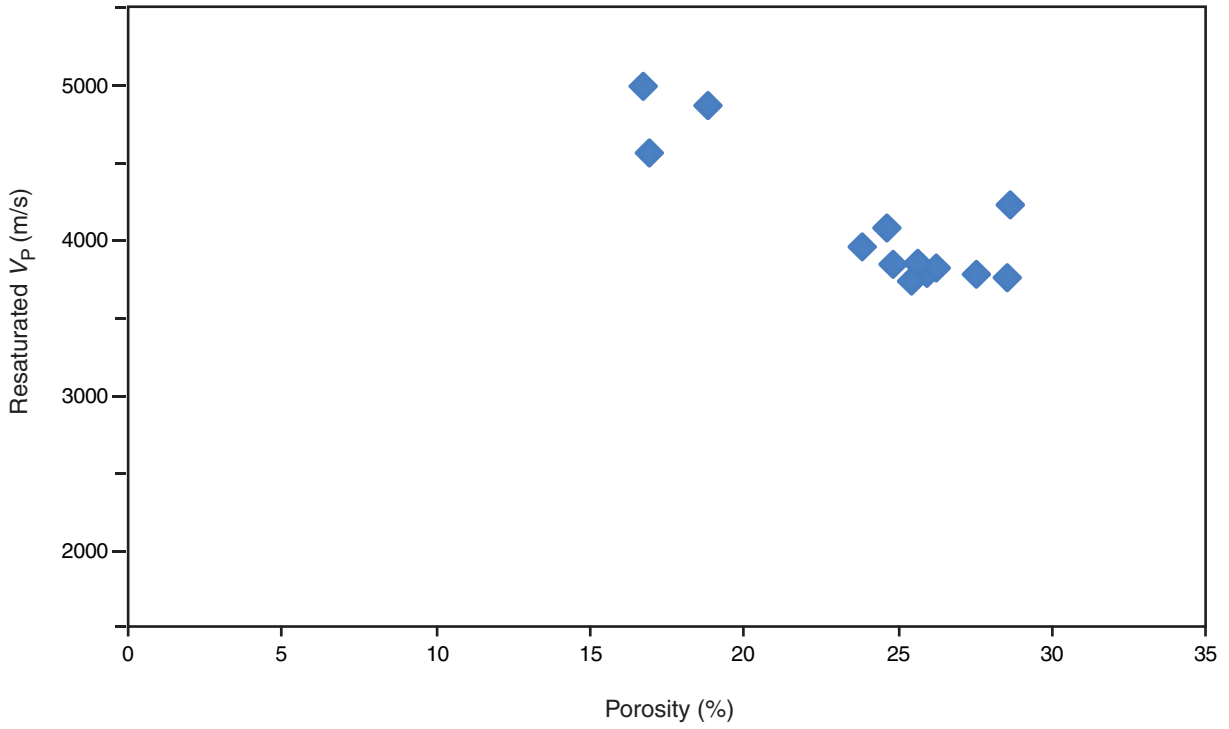


Figure F25. Color reflectance, L^* (%), for all holes along the HYD-02A transect in order from shallow water to deep water (left to right), Expedition 325.

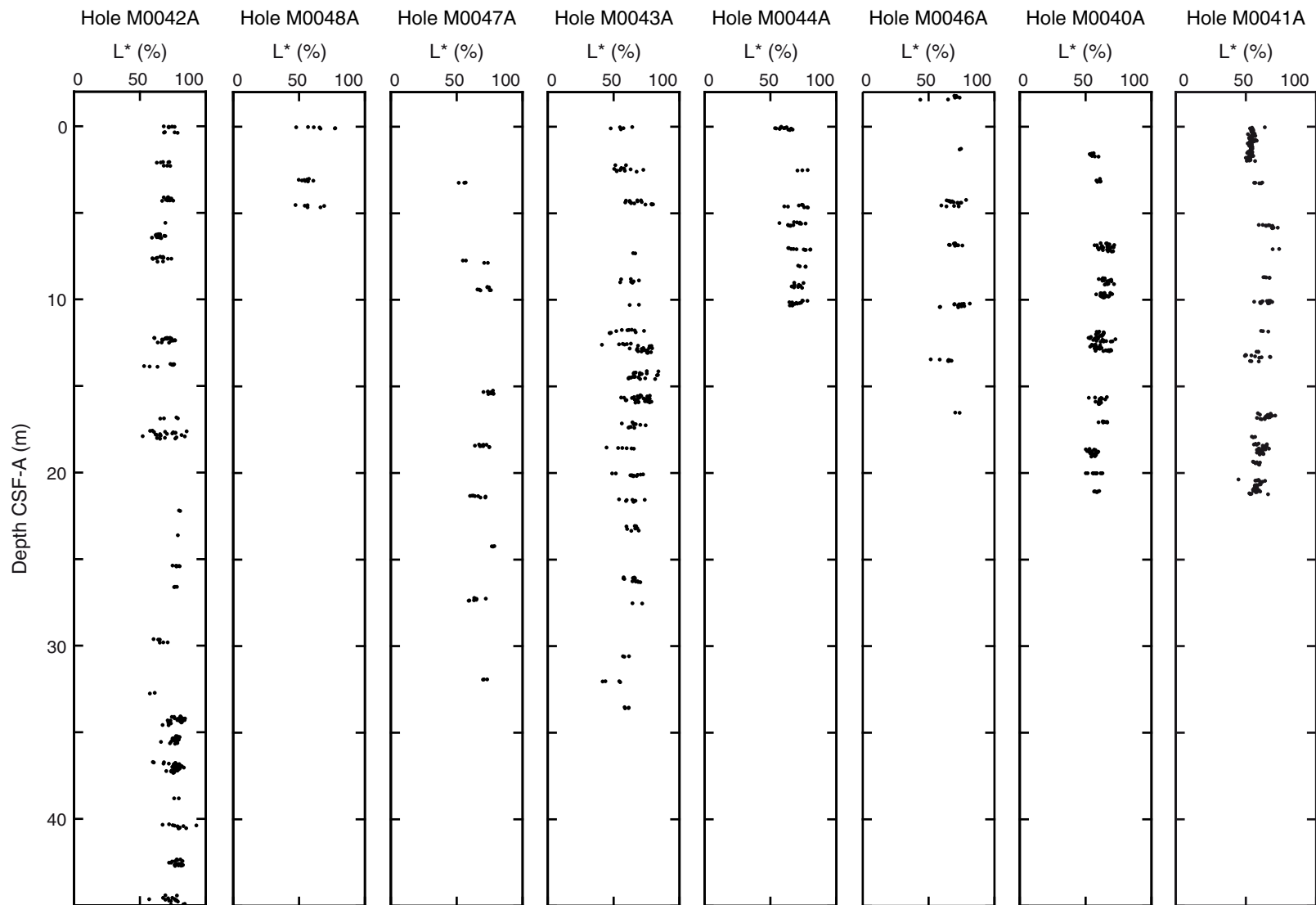


Figure F26. Transect summary of holes forming the RIB-02A transect showing recovery, facies units, location within each hole of core catcher samples taken for preliminary dating, and distance between each hole/group of holes, Expedition 325. Depth shown in meters below present-day sea level (LAT taken from corrected EM300 multibeam bathymetry).

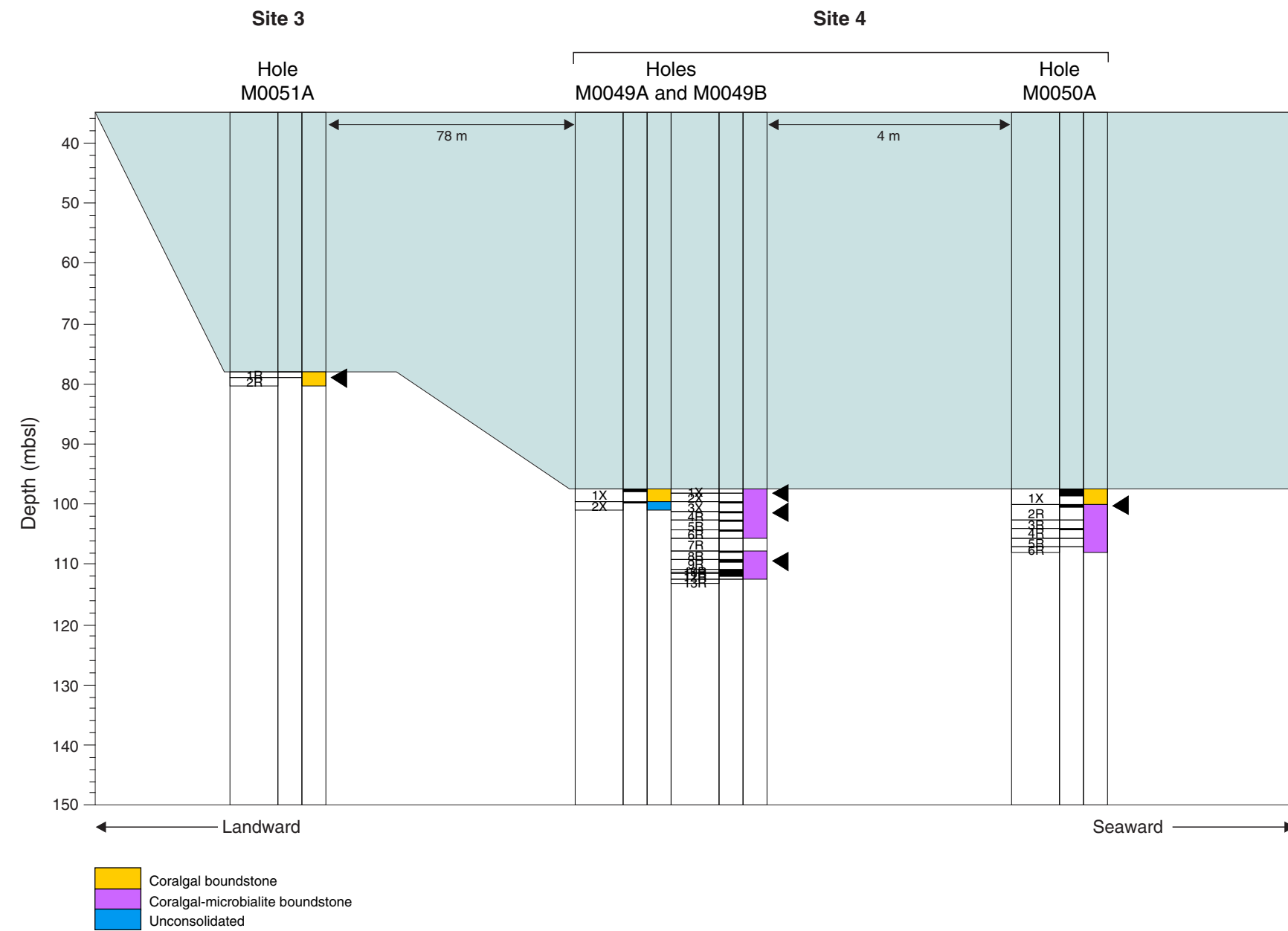


Figure F27. Porosity of discrete samples for all holes measured along the RIB-02A transect in order from shallow water to deep water (left to right), Expedition 325.

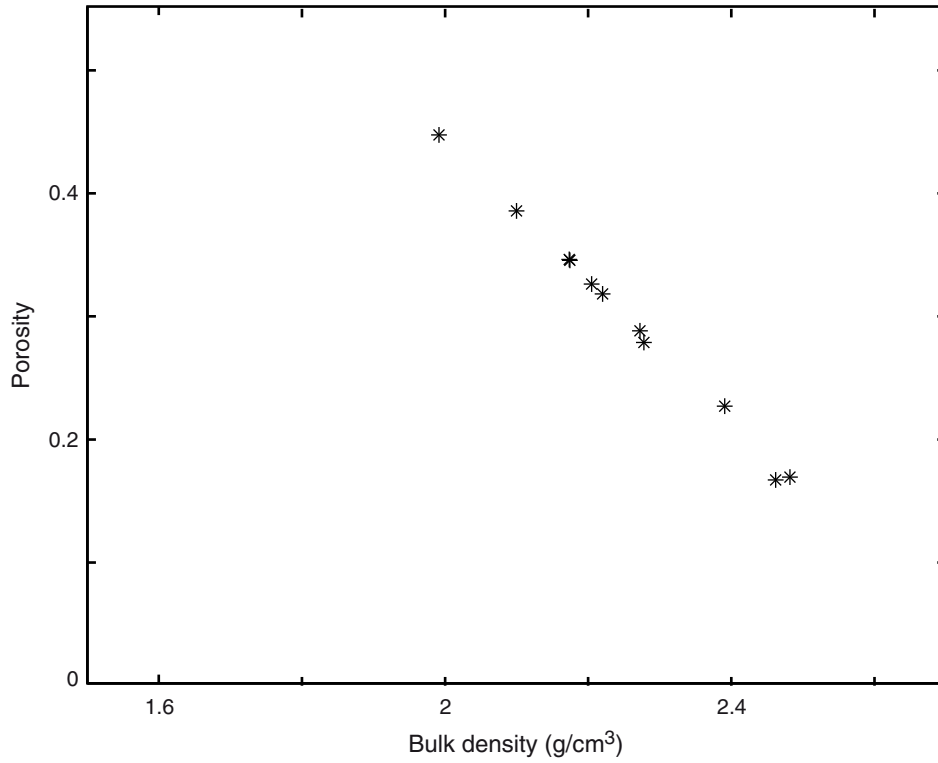


Figure F28. Crossplot showing porosity against bulk density measured in discrete samples from the RIB-02A transect, Expedition 325.

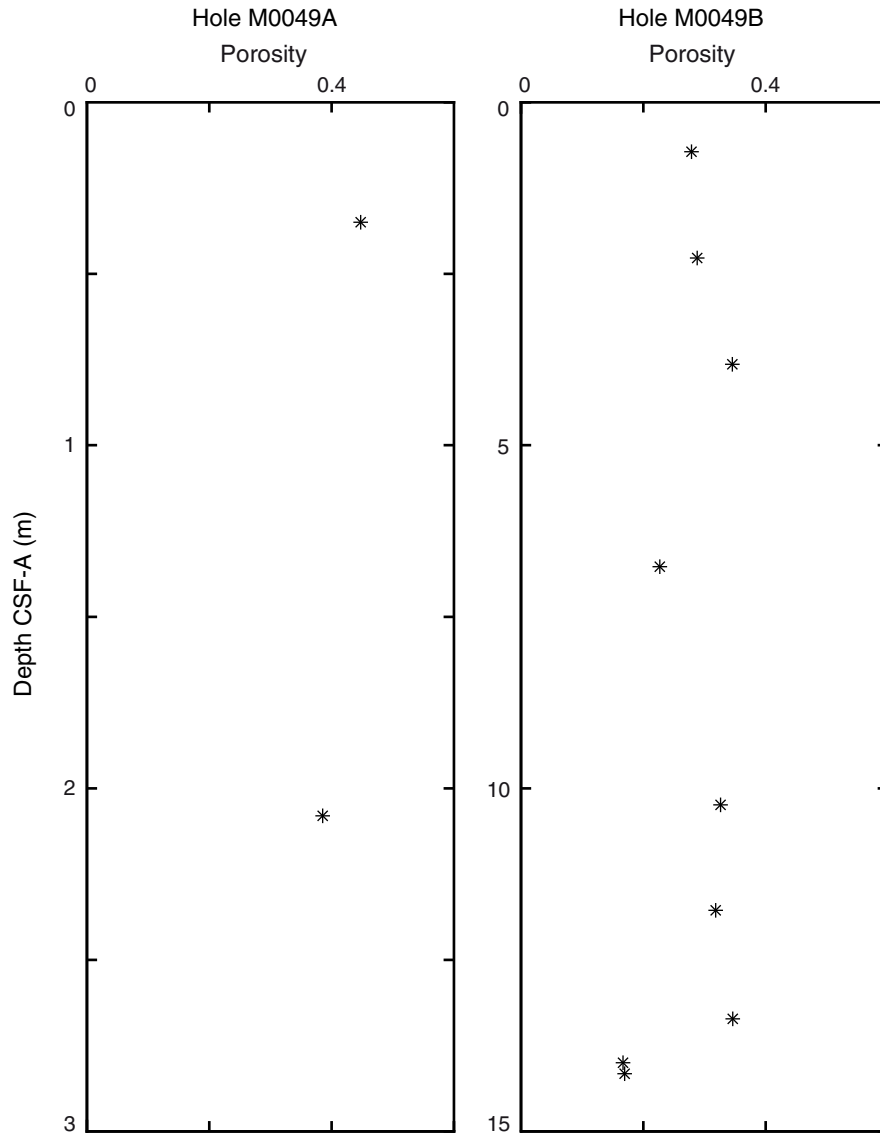


Figure F29. Crossplot of all porosity and V_p measurements from discrete sample analysis from all holes in the RIB-02A transect, Expedition 325.

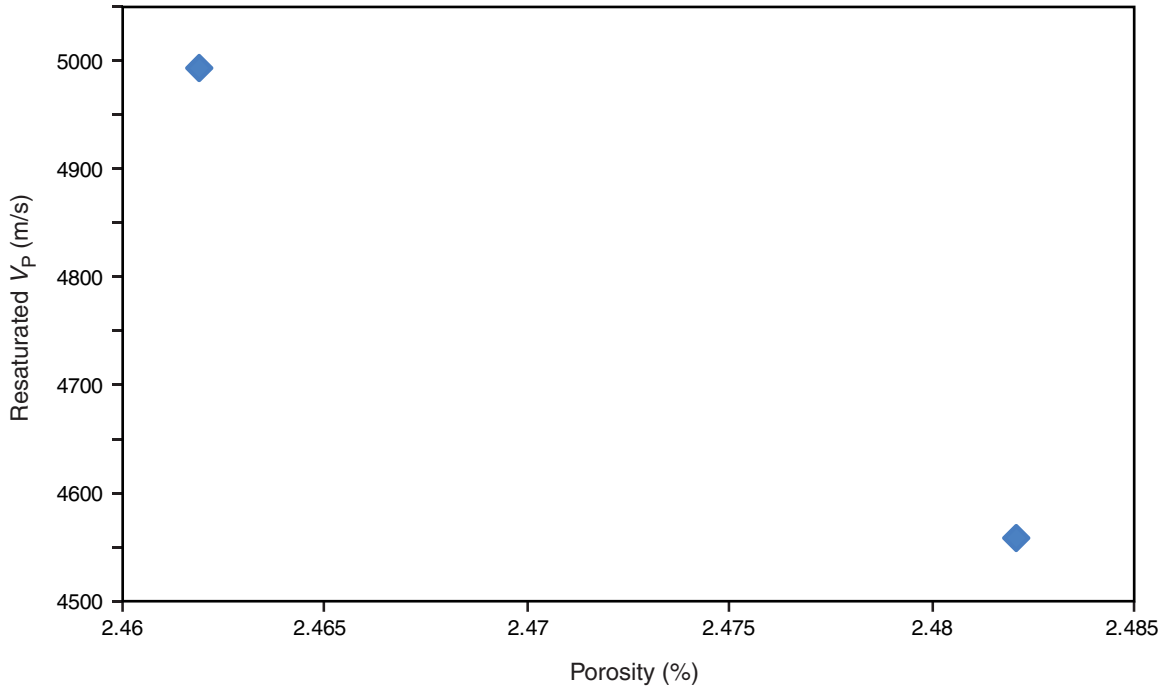


Figure F30. Color reflectance, L^* (%), for all holes along the RIB-02A transect in order from shallow water to deep water (left to right), Expedition 325.

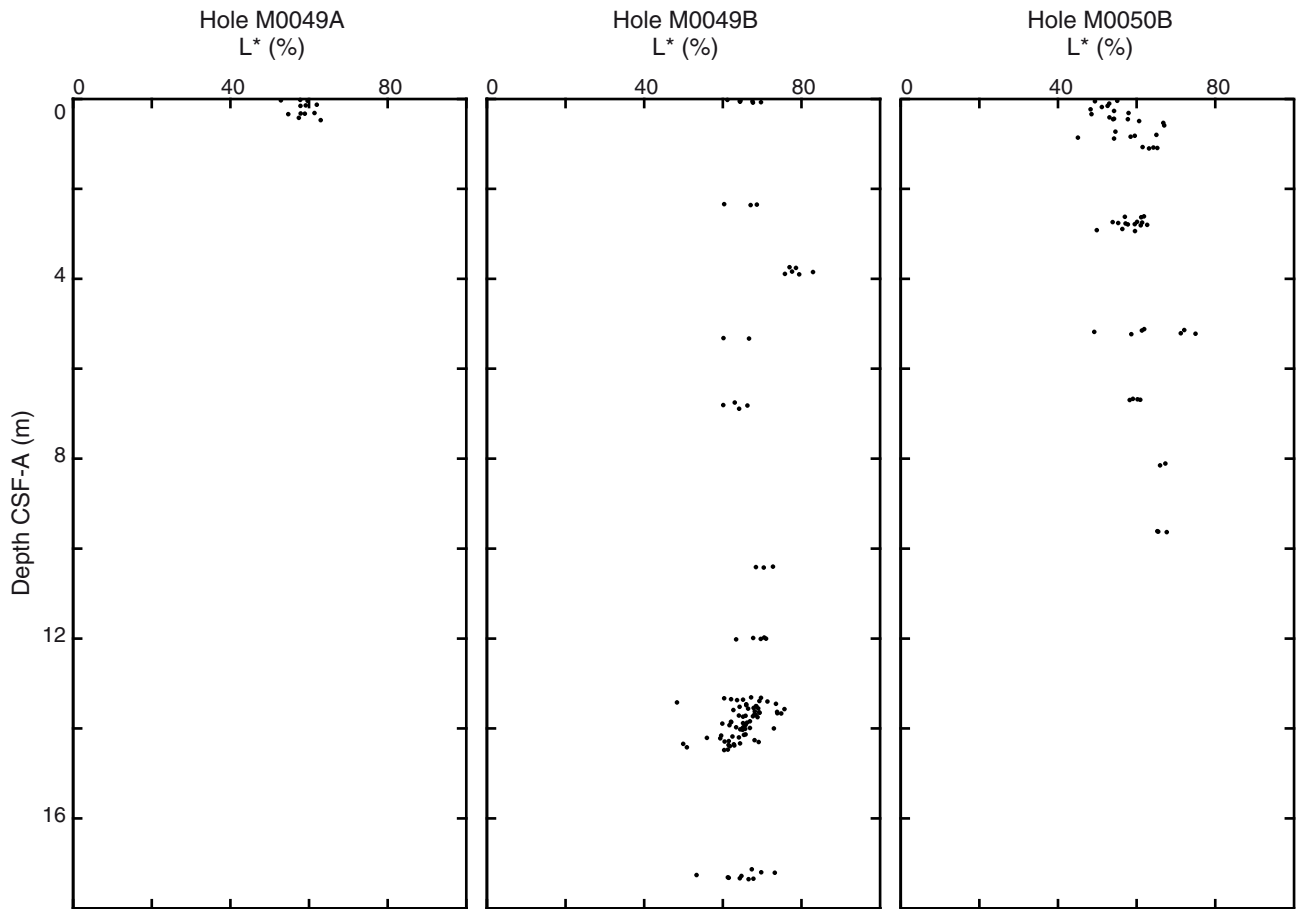


Figure F31. Transect summary of the holes forming the NOG-01B transect showing recovery, facies units, location within each hole of core catcher samples taken for preliminary dating, and distance between each hole/group of holes, Expedition 325. Depth shown in meters below present-day sea level (LAT taken from corrected EM300 multibeam bathymetry).

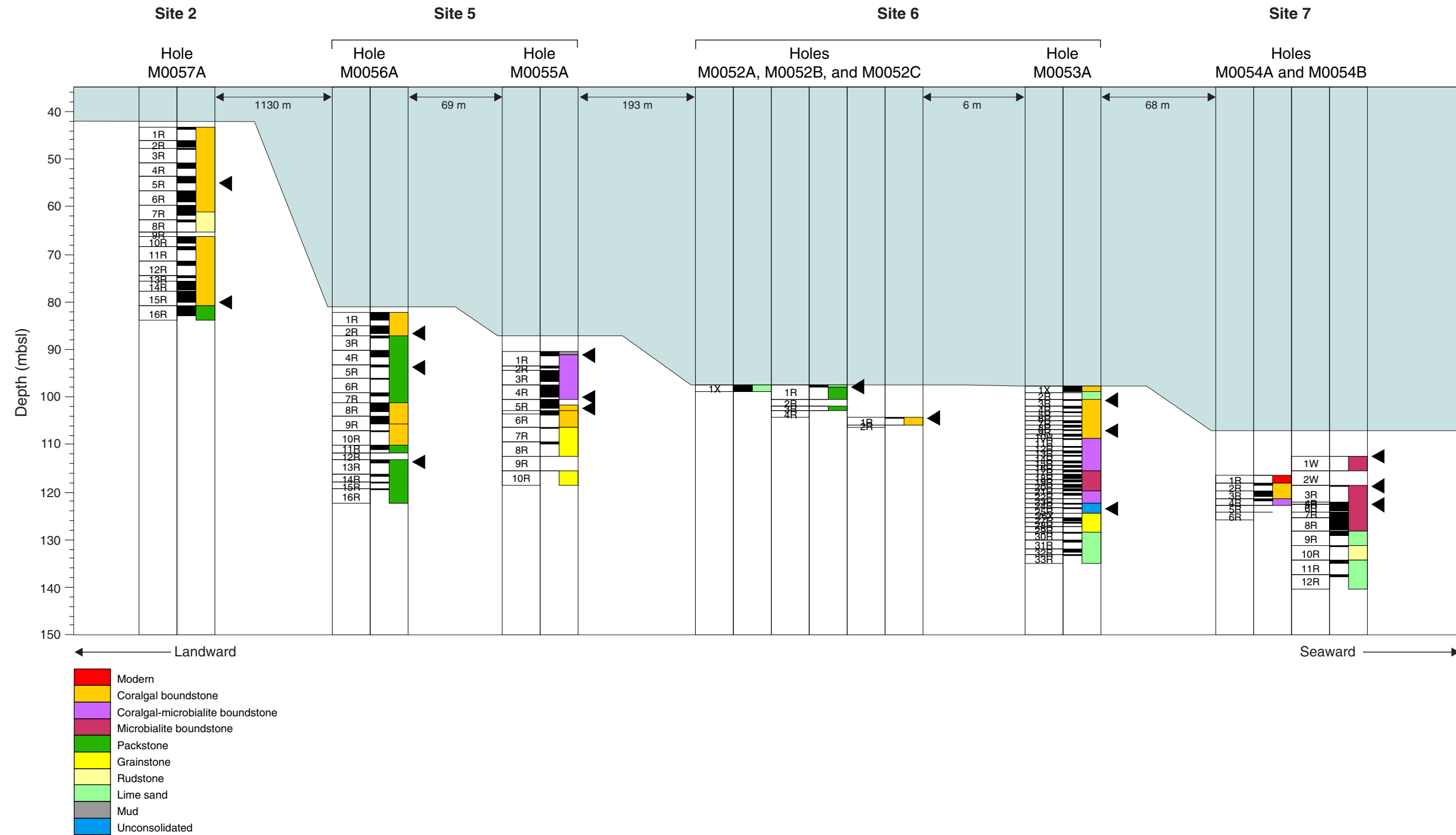


Figure F32. Porosity of discrete samples for all holes measured along the NOG-01B transect in order from shallow water to deep water (left to right), Expedition 325.

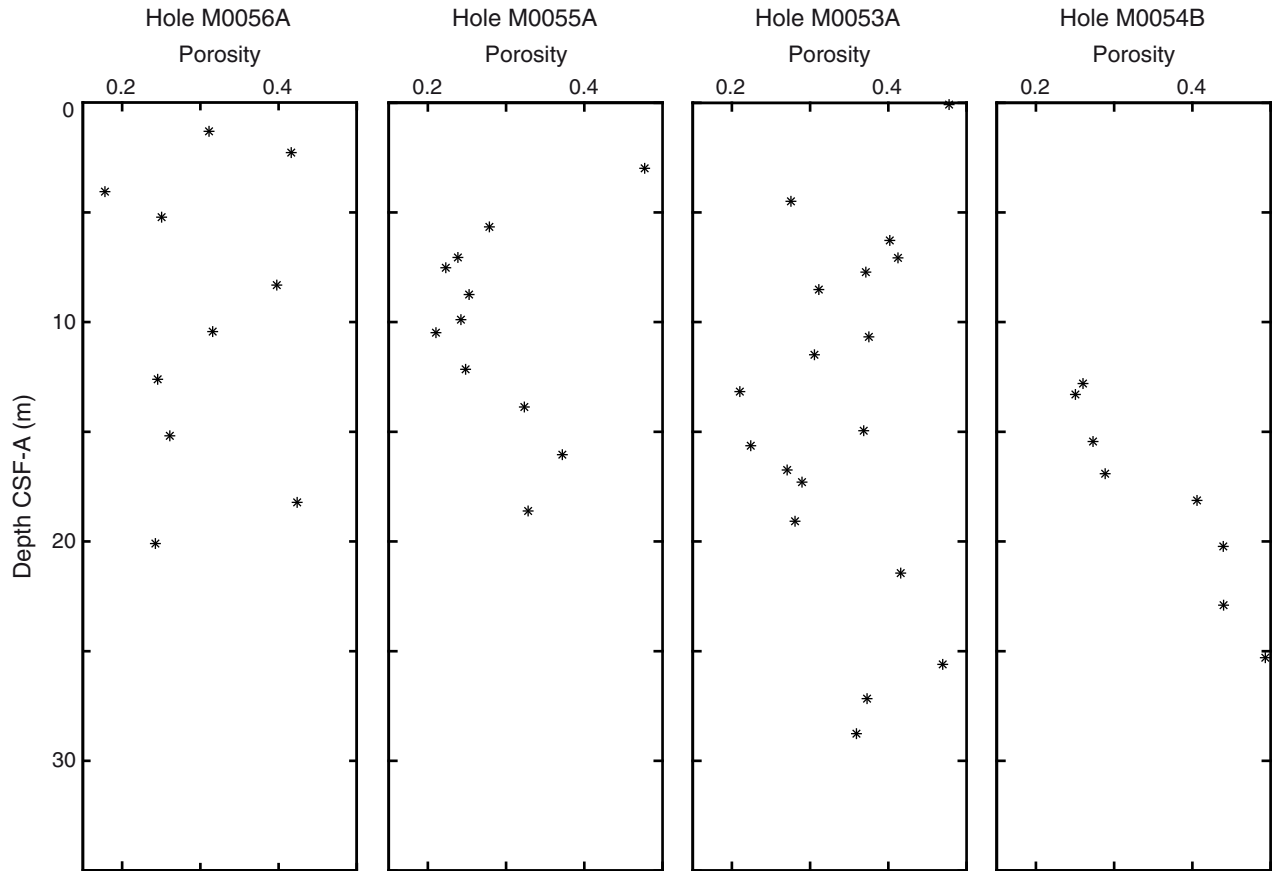


Figure F33. Crossplot showing porosity against bulk density measured in discrete samples from the NOG-01B transect, Expedition 325.

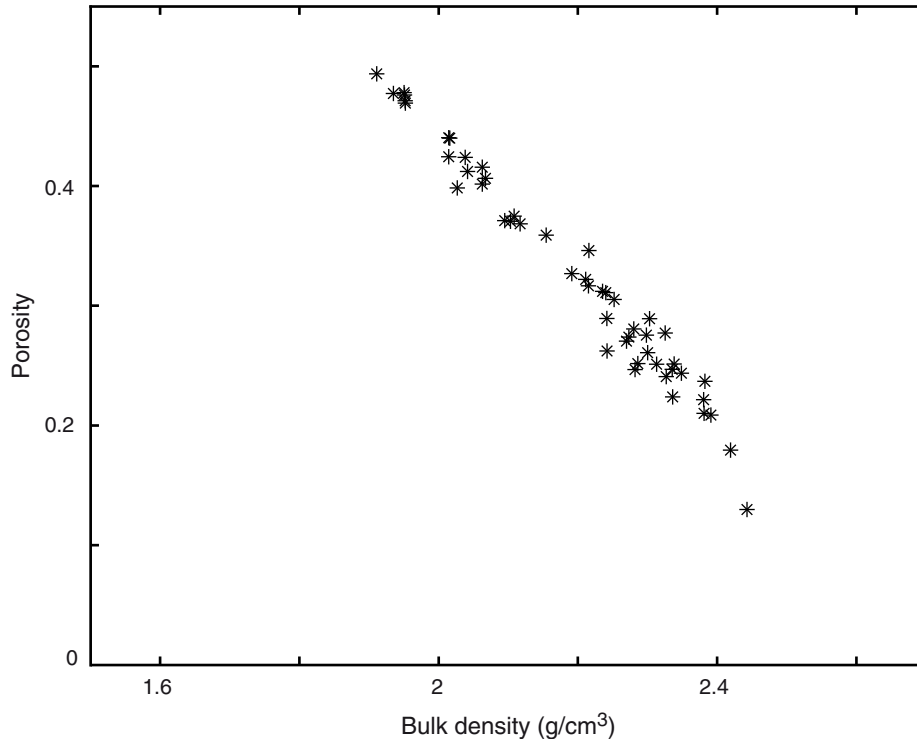


Figure F34. Crossplot of all porosity and V_p measurements from discrete sample analysis from all holes in the NOG-01B transect, Expedition 325.

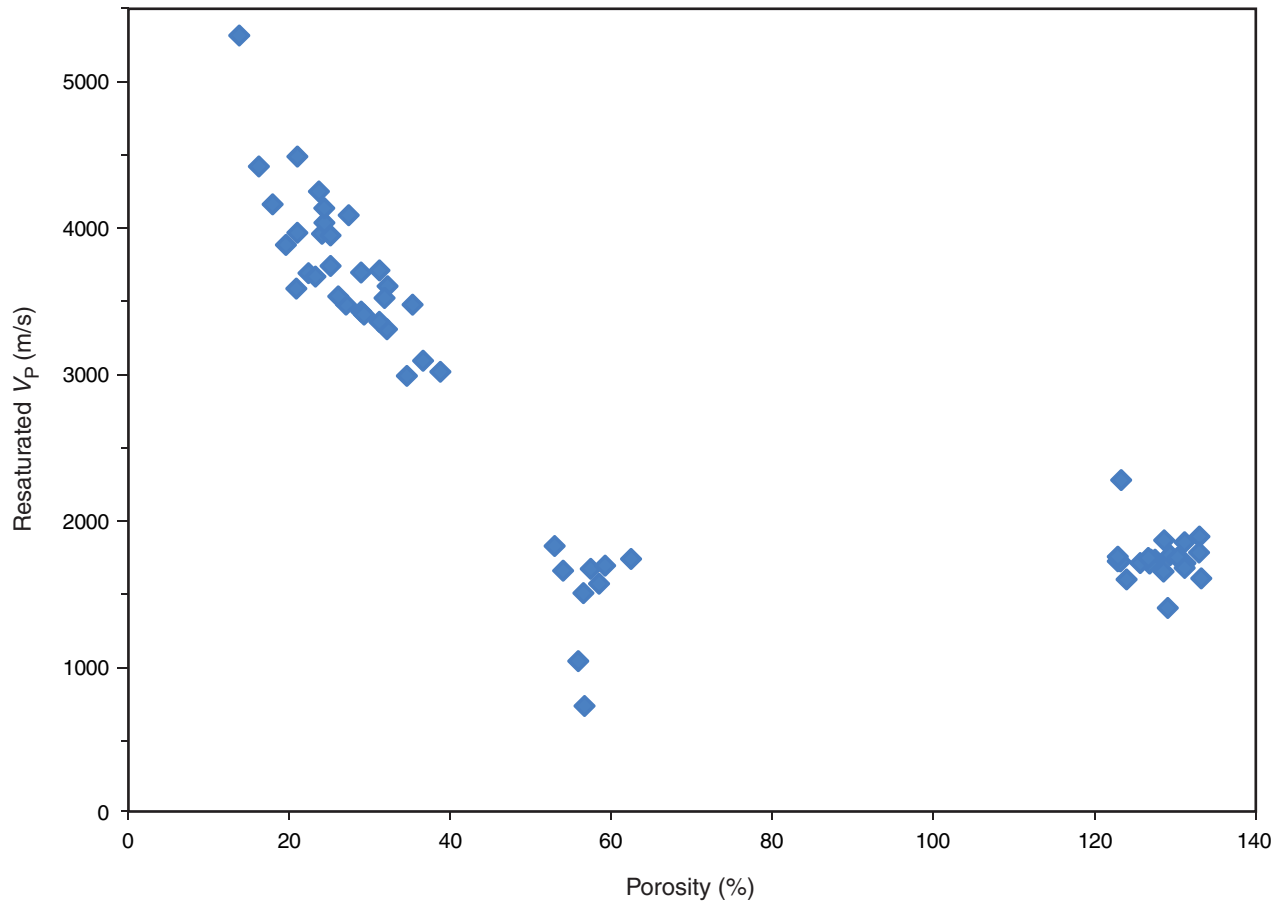


Figure F35. Color reflectance, L^* (%), for all holes along the NOG-01B transect in order from shallow water to deep water (left to right), Expedition 325.

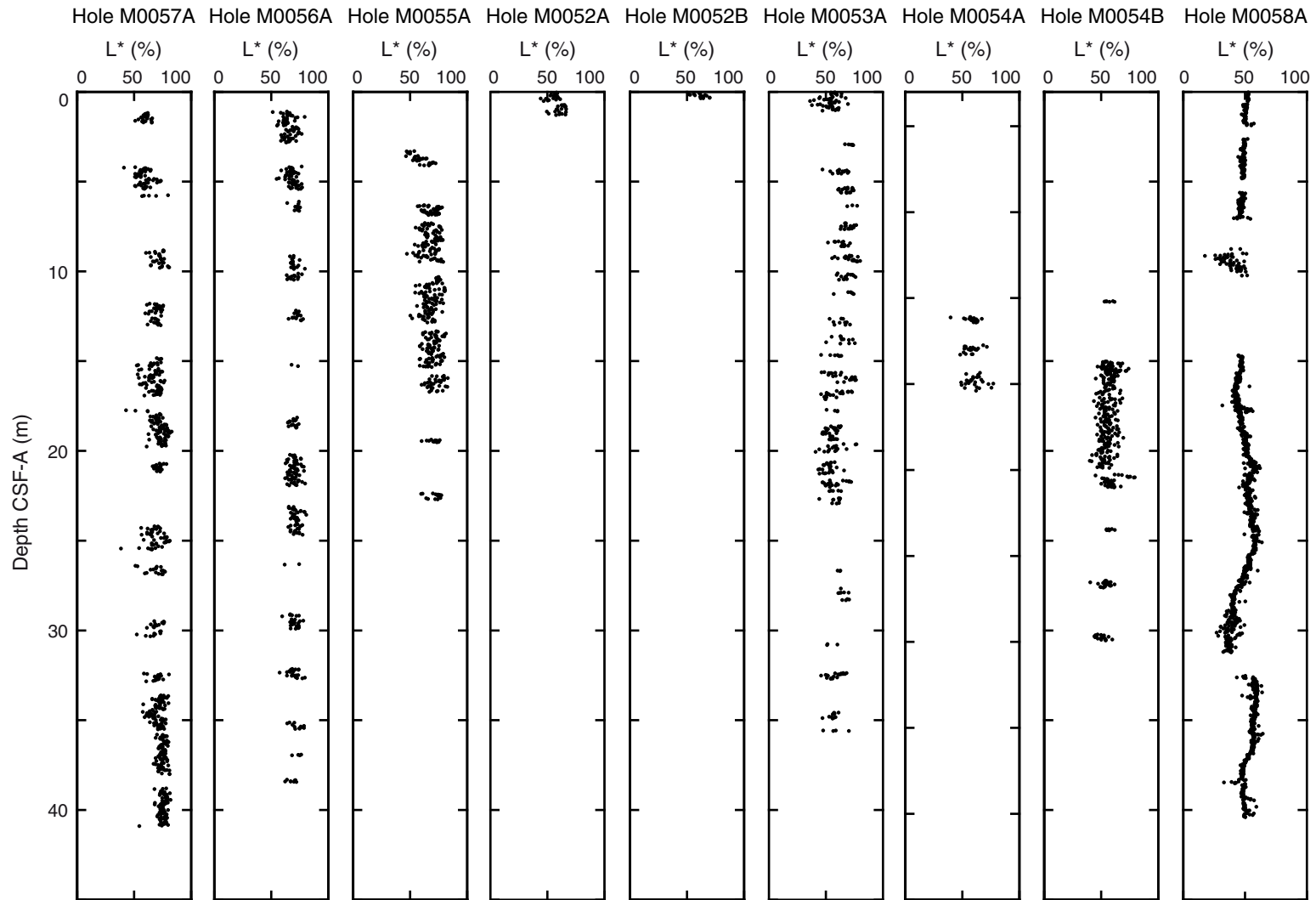


Figure F36. Composite illustrating the detail acquired by the acoustic imaging tool (ABI40) and 3-D virtual borehole. ABI40 traveltime image is overlain by total gamma ray (TGR) (open hole [OH]) and the caliper log.

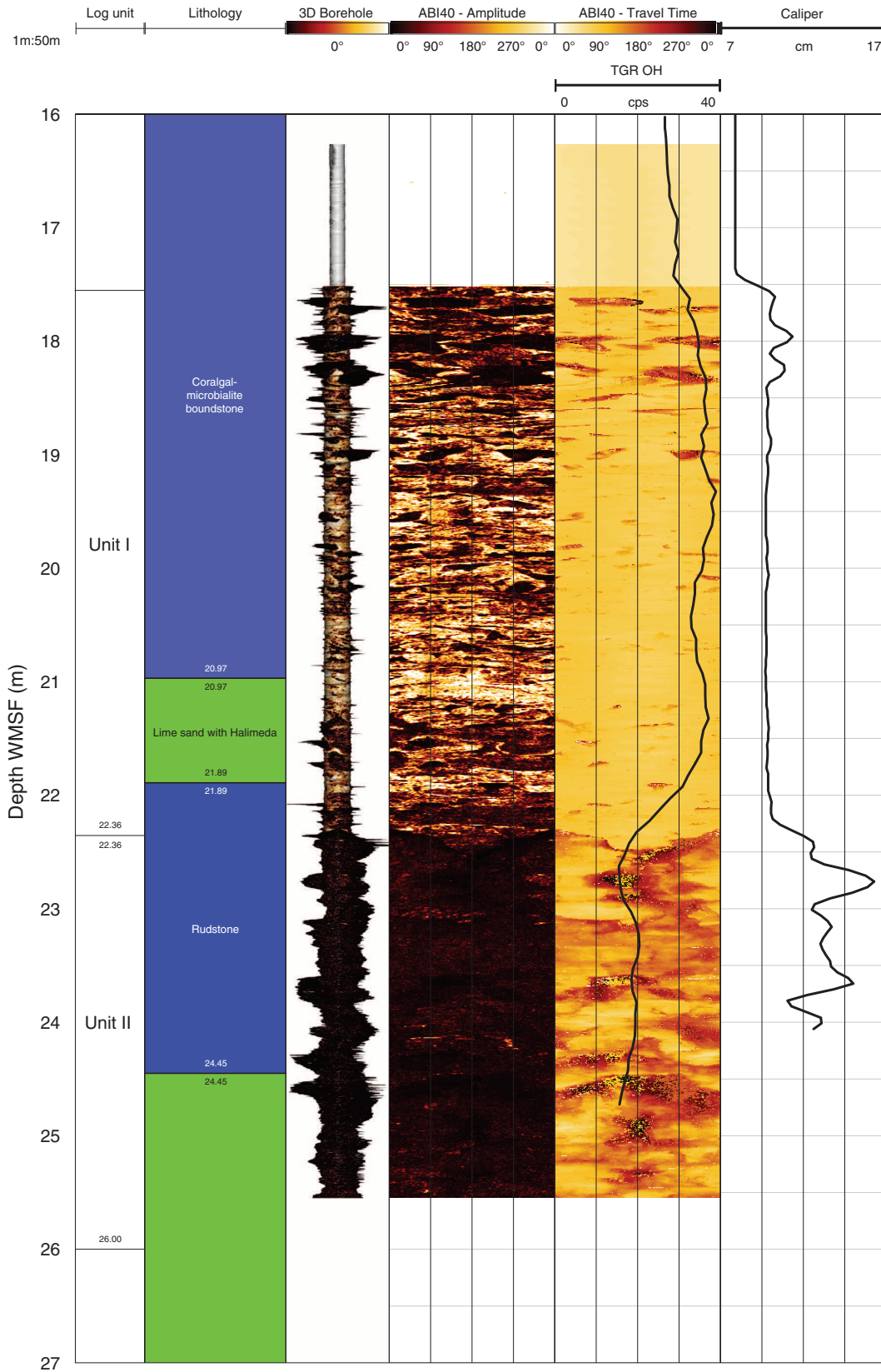


Figure F37. Histogram showing preliminary chronology measurements on core catcher materials recovered during Expedition 325. Age distribution clearly indicates that the recovered fossil coral reef cores span key periods of interest for sea level change and environmental reconstruction, including the last glacial maximum (LGM) and Heinrich Events 1 and 2 (H2, H3), Bølling-Allerød (B/A), and Younger Dryas (YD). Previously published data on relative sea level from 20 cal y. BP through present (upper symbols) along with GISP2 $\delta^{18}\text{O}$ (proxy for temperature over Greenland; black line) are plotted for comparison. MWP-1A = meltwater pulse 1A. Source of data: Tahiti = Bard et al., 1996, 2010. Huon Peninsula = Chappell and Polach 1991; Edwards et al., 1993; Yokoyama et al., 2001a, 2001b. Huon drill core = Cutler et al., 2003. Sunda shelf = Hanebuth et al., 2000. Barbados = Fairbanks, 1989; Bard et al., 1990. GISP2 = Stuiver and Grootes, 2000).

